DOPAMINE D1/5 RECEPTOR MODULATION OF EXCITATORY NEUROTRANSMISSION AND SYNAPTIC PLASTICITY

APPROVED BY SUPERVISORY COMMITTEE

Robert W. Greene, Ph.D. (Supervisor)

Craig Powell, Ph.D. (Chair)

Kimberley Huber, Ph.D.

James Bibb, Ph.D.

Ege Kavalali, Ph.D

DEDICATION

For my husband Don, my children Channing and Jaxson, and my parents Joe and Barbara (who encouraged me to attend fine arts school).

DOPAMINE D1/5 RECEPTOR MODULATION OF EXCITATORY NEUROTRANSMISSION AND SYNAPTIC PLASTICITY

by

LEAH SCHAAL LEVERICH

DISSERTATION

Presented to the Faculty of the Graduate School of Biomedical Sciences

The University of Texas Southwestern Medical Center at Dallas

In Partial Fulfillment of the Requirements

For the Degree of

DOCTOR OF PHILOSOPHY

The University of Texas Southwestern Medical Center at Dallas

Dallas, Texas

March 2009

DOPAMINE D1/5 RECEPTOR MODULATION OF EXCITATORY NEUROTRANSMISSION AND SYNAPTIC PLASTICITY

LEAH SCHAAL LEVERICH, Ph.D.

The University of Texas Southwestern Medical Center at Dallas, 2009

ROBERT W. GREENE, M.D., Ph.D.

Dopamine D1/5 receptor (D1/5R) activation modulates glutamate-dependent neuroplasticity thought to underlie learning and memory. Disturbances in dopamine-glutamate signaling have been implicated in neuropsychiatric disorders such as schizophrenia and addiction. Despite its importance, a mechanism responsible for D1/5R modulation of glutamate-dependent neuroplasticity remains unknown. Here we present evidence using field potential recordings from hippocampal slices showing that D1/5R activation establishes a prolonged temporal window for the induction of NMDA receptor-dependent

synaptic plasticity. We found that D1/5R activation increases synaptic responses and long-term potentiation (LTP) expression through a pathway involving NR2B-NMDARs, PKA, PKC, PKM zeta, and src-family tyrosine kinases. D1/5R activation produced sustained increases in the surface expression of NR2B and GluR1 subunits in hippocampal slices, and this increase required the activity of NR2B-NMDARs. Consistent with our field potential recordings, D1/5R activation during memory consolidation facilitates extinction learning to conditioned fear, providing functional relevance for a prolonged window of synaptic potentiation mediated by D1/5Rs at the level of behavioral output.

TABLE OF CONTENTS

PRIOR PUBLICATIONS

Varela JA, Hirsch SJ, Chapman D, **Leverich LS**, Greene RW. D1/5 modulation of synaptic NMDA receptor currents. *Journal of Neuroscience.* In press.

Leverich LS, Lane CE, Cooper DC, Greene RW. Dopamine D1/5R receptor activation induces synaptic plasticity via a novel NR2B-dependant mechanism. *Journal of Neuroscience.* Submitted.

Hale CF, Dietz K, **Leverich LS**, Varela J, Zirlin B, Greene RW, Cowan CW. Vav family GEFs mediate brain-derived neurotrophic factor-induced dendritic spine and synaptic plasticity. In preparation.

TABLE OF FIGURES

LIST OF ABBREVIATIONS

6-OH-DA, 6-Hydroxydopamine

ACSF, artificial cerebrospinal fluid

AMPA, alpha-amino-3-hydroxy-5-methyl-4-isoxazolepropionic acid

AMPAR, AMPA receptor

AMY, amygdala

ANOVA, analysis of variance

APV, ((2R)-amino-5-phosphonovaleric acid; AP5, (2R)-amino-5-phosphonopentanoate)

CA1, *Cornu Ammonis* 1

CamKII, calcium / calmodulin-dependent protein kinase II

D1, dopamine D1 receptor

D1/5R, dopamine D1/D5 receptor family

D2, dopamine D2 receptor

DA, dopamine

DG, dentate gyrus

EC, entorhinal cortex

EPSC, excitatory postsynaptic current

fEPSP, field excitatory postsynaptic potential

$GABA_A$, Gamma-aminobutyric acid type A

GluR1, AMPAR subunit type 1

GluR2, AMPAR subunit type 2

GluR3, AMPAR subunit type 3

GluR4, AMPAR subunit type 4

GPCR, g-protein coupled receptor

G-protein, guianine nucleotide regulatory protein

HFS, high frequency stimulation

I.P., intra-peritoneal

Ifenprodil, (1R*,2S*)-erythro-2-(4-Benzylpiperidino)-1-(4-hydroxyph enyl)-1-propanol hemitartrate

KT5720, (9R,10S,12S)-2,3,9,10,11,12-Hexahydro-10-hydroxy-9-meth yl-1-oxo-9,12-epoxy-1H-diindolo[1,2,3-fg:3',2',1'-kl]py rrolo[3,4-i][1,6]benzodiazocine-10-carboxylic acid, hexyl ester

LTD, long-term depression

LTP, long-term potentiation

mGluR, metabotropic glutamate receptor

mPFC, medial prefrontal cortex

NAc, nucleus accumbens

NBQX, 1, 2,3,4-tetrahydro-6-nitro-2,3-dioxo-benzo[f]quinoxaline-7-sulfonamide

NMDA, N-methyl D-aspartate

NMDAR, NMDA receptor

NR1, NMDAR subunit type 1a-1

NR2A, NMDAR subunit type 2A

NR2B, NMDAR subunit type 2B

NR2C, NMDAR subunit type 2C

PKA, cAMP-dependent protein kinase A

PKC, protein kinase C

PKMζ, atypical protein kinase C form zeta

PP2, 4-amino-5-(4-chlorophenyl)-7-(t- butyl)pyrazolo[3,4-d]pyramidine

GFX109203X, bisindolylmaleimide I

PPF, paired pulse facilitation

PPR, paired pulse ratio

SCH-23390, (R)-(+)-7-Chloro-8-hydroxy-3-methyl-1-phenyl-2,3,4,5-te trahydro-1H-3-benzazepine hydrochloride

SCH-39166, (6aS-trans)-11-Chloro-6,6a,7,8,9,13b-hexahydro-7-methyl -5H-benzo[d]naphth[2,1-b]azepin-12-ol hydrobromide

SKF-81297, R-(+)-6-Chloro-7,8-dihydroxy-1-phenyl-2,3,4,5-tetrahydro-1H-3-benzazepine hydrobromide

SR, striatum radiatum

SUB, subiculum

TBS, theta burst stimulation

TBS, tris-buffered saline

t-test, student’s t-test

VGCC, voltage-gated calcium channel

VTA, ventral tegmental area

ZIP, protein inhibitor of atypical protein kinase C form zeta

CHAPTER ONE

REVIEW OF DOPAMINE D1/5 RECEPTOR MODULATION IN THE HIPPOCAMPUS

Introduction:

Mesolimbic dopamine (DA) has been essential to the ability of organisms across species and throughout evolution to execute behaviors that require planning and to form and retain memories of emotional salience. The mesolimbic DA system is responsible for governing the motivation required to initiate behavioral output, and in conjunction with the nigrostriatal DA system, coordinates cognitive processing with motor function to produce goal-oriented behavior (Philpson 1979, Mogenson et al 1980, Berrige and Robinson 1998, Everitt et al 1999, Gardner and Ashby 2000). The mesolimbic DA system is composed of two projections originating from DA neurons in the ventral tegmental area (VTA): The mesoaccumbens projection terminates in the nucleus accumbens (NAc), while the mesocortical projection terminates the medial prefrontal (mPFC) and anterior cingulate corticies (Bannon and Roth, 1983). Upon release, DA modulates the limbic system and establishes associations

between emotional salience (reward or aversion) and environmental stimuli. Thus, modulation by DA allows organisms to plan behavioral strategies to approach rewarding, while avoiding aversive stimuli in the environment.

Anatomy: Hippocampus as part of the Limbic Circuit

The limbic system is a group of interconnected, evolutionarily conserved structures within the brain that mediate emotional behaviors (such as pleasure or fear) to environmental stimuli and are involved in memory formation surrounding emotionally salient events. Disruptions of DA signaling within the limbic system are characteristic of psychiatric disorders such as schizophrenia, addiction, and attention deficit disorder (Weinberger DR 1987, Gray et al 1991, Barkley RA 1998, Berger and Posner 2000, Nestler EJ 2005). Many pharmacological treatments for these diseases target DA to regulate limbic function.

The hippocampus is a key component of the limbic system, along with the amygdala (AMY), mPFC, NAc, thalamus, and hypothalamus. The hippocampus is required for spatial navigation, contextual memories, and consolidation of short-term into long-term memories (O'Keefe and Dostrovsky 1971, Squire et al 1984, Jarrard JE 1993). Area CA1 of the hippocampus receives excitatory glutamatergic input from the ehtorhinal cortex (EC) and sends excitatory glutamatergic projections via the subiculum to the NAc, AMY, mPFC, EC, hypothalamus, and septal nuclei (Fig. 1A). The hippocampus also receives DA

input from the ventral tegmental area (VTA) (Gasbarri et al 1997). This convergence allows the hippocampus to balance mesolimbic DA activity and limbic circuit output. Within the hippocampus, there exists a highly organized tri-synaptic circuit for information processing. Inputs from layer III of the EC send glutamatergic projections to granule cells in the dentate gyrus (DG), which send glutamatergic projections to CA3 pyramidal cells, terminating proximally on CA1 dendrites via the schaffer collaterals (SC) (Fig. 1B). A second, direct input from layer II of the EC terminates on distal dendrites of CA1 pyramidal neurons. Interactions between these direct and processed inputs gate the output of CA1 neurons and influence hippocampal information processing. Because of its highly organized circuitry, hippocampal SC-CA1 synapses have been used extensively in the study of cellular learning and memory.

Dopamine Receptor Subtypes and Distribution

DA exerts a strong influence in regulating limbic function, which it accomplishes by activation of DA receptors that occupy different anatomical and cellular distributions and are coupled to distinct signaling mechanisms. In area CA1 of the hippocampus, DA is released from the presynaptic terminals of VTA neurons that terminate in CA1 via the mesolimbic DA projection (Gasbarri et al 1997). DA diffuses across the synaptic cleft and binds to post-synaptic DA receptors on CA1 neurons. This causes both rapid and sustained cascades of

events that modulate the electrical, biochemical, translational, and transcriptional properties of the post-synaptic neuron.

Two families of DA receptors are distinguished based on their coupling to guianine nucleotide regulatory (G) proteins. The D1 receptor family (D1/5R) consists of D1 and D5 receptors and is positively coupled to adenylyl cyclase by G_s/G_o proteins, while the D2 receptor family contains the remaining D2, D3, and D4 subtypes and is negatively coupled to adenylyl cyclase by G_i proteins (Girault and Greengard 2004). The two receptor classes also differ in synaptic localization. DA neurons that terminate in the hippocampus and express D2 auto-receptors which serve to inhibit DA release, while post-synaptic CA1 pyramidal neurons express both D1 and D2 -type receptors (Baldessarini and Tarazi 1996, Hsu KS 1996, Tarazi and Baldessarini 1999). Both families of DA receptors have 7 transmembrane segments and are widely distributed throughout limbic structures, including the hippocampus (Girault and Greengard 2004, www.brainmap.org,).

Glutamate Receptor Subtypes and Distribution

While G-protein coupled receptors (GPCRs) primarily exert a slow modulatory influence on neuronal function, receptors that bind the amino acid glutamate have the ability to rapidly influence membrane potential and action potential output, in addition to exerting slower modulatory influences. Glutamate is the primary excitatory neurotransmitter in the central nervous system. It is

released by pyramidal cells within the hippocampus, and is responsible for transmitting processed hippocampal output by exciting neurons in other limbic regions. Two classes of glutamate receptors exist: Ionotropic glutamate receptors, which act as ligand-gated ion channels and depolarize the resting membrane potential, and metabotropic glutamate receptors (mGluRs), which are coupled to G-proteins and exert slower modulatory influences. Three types of ionotropic glutamate receptors are present in the hippocampus: Alpha-amino-3-hydroxy-5-methyl-4-isoxazolepropionic acid (AMPA) receptors, N-methyl D-aspartate (NMDA) receptors, and Kainate receptors (Sweatt JD 2003). Because of their involvement in synaptic plasticity, AMPA receptors (AMPARs) and NMDA receptors (NMDARs) will be discussed in detail.

AMPA receptors are responsible for rapid excitatory neurotransmission in the central nervous system. Four homologous alpha subunits (GluR1-GluR4) combine to form a tetrameric AMPA receptor complex (Mayer M 2005, Greger et al 2007). In the hippocampus, the predominant subunit compositions are GluR2/3 and GluR1/2 heteromers and GluR1 homomers, with each receptor subtype having unique electrophysiological properties. AMPA receptors that contain GluR2 have the property of inward rectification, which is a non-linearity in their current-voltage relationship that occurs at voltages greater than zero (Jonas P and Sackman B 1992). The rectification results from a lack of calcium permeability conferred by GluR2 subunits (Jonas P 1993). AMPA receptors that lack GluR2

subunits, however, are permeable to calcium, pass current in a linear manner, and are sensitive to polyamine block at depolarized voltages (Mayer M 2005). Each AMPA subunit binds one molecule of glutamate; with the channel passing more current as more glutamate is bound and rapidly desensitizing (Rosenmund et al 1998). AMPA receptor conductance and trafficking are modulated by phosphorylation, and phosphorylation of GluR1 has been extensively studied. GluR1 subunits contain phosphorylation sites at S845 (PKA), S831 (PKC/CamKII), S818 (PKC), and T840 (Banke et al 2000, Hayashi et al 2000, Boehm et al 2006, Delgado et al 2007). Phosphorylation at S845 increases channel open probability, membrane insertion, and has been implicated in LTD and de-depression (Banke et al 2000, Lee et al 2000). Phosphorylation at S831 increases single channel conductance and is associated with LTP and depotentiation, a process by which synapses that have undergone LTP revert towards their baseline response (Derkach et al 1999, Lee et al 2000). Phosphorylation at S818 is also involved in LTP, and de-phosphorylation at S818 has been implicated in LTD (Bohem et al 2006, Delgado et al 2007)

Like AMPA receptors, NMDA receptors bind glutamate; however they have properties that distinguish them from AMPA receptors. While AMPA receptors activate immediately upon glutamate binding, NMDA receptors contain a magnesium ion that blocks the channel pore at resting membrane potential (Sweatt DJ 2003). Membrane depolarization via AMPARs removes the

magnesium block, and when postsynaptic depolarization is coincident with presynaptic glutamate, NMDARs open and flux not only sodium and potassium, but calcium as well (Sweatt JD 2003). Because both pre- and post-synaptic activity are simultaneously required for NMDARs to open, they are considered molecular "coincidence detectors" that are essential to neuroplasticity (Sweatt JD 2003). Calcium flux through NMDARs activates numerous intracellular signaling cascades, leading to lasting modifications in synaptic strength.

The NMDA receptor is composed of four subunits; two NR1 subunits and two NR2 subunits. Eight NR1 subunits exist with NR1a-1 predominating in the hippocampus (Sweatt JD 2003). Of the four NR2 subunits, NR2A and NR2B are predominant in the hippocampus, with mostly NR2B at birth an increase in NR2A contribution towards adulthood (Dunah et al 1998, Cull-Candy et al 2001). NR1 subunits are phosphorylated by PKA and PKC at a number of sites, altering synaptic localization, membrane insertion, channel properties, and calcium permeability (Markram and Segal 1992, Raman et al 1996, Lu et al 1999, Lan et al 2001, Crump et al 2001, Skeberdis et al, 2006). NR2A and NR2B subunits can be also phosphorylated by PKA and PKC at a number of residues, modulating receptor localization and channel function (Chen and Roche 2007). Unlike the NR1 subunit, NR2A and NR2B subunits undergo extensive tyrosine phosphorylation by src and fyn, which increases NR2A and NR2B current and surface expression. In particular, fyn phosphorylates NR2B subunits at T1472

and increases NR2B surface expression (Kohr and Seeburg 1996, Dunah et al 1998, Zheng et al 1999, Nakazawa et al 2001, Takasu et al 2002).

Functional NMDARs in the adult hippocampus are composed of NR1/NR2A and NR1/NR2B homers and heteromeric NR1/NR2A/NR2B. NR2A and NR2B NMDA receptors differ in their electrophysiological properties, developmental expression, and pharmacological sensitivity. NR2A-NMDARs desensitize greatly and deactivate rapidly, while NR2B-NMDARs desensitize less and deactivate slowly (Cull-Candy et al 2001). NMDARs that contain NR2B subunits are selectively inhibited by the drug ifenprodil (Williams et al 1993). Ifenprodil reduces channel opening without changing single channel conductance, and was initially reported to bind NMDARs independently of channel opening, however dispute exists regarding its mechanism of action (Legendre and Westbrook 1991). More recent work indicates NMDAR antagonism by ifenprodil may be activity-dependent, however the complete binding site and mechanism of action of ifenprodil remain unknown (Williams 2001). Members of the glutamate receptor family are diverse, and the unique properties of AMPA and NMDA receptors underlie the ability of neurons to store memory of past activity at individual synapses within the hippocampus.

Glutamate Receptors and NMDAR-dependent Long-Term Potentiation

Neuroplasticity refers to the property of a neuron to modify its response to a given synaptic input. Depending on many factors in the electrical, chemical, and temporal environment, neurons can react to synaptic activation with a response that lessens or becomes larger. The latter is a process known as long-term potentiation (LTP). LTP is a persistent increase in synaptic strength following coincident high-frequency synaptic activation and postsynaptic membrane depolarization. LTP is widely accepted as the cellular correlate of learning and memory, and LTP underlies learning and memory exhibited at the level of behavioral output.

LTP can be divided into three phases: Induction, expression, and maintenance, with each of these phases utilizing unique properties of ionotropic glutamate receptors. LTP induction refers to events that occur transiently and trigger lasting potentiation. Because NMDARs require both synaptic glutamate and depolarized membrane potentials for activity, they detect coincident activation of both pre- and postsynaptic neurons and are necessary for LTP induction (Mueller et al 1988) Expression of LTP occurs when calcium influx through activated NMDARs triggers persistent biochemical signals that upregulate AMPAR number, function, and location, while maintenance of LTP occurs when upregulated AMPAR function persists persists (Kaur et al 1988, Muller et al 1988, Muller and Lynch 1988, Lu et al 2001). Thus, when simultaneous release of synaptic glutamate and postsynaptic depolarization occur

in a particular temporal pattern, the connections between two neurons can be persistently modified. Built from foundations on unique properties of AMPA and NMDA receptors, neuroplasticity such as LTP stabilizes neuronal responses to environmental stimuli and directs future behavioral output.

Interactions between Dopamine D1/5 Receptors and NMDA Receptors

Because LTP induction occurs through NMDARs and NMDARs are modulated by D1/5Rs, D1/5R activation has the potential to modulate the induction of LTP. NMDAR modulation by D1/5R activation been well characterized. D1/5R activation increases NR1 and NR2B surface expression in striatal slices and cultures, in prefrontal cortical cultures, and in VTA slices, with only one study indicating an increase in NR2A (Dunah and Standeart 2001, Dunah et al 2004, Hallett et al 2006, Schilstrom et al 2006, Gao and Wolf 2008). Some studies found D1/5R induced increases in surface expression were accompanied by an increase in p-T1472, a residue on NR2B that is phosphorylated by fyn tyrosine kinase (Dunah et al 2004, Hallett et al 2006, Gao and Wolf 2008) while another study found an increase in PKA-dependent NR2B surface expression following D1/5R activation without (Schilstrom et al 2006).

D1/5R modulation of NMDAR currents has also been extensively studied. D1/5R activation potentiates NMDAR currents via PKA and src-tyrosine kinases (Yang 2000, Whitmann et al 2005, Schilstrom et al 2006), and further evidence

has been presented for a physical interaction between NR2A subunits and D1 receptors that inhibits NMDA currents (Cepeda and Levine 2006). Additionally, we have reported D1/5R-induced potentiation of NMDAR currents occurs via NR2B subunits, while D1/5R-inhibition of NMDAR currents occurs through NR2A subunits (Varela et al, 2009). These results are summarized in Table 1.1.

Interactions between Dopamine D1/5 Receptors and AMPA Receptors

Because LTP expression occurs through AMPARs and AMPARs are modulated by D1/5Rs, D1/5R activation has the potential to modulate the expression of LTP. D1/5R activation increases AMPA currents in hippocampal CA1 and NAc neurons through a mechanism requiring PKA (Prince et al 1999, Yang 2000). Surface expression and synaptic incorporation of GluR1 subunits is increased following D1/5R activation in cultured hippocampal, VTA, NAc, and PFC neurons, and is accompanied by an increase in PKA phosphorylation at S-845 GluR1 (Wolf et al 2004, Gao et al 2006, Gao et al 2007). In hippocampal and PFC-VTA co-cultures, the increase in GluR1 surface expression is NMDAR-dependent (Gao et al 2006, Gao and Wolf 2007), and in the PFC, the increase in GluR1 synaptic incorporation requires CamKII in addition to PKA (Gao et al 2006). These results are summarized in Table 1.2. D1/5R activation modulates both AMPAR and NMDAR phosphorylation, cellular localization, and current, which gives D1/5Rs the ability to influence multiple stages of synaptic plasticity.

Modulation of Synaptic Plasticity by Dopamine D1/5 Receptors

Synaptic plasticity, the cellular correlate of learning and memory, is extensively modulated by D1/5R activation. Both *in vivo* and *in vitro*, D1/5 agonists enhance the magnitude of LTP (Otmakhova and Lisman 1996, Lemon and Manahan-Vaughn 2006). Mice lacking the D1 receptor do not express late-phase LTP *in vitro*, and D1/5R antagonists decrease the magnitude of LTP *in vivo* (Matthies et al 1997, Lemon and Manahan-Vaughn 2006). Moreover, D1/5R agonists inhibit depotentiation and reverse long-term depression (LTD) (Otmakhova and Lisman 1998, Mockett et al 2007). It has been reported D1/5R activation produces a slow-onset potentiation in the absence of LTP-inducing stimuli, yet the precise mechanism has not been described (Huang and Kandel 1995, Navakkode et al 2007). Collectively, this data shows that D1/5R activation promotes the maintenance of increased synaptic strength in response to DA release (Table 1.3).

Dopamine D1/5R Modulation of Hippocampal Behaviors in Rodents

Consistent with modulation of hippocampal synaptic plasticity by D1/5R activation, a number of learning and memory behaviors mediated by the hippocampus are modulated by D1/5R signaling. Intra-CA1 injections of D1/5R

agonist facilitate radial maze learning, while spatial memory measured by a Barnes circular maze is also enhanced by systemic D1/5R activation (Packard and White 1991, Bach et al 1999). In addition, memory consolidation measured during a step-down inhibitory avoidance task is enhanced following intra-CA1 D1/5R agonist injections (Bernabeau et al 1997). Inhibiting D1/5R signaling with 6-OH-DA lesion impairs spatial learning in the Morris water maze, while genetic deletion of the D1R produces a similar impairment (Gasbarri et al 1996, Granado et al 2007). These studies are summarized in Table 1.4.

As D1/5R activation facilitates learning and memory at the level of individual synapses, it also produces facilitation of learning and memory at the level of behavioral output. Pathologies in DA signaling may lead to disturbances in behavioral cognition, and have been implicated in a number of psychiatric disorders, such as schizophrenia and addiction. Understanding D1/5R modulation of excitatory neurotransmission may reveal novel therapeutic strategies to treat psychiatric disorders.

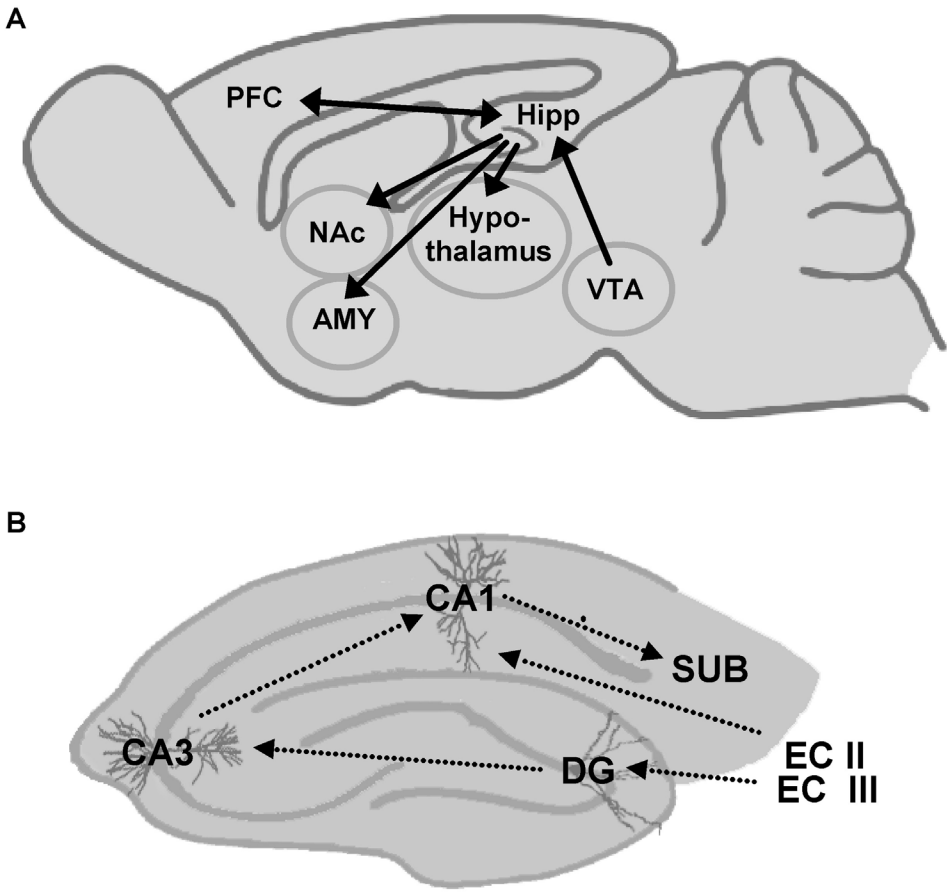

Figure 1.1: Limbic and Hippocampal Cicuitry

A) Location of the hippocampus within limbic circuitry. The hippocampus receives glutamatergic innervation from the entorhinal cortex and DA input from the VTA. The hippocampus sends glutamatergic projections to the NAc, amygdala, PFC, entorhinal cortex, hypothalamus, and septal nuclei. B) Circuitry within the hippocampus. Tri-synaptic pathway: Pyramidal cells in layers II/III of entorhinal cortex project to the dentate gyrus (DG). Dentate granule cells project to CA3 via mossy fibers. CA3 pyramidal cells project to proximal CA1 pyramidal cell dendrites via the Schaffer Collaterals (SC). Direct cortical pathway: Layers IV/V of the entorhinal cortex project directly onto distal CA1 pyramidal dendrites.

Table 1.1: Effect of D1/5R Activation on NMDAR Function						
D1/5 Activation	**Effect on NMDA EPSC**	**Surface Expression**	**Phosphorylation**	**Kinase Required**	**Prep**	**Ref.**
SKF-82958	n/a	Increase NR2B	increase P-T1472 NR2B	Tyrosine Kinase	Striatal cultures	Hallett et al 2006
SKF-82958	n/a	Increase NR2A Increase NR2B	Increase total p-T-NR2B	Tyrosine Kinase (Fyn)	Striatal tissue	Dunah et al 2004
Cocaine	n/a	Increase NR2B	No change p-T1472 NR2B	PKA	VTA slices	Schilstrom et al 2006
SKF-81297	n/a	Increase NR2B	Increase p-T1472 NR2B	PKA	PFC cultures	Gao and Wolf 2008
SKF-81297	Enhance	n/a	n/a	PKA	Hipp. Slice	Yang 2000
SKF-82958	Enhance	n/a	n/a	Fyn PKA	Hipp. Slice	Whitmann et. al. 2005
Cocaine + D2 antagonist	Enhance	n/a	n/a	PKA	VTA slice	Schilstrom et al 2006
SKF-81297	Enhance NR2B InhibitNR2A	n/a	n/a	n/a	Hipp. Slice	Varela et al 2008

Table 1.1: Effect of D1/5R activation on NMDAR function

Table 1.2: Effect of D1/5R Activation on AMPAR Function				
	AMPA EPSCs	**AMPA subunit phosphorylation**	**AMPA surface expression**	**AMPA synaptic incorporation**
Effect of D1/5R activation	Potentiation	Increase GluR1 P-Ser845 No change P-Ser831	Increase GluR1	Increase GluR1
Mechanism	PKA	PKA	PKA	PKA and CamKII
Protein Synth. Dependent?	N/A	N/A	no	no
Requires NMDAR?	No	no	Yes	N/A
Area / Prep.	Hipp. CA1, NAc	NAc	VTA – PFC co-cultures, Hipp. CA1 cultures	Hipp. CA1 cultures
Ref.	Yang 2000 Prince et al 1999	Wolf 2004	Gao and Wolf 2007 Gao et al 2006	Gao et al 2006

Table 1.2 Effect of D1/5R activation on AMPAR function

Table 1.3: Effect of D1/5R Activation on Synaptic Plasticity					
Plasticity	**D1/5 Effect**	**Manipulation**	**Induction**	**Prep**	**Ref**
LTP	**Enhance**	D1/5 Agonist and antagonist	HFS	In Vivo SC-CA1	Lemon and Vaughn 2006
		D1/5 Agonist	HFS	Acute Slice SC-CA1	Otmakhova and Lisman 1996
		D1 KO Mice	HFS	Acute Slice SC-CA1	Mathies et al 1997
		D1 KO Mice	HFS	Acute Slice SC-CA1	Granado et al 2007
Depotentiation	**Inhibit**	D1/5 Agonist	LFS	Acute Slice SC-CA1	Otmakhova and Lisman 1998
LTD	**Reverse**	D1/5 Agonist	LFS	Acute Slice SC-CA1	Mockett et al 2007
Synaptic Potentiation	**Induce**	D1/5 Agonist	N/A	Acute Slice SC-CA1	Huang and Kandel 1995 Navakkode et al 2007

Table 1.3: Effect of D1/5R activation on synaptic plasticity

Table 1.4: Effect of D1/5R Activation on Hippocampal Behavior				
Task Measured	**Effect on learning / memory task**	**Drug**	**Method**	**Ref**
Learning	↑ Radial Maze performance	SKF-38393 (5 ug)	Dorsal Intra-CA1 injection	Packard and White 1991
Memory consolidation	↑ Step-down inhibitory avoidance	SKF-38393 (7.5 ug)	Dorsal Intra-CA1 injection	Bernabeu et al 1997
Spatial Memory	↑ performance of aged mice on Barnes circular maze	SKF-38393 (6 mg/kg)	IP injection	Bach et al 1999
Spatial memory	↓performance on Morris water maze	6-OH-DA	CA1 / SUB injection	Gasbarri et al 1996
Spatial Memory	↓performance on Morris water maze	NA	D1 KO Mice	Granado et al 2007

Table 1.4: Effect of D1/5R activation on hippocampal behavior

CHAPTER TWO

MECHANISM OF DOPAMINE D1/5 RECEPTOR-MEDIATED ENHANCEMENT OF LONG-TERM POTENTITION

Summary:

While the effects of D1/5R activation on glutamate receptors underlying synaptic plasticity have been characterized, the mechanism responsible D1/5R LTP potentiation remains unknown. We report that brief D1/5R activation prior to LTP induction enhances LTP in the hippocampus through a post-synaptic mechanism requiring NR2B-NMDARs, PKA, and src-family tyrosine kinase signaling and occurs independently of NR2A-NMDARs and fyn tyrosine kinase. Determining a mechanism for D1/5R modulation of LTP within the hippocampus will help clarify the role of DA in hippocampal behaviors and in diseases of aberrant DA signaling in the hippocampus.

Introduction:

D1/5R activation enhances cognition during hippocampal-dependent learning and memory behaviors (Packard and White 1991, Gasbarri et al 1996,

Bernabeu et al 1997, Bach et al 1999). Synaptic plasticity, a cellular correlate of learning, is modulated by changes in D1/5R signaling as well. Both *in vivo* and *in vitro*, D1/5R activation increases hippocampal long-term potentiation (LTP), while decreasing D1/5R signaling reduces hippocampal LTP (Otmakhova and Lisman 1996, Matthies et al 1997, Williams et al 2006, Lemon and Manahan-Vaughn 2006, Granado et al 2008). Additionally, D1/5R activation inhibits depotentiation, reverses long-term depression (LTD), and induces late-phase potentiation (Otmakhova and Lisman 1998, Mockett et al 2007, Navakkode et al 2007). Collectively, this data suggests D1/5R activation biases glutamatergic neurotransmission towards potentiation. While the effects of D1/5R activation on synaptic plasticity have been characterized, the mechanism responsible for D1/5R potentiation of LTP remains unknown. Determining a mechanism for D1/5R modulation of LTP within the hippocampus may clarify the role of DA in hippocampal behaviors and in diseases of aberrant DA signaling in the hippocampus.

Electrophysiological and biochemical studies found that D1/5R activation potentiates NMDA EPSCs in CA1 pyramidal neurons and selectively increases both src-family kinase phosphorylation and surface expression of NR2B NMDAR subunits (Yang 2000, Dunah and Standaert 2001). Additionally, both D1/5R potentiation of NMDAR currents and D1/5R-mediated increases in NR2B surface expression require the activity of PKA and src-family tyrosine kinase (Hatt et al

1995, Zheng et al 1999, Chen et al 2002, Dunah et al 2004, Tseng and O'Donnell 2004, Wirkner 2004, Whitman et al 2005, Hallett et al 2006, Gao and Wolf 2008).

NMDARs are critical to the induction of LTP (Sarvey et al 1989). Because it is known that NMDAR current is increased following D1/5R activation, we hypothesized that D1/5R enhancement of LTP occurs by enhancing LTP induction through NMDARs. Additionally, it is known that D1/5R potentiation of NMDARs requires NR2B subunits, PKA and src-family kinases. We further hypothesized that NR2B NMDARs, PKA, and src-family kinases are required for D1/5R enhancement of LTP. Using synaptic field recordings in acute hippocampal slices, we pharmacologically manipulated intracellular signaling cascades and present evidence that D1/5R enhancement of LTP occurs through a pathway requiring NR2B NMDARs, PKA, and src-family kinases.

Experimental Procedures:

Acute Hippocampal Slice Preparation

Adult 6-12 wk. C57/BL6 mice (Jackson Labs) were anesthetized with isoflurane, rapidly decapitated, and brains were immediately placed in ice-cold cutting solution (in mM): sucrose 254, dextrose 10, NaH_2PO_4 1.25, $NaHCO_3$ 24, $CaCl_2$*2(H_2O) 2, $MgSO_4$*7(H_2O) 2, KCl 3) saturated with carbogen gas (95% O_2, 5% CO_2). 400 μm para-transverse hippocampal slices were made using a

vibrating tissue slicer (Vibratome, St. Louis, MO) and transferred to a holding chamber containing room temperature ACSF. Slices were allowed to recover at least one hour before use.

Synaptic Field Recording

Acute hippocampal slices were placed in a RC-26 submersion recording chamber (Warner, Hamden, CT) at room temperature. A stimulating electrode (CED255, FHC, Bowdoin, ME) was placed in the Schaffer Collaterals near CA2 and a glass recording electrode (1-2 MΩ) filled with ACSF was placed in the Schaffer Collaterals in CA1. Field responses were elicited with a biphasic stimulus delivered via a stimulus isolator (BSI-950, Dagan, Minneapolis, MN) and stimulation intensity was adjusted until field responses were within 30-60% of the linear response range. Field responses were recorded with an Axoclamp 2B amplifier (Axon instruments, Foster City, CA) and digitized using an ITC-18 digital/analog converter (Instrutech, Port Washington, NY). Responses were stored on a Dell PC. Data acquisition and analysis was conducted using custom software in Igor Pro (Wavemetrics).

Drugs and Solutions

Artificial cerebrospinal fluid (ACSF) for slice experiments consisted of (in mM); NaCl 125, KCl 2.5, NaH_2PO_4 1.25, $MgCl_2$*6(H_2O) 1, $CaCl_2$*2(H_2O) 2,

$NaHCO_3$ 25, and Dextrose 25. All drugs were aliquoted and stored at -20°C. Fresh drug aliquots were used for each experiment. To activate D1/5R receptors SKF-81297 (Tocris) in DMSO was added to ACSF to a final concentration of 10 μM. To block NR2B NMDARS, Ifenprodil (Tocris) in ethanol was used at 3 μM. To block $GABA_A$ signaling, picrotoxin (Sigma-Aldrich) in ethanol was used at 50 μM. To block L-type VGCCs, nimodipine (Tocris) was used at 10 μM. To inhibit PKA signaling, H89 (Tocris) in DMSO was used at 10 μM. To inhibit src-family tyrosine kinases, PP2 (Tocris) in DMSO was used at 10 μM.

Statistics and analysis:

Experimental conditions were interleaved and group comparisons were made using unpaired two-tailed student's t-tests. Results were considered statistically significant if P value was less than 0.05.

Results:

D1/5R-mediated enhancement of E-LTP requires NR2B NMDARs

As reported by others, we found that brief D1/5R activation produced an enhancement of LTP (Figure 2.1A, 30.3 ± 9.8% above control LTP, n = 7 control, n = 7 SKF-81297, $p < 0.05$) under our experimental conditions. To confirm that D1/5R works by modulating post-synaptic signaling and not through effects on

presynaptic neurotransmitter release, we used a paired pulse ratio (PPR) measurement and found no D1/5-induced changes during SKF-81297 application (Figure 2.1B) or 30 minutes after SKF-81297 washout (supplemental Figure 2.1).

We next sought to determine the role of NMDAR subtypes in the effect of D1/5R activation on LTP using extracellular synaptic field recording. Responses were elicited by single pulse stimulation of Schaffer Collateral (SC) projections to the apical dendrites of area CA1 pyramidal neurons in hippocampal slices from adult (6-12 weeks of age) mice. It has previously been shown that D1/5R activation can decrease inhibitory $GABA_A$ signaling and can increase currents through L-type voltage-gated calcium channels (VGCCs; Byrnes et al 1997, Galarraga et al 1997, Hernandez-Lopez et al 1997, Liu et al 2004, Hernández-Echeagaray et al 2006). To rule out such mechanisms, we included picrotoxin (50 μM) and nimodipine (10 μM) in the bath of all experiments to block $GABA_A$ receptors and L-type VGCCs respectively. Following baseline recording, the selective D1/5R agonist SKF-81297 (10 μM) was bath-applied for 10 minutes prior to theta-burst stimulation (TBS, 3 trains of 10 bursts delivered every 15 seconds, each burst consisting of 4 pulses at 100Hz, every 200 ms) induced LTP.

SKF-81297 was washed out immediately following TBS. In all experiments, early-phase LTP was measured 30-40 minutes after TBS and control and drug-treated experiments were interleaved to avoid systematic bias.

To determine if NR2A-NMDARs were necessary for D1/5R enhancement, we tested the LTP response in slices from homozygous NR2A-deficent mice (a gift from Drs. Masayoshi and Lovinger) and found LTP enhancement by D1/5R activation intact (Figure 2.1C, open circles, 23.5 ± 7.3%, n = 7 control, n = 5 SKF-81297, $p < 0.01$). LTP was prevented by ifenprodil (3 μM) in these mice (Figure 1C, grey circles, n = 5, $p > 0.05$), suggesting NR2B NMDARs were the only subtype available.

Furthermore, wild-type mice with intact NR2A function show positive modulation of NR2B-NMDARs following D1/5R activation (Dunah and Standaert 2001, Dunah et al 2004, Hallett et al 2006, Gao and Wolf 2008) we hypothesized that D1/5R activation would increase NR2B-NMDAR function during LTP induction and result in enhanced LTP. Under conditions of NR2B blockade by the selective NR2B antagonist ifenprodil (3 μM), we found no significant SKF-81297-induced enhancement of LTP between control and drug experiments (Figure 1D, 2.2 ± 8.5%, n = 6 control, n = 7 SKF-81297, $p > 0.05$). These results indicate a necessary role for NR2B and not NR2A NMDARs in D1/5R enhancement of LTP.

D1/5R enhancement of LTP requires Src tyrosine kinase and PKA activity

Previous studies indicate that following D1/5R activation, the src family tyrosine kinase fyn phosphorylates NR2B NMDARs at T1472 leading to

increased NR2B surface expression and NMDA currents (Dunah and Standaert 2001, Dunah et al 2004, Whitman et al 2005, Hallett et al 2006, Gao and Wolf 2008). To determine if D1/5R activation modulates NR2B function via fyn to enhance LTP, we tested the LTP response in slices made from fyn knockout mice (Jackson Labs) and found normal D1/5R enhancement (Figure 2.2A, 36.1 ± 12.5%, n = 9 control, n = 11 SKF-81297, $p < 0.05$). It is possible that the continued ability of D1/5R activation to enhance LTP in fyn deficient mice is due to compensation by another src-family kinase. Consistant with this, we tested the LTP response in the presence of the broad src-family kinase inhibitor PP2 (10 μM) and found no LTP enhancement following D1/5R activation (Figure 2.2B, 2.9 ± 10.5, n = 8 control, n = 7 SKF-81297, $p > 0.05$).

A role for PKA in D1/5R-mediated enhancement of NMDAR currents has previously been reported (Whitman et al 2005, Yang 2000). To determine if PKA activity was required for D1/5R enhancement of LTP, we tested the LTP response in the presence of the PKA inhibitor H89 (10 μM) and found no LTP

enhancement following D1/5R activation (Figure 2.2C, 9.4 ±12.6%, n = control, n = 6 SKF-81297, $p > 0.05$). These results indicate that potentiation of LTP by D1/5R activation, like D1/5R potentiation of NMDAR currents, requires PKA and src-family kinase.

Discussion:

D1/5R activation during TBS enhances the magnitude of LTP in hippocampal SC-CA1 synapses (Otmakova and Lisman 1996), yet the precise mechanism for this remains unknown. Illuminating the effects of D1/5R activation on LTP is relevant to understanding the broad cognitive-enhancing properties of D1/5R activation on behaviors mediated by the hippocampus and other brain regions, which rely on modulation of synaptic plasticity (Packard and White 1991, Bernabeu et al 1997, Bach et al 1999, Gasbarri et al 1996). Based on evidence for positive modulatory interactions between D1/5R activation and NR2B-NMDARs (Dunah and Standaert 2001, Dunah et al 2004, Hallett et al 2006, Gao and Wolf 2008) and evidence supporting a role for NR2B in LTP (reviewed in Yashiro and Philpot 2008) we hypothesized that NR2B-NMDARs mediated the enhancing effect of D1/5R activation on LTP. Since NMDARs are necessary for LTP induction, we sought to determine which NMDA subunit was responsible for the effect of D1/5R activation on LTP. We found that NR2B-NMDARs were required for D1/5R enhancement of LTP. Further evidence suggested a role for PKA and src-family kinases in positive D1/5R modulation of NR2Bs (Hatt et al 1995, Zheng et al 1999, Chen et al 2002, Dunah et al 2004, Tseng and O'Donnell 2004, Wirkner 2004, Whitman et al 2005, Hallett et al 2006, Gao and Wolf 2008), and we hypothesized that D1/5R modulation of LTP

requires PKA and src-family tyrosine kinases, in particular fyn kinase. While we showed that indeed PKA and src-family kinases are required for D1/5R enhancement of LTP, we did not find a role for fyn tyrosine kinase as suggested by previous studies. The continued ability of D1/5R activation to enhance LTP in fyn KO mice may be due to compensation by another src-family kinase in the knockout animal. Despite the potential role of D1/5R modulation of synaptic plasticity in mediating hippocampal behaviors and in neuropsychiatric disorders, a mechanism for the effect of D1/5R modulation of synaptic plasticity remained uncharacterized. Our novel findings that D1/5R activation potentiates LTP through a NR2B, PKA, and src-family kinase dependent pathway may have future therapeutic implications in memory and in the treatment of neuropsychiatric disorders resulting from aberrant dopamine function in the hippocampus.

Conclusion:

We conclude that brief D1/5R activation prior to LTP induction in SC-CA1 of the hippocampus leads to enhanced LTP in the absence of changes in inhibitory signaling or L-type VGCCs through a post-synaptic mechanism. Using manipulation of synaptic field recordings in acute hippocampal slices with pharmacological inhibitors and knockout mice, we found D1/5R enhancement of LTP required NR2B-NMDARs, PKA, and src-family kinases, and does not

require NR2A-NMDARs or fyn tyrosine kinase. This novel finding is relevant to understanding the broad cognitive enhancing properties of D1/5R agonists, and to understanding neuropsychiatric disorders such as schizophrenia and addiction.

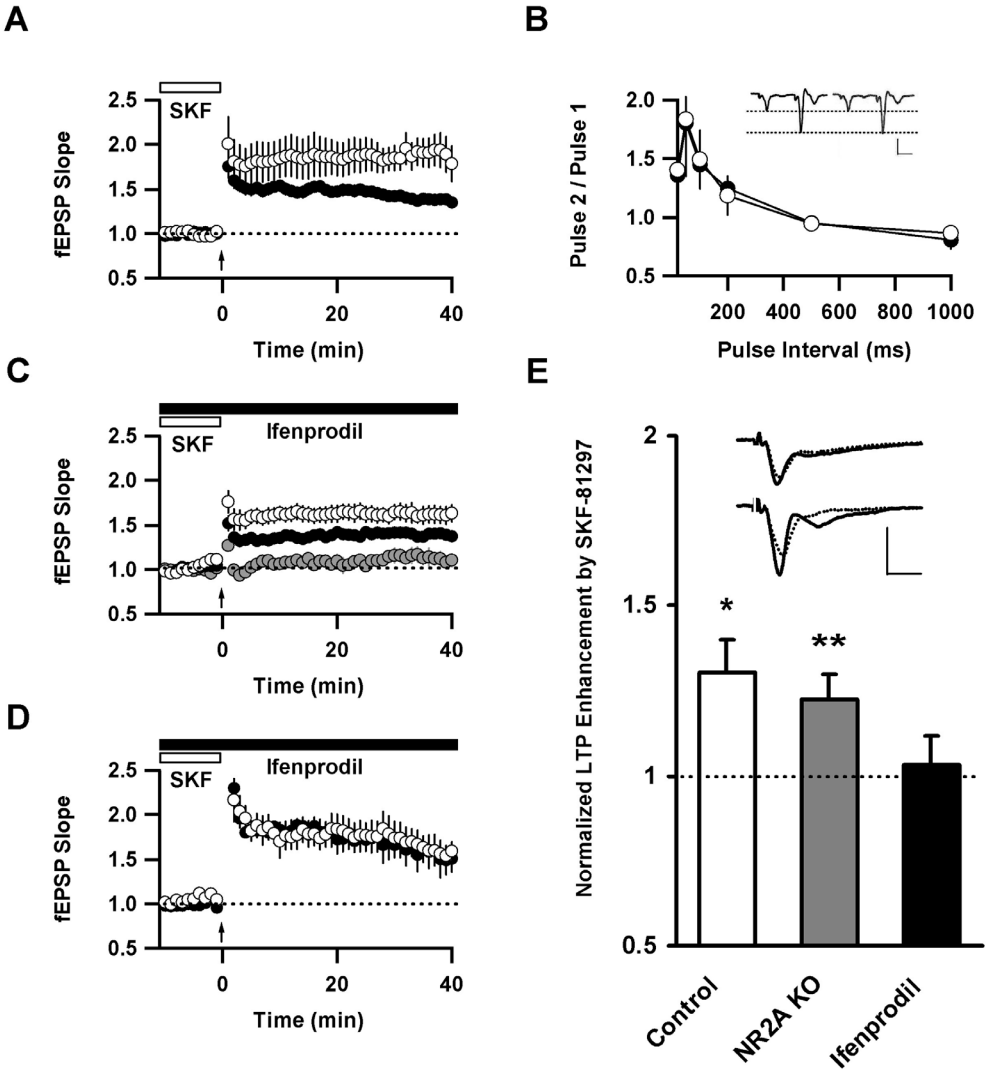

Figure 2.1: D1/5R potentiation of LTP requires NR2B-NMDARs. A) D1/5R activation enhances LTP. For all panels: filled circles, control; open circles, SKF-81297; arrow, LTP induction by 30 TBS; open bar, SKF-81297. B) SKF-81297 does not change paired pulse facilitation. Inset, representative paired pulse response for 50 ms. Scale, y-axis 1 mV, x-axis 10 ms. C) NR2A receptors are not required for D1/5 enhancement of LTP. Grey circles, ifenprodil. D) Ifenprodil blocks D1/5R enhancement of LTP. Closed bar, ifenprodil. E) Bar graph representing enhancement of LTP by SKF-81297. Top inset, representative field response during control LTP experiment. Bottom inset, representative field

response with D1/5R activation prior to LTP induction. Scale: y-axis 1 mV, x-axis 5 ms.

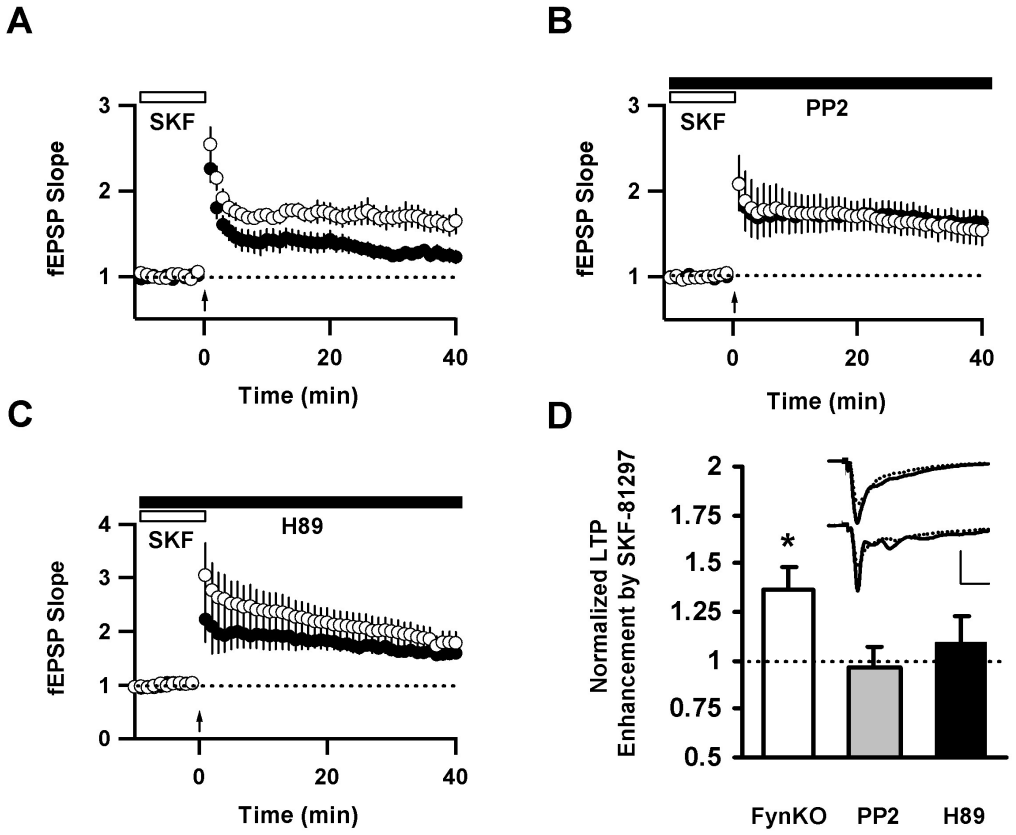

Figure 2.2: D1/5R potentiation of LTP requires Src-family kinase and PKA activity. A) D1/5R enhancement of LTP is present in fyn knockout mice. For all panels: filled circles, control; open circles, SKF-81297; arrow, LTP induction by 30 TBS; open bar, SKF-81297. B) The src-family tyrosine kinase inhibitor PP2 blocks D1/5R enhancement of LTP. Closed bar, PP2. C) The PKA inhibitor H89 blocks D1/5R enhancement of LTP. Closed bar, H89. D) Bar graph representing enhancement of LTP by SKF-81297. Top inset, representative field response during control LTP experiment. Bottom inset, representative field response with D1/5R activation prior to LTP induction. Scale: y-axis 1 mV, x-axis 5 ms.

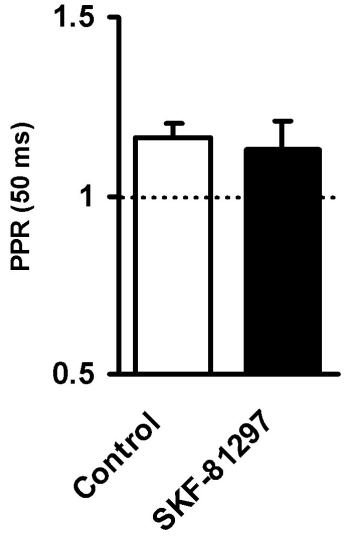

Supplemental Figure 2.1. Paired pulse ratio (50 ms inter-stimulus interval) is not changed following 30 min. washout of SKF-81297.

CHAPTER THREE

D1/5R ACTIVATION INDUCES E-LTP IN THE ABSENCE OF THETA-BURST STIMULATION AND OCCLUDES D1/5R ENHANCEMENT OF LTP

Summary:

Using field recordings in acute hippocampal slices, we present evidence that brief D1/5R activation produces a delayed potentiation of synaptic field responses with a similar time scale to that for D1/5R enhancement of LTP. We found that potentiation by D1/5R activation occluded D1/5R enhancement of LTP, and that LTP occluded D1/5R potentiation. This evidence indicates that D1/5R enhancement of LTP and D1/5R potentiation of synaptic responses are a result of the same phenomenon.

Introduction:

Previous work has shown an NMDA-dependent enhancement of dopamine on synaptic field responses at SC-CA1 synapses and a late-phase, stimulation-dependent enhancement of synaptic field responses that is not expressed until

hours after D1/5R activation (Huang and Kandel 1995, Kaphzan et al 2006, Navakkode et al 2007). Because D1/5R activation potentiates AMPAR current and increases AMPAR phosphorylation and surface expression (Prince et al 1999, Yang 2000, Wolf et al 2004, Gao and Wolf 2007, Gao et al 2006), we sought to address the hypothesis that D1/5R activation enhances LTP by modulating AMPARs during LTP expression rather than by modulating NMDARs during LTP induction. Although we saw no effect of SKF-81297 on baseline synaptic transmission, we sought to determine if, in the absence of TBS, D1/5R activation could affect the field response at a time point corresponding to our LTP measurements. Using field recordings in acute hippocampal slices, we present evidence that brief (10 min.) D1/5R activation produces a delayed potentiation of synaptic field responses with a similar time scale to that for D1/5R enhancement of LTP. Because D1/5R enhancement of LTP is occluded by D1/5R potentiation and both share a similar time course, we suggest that D1/5R enhancement of LTP results from the expression of D1/5R potentiation following TBS and not through modulation of LTP induction during TBS.

Experimental Procedures:

Drugs and Solutions

Artificial cerebrospinal fluid (ACSF) for slice experiments consisted of (in mM); NaCl 125, KCl 2.5, NaH_2PO_4 1.25, $MgCl_2$*6(H_2O) 1, $CaCl_2$*2(H_2O) 2, $NaHCO_3$ 25, and Dextrose 25. All drugs were aliquoted and stored at -20°C. Fresh drug aliquots were used for each experiment. To activate D1/5R receptors SKF-81297 (Tocris) in DMSO was added to ACSF to a final concentration of 10 µM.

Acute Slice Preparation:

Adult 6-12 wk. C57/BL6 mice (Jackson Labs) were anesthetized with isoflurane, rapidly decapitated, and brains were immediately placed in ice-cold cutting solution (in mM): sucrose 254, dextrose 10, NaH_2PO_4 1.25, $NaHCO_3$ 24, $CaCl_2$*2(H_2O) 2, $MgSO_4$*7(H_2O) 2, KCl 3) saturated with carbogen gas (95% O_2, 5% CO_2). 400 µm para-transverse hippocampal slices were made using a vibrating tissue slicer (Vibratome, St. Louis, MO) and transferred to a holding chamber containing room temperature ACSF. Slices were allowed to recover at least one hour before use.

Field Potential Recording:

Acute hippocampal slices were placed in a RC-26 submersion recording chamber (Warner, Hamden, CT) at room temperature. A stimulating electrode (CED255, FHC, Bowdoin, ME) was placed in the Schaffer Collaterals near CA2

and a glass recording electrode (1-2 MΩ) filled with ACSF was placed in the Schaffer Collaterals in CA1. Field responses were elicited with a biphasic stimulus delivered via a stimulus isolator (BSI-950, Dagan, Minneapolis, MN) and stimulation intensity was adjusted until field responses were within 30-60% of the linear response range. Field responses were recorded with an Axoclamp 2B amplifier (Axon instruments, Foster City, CA) and digitized using an ITC-18 digital/analog converter (Instrutech, Port Washington, NY). Responses were stored on a Dell PC. Data acquisition and analysis was conducted using custom software in Igor Pro (Wavemetrics). Group comparisons were made using paired or unpaired t-tests where appropriate.

Results:

D1/5R activation induces E-LTP of synaptic responses in the absence of theta-burst stimulation

We report that brief SKF-81297 application induces early-phase potentiation of synaptic field responses (Figure 3.1A, 31.1 ± 1.8%, $n = 8$, $p < 0.001$). Perfusion of vehicle produced no change in the magnitude of field response (Figure 3.1A, $n = 5$, $p > 0.05$) nor did application of SKF-81297 in the presence of the D1/5R antagonist SCH-23390 (10 μM, Figure 3.1B, $n = 5$, $p >$

0.05). SKF-81297 also induced potentiation in the absence of picrotoxin (Supplemental Figure 3.1, 33.9 ± 6.5%, n = 4, $p < 0.05$). While previous work at SC-CA1 synapses has shown that dopamine produces NMDA-dependent enhancement of synaptic field responses and that D1/5R activation induces late-phase, stimulation-dependent enhancement of synaptic field responses (Huang and Kandel 1995, Kaphzan et al 2006, Navakkode et al 2007), our report is the first showing early-phase D1/5R-induced potentiation. Although we saw no effect of SKF-81297 on baseline synaptic transmission after 10 minutes during LTP experiments, we sought to determine if, in the absence of TBS, D1/5R activation could affect the field response at a time point corresponding to our LTP measurements. As a positive control for SKF-81297 activity, SKF-81297-only experiments were interleaved and monitored for potentiation and all experiments were conducted in the presence of picrotoxin (50 μM) unless otherwise stated. After baseline recording, SKF-81297 (10 μM) was bath-applied for 10 minutes and the field response was measured 30-40 minutes after SKF-81297 washout. The effect was similar in magnitude and time scale to that of SKF-81297 on LTP, raising the possibility that D1/5R enhancement of LTP occurs during LTP expression rather than LTP induction.

LTP induction occludes D1/5R potentiation and D1/5R potentiation occludes D1/5R enhancement of LTP

We next sought to determine if potentiation by D1/5R activation and potentiation by TBS share similar mechanisms and if D1/5R enhancement of LTP results from D1/5R potentiation. To determine if LTP induction occluded D1/5R potentiation, LTP was induced with TBS and 30 minutes after LTP induction, SKF-81297 (10 μM) was applied for 10 minutes. Synaptic responses were monitored for another 40 minutes for further enhancement following D1/5R activation. Control LTP experiments with were interleaved with drug LTP experiments. When SKF-81297 was applied during LTP expression (40 minutes post-TBS), no effect of D1/5R activation on synaptic responses was observed (Figure 3.2A, 0 ± 4.8%, n = 5, $p > 0.05$). This indicates that potentiation by TBS and D1/5R activation may share a similar mechanism, and it is possible that this mechanism is saturated by LTP induction which blocks further modulation by D1/5R activation.

To determine if D1/5R potentiation was responsible for D1/5R enhancement of LTP, we induced potentiation with SKF-81297 (Figure 3.2B inset) and after expression of D1/5R potentiation stabilized, LTP was induced with TBS. No difference in magnitude of LTP was found between control and SKF-81297 conditions (Figure 3.2B, 92.5 ± 8.1% control, 93.2 ± 9.7% SKF-81297, n = 8 control, n = 5 SKF-81297, $p > 0.05$), likely because D1/5R potentiation had already been expressed. TBS still induced potentiation of D1/5R potentiated responses, possibly because D1/5 activation did not saturate the

induction mechanism as did LTP. From our results, we conclude that D1/5R potentiation and LTP may share a similar mechanism and that inducing D1/5R potentiation prior to LTP induction with TBS occludes D1/5R enhancement of LTP., suggesting that D1/5R enhancement of synaptic field response and D1/5R enhancement of LTP may be a result of the same phenomenon.

Discussion:

We reported that brief D1/5R activation produces a delayed, sustained enhancement of synaptic responses in the absence of theta burst stimulation. Further, we showed that D1/5R activation potentiates both LTP and synaptic responses with similar time courses and similar magnitudes of potentiation. Although a late-phase (>120 min), synapse-specific, protein synthesis-dependent form of D1/5R potentiation has previously been reported (Huang and Kandel 1995, Navakkode et al 2007), our description is the first to report an early-phase D1/5R potentiation and the first to provide a mechanism linking early-phase D1/5R potentiation to D1/5R potentiation of synaptic plasticity.

We found that LTP occluded the effects of D1/5R activation, indicating that D1/5R potentiation and LTP may share some mechanistic similarities. We attempted the reverse by inducing potentiation with D1/5R activation and then inducing LTP with TBS and found that D1/5R potentiation did not occlude LTP.

This is possibly because D1/5R activation produced approximately 30% potentiation and did not saturate the mechanism of potentiation as did TBS. However, we found no difference in the magnitude of LTP between slices that had been pre-potentiated by D1/5R activation and slices that had not been treated, supporting supports our hypothesis that D1/5R potentiation of LTP and D1/5R potentiation of synaptic responses are results of the same phenomenon. It is possible that this mechanism is also responsible for the reversing effect of D1/5R activation LTD and the inhibitory effect of D1/5R activation on depotentiation. In summary, potentiation by D1/5R activation like LTP is delayed in onset and sustained in magnitude long after induction.

Our results suggest that D1/5R activation produces TBS-independent potentiation of synaptic responses and D1/5R potentiation is likely responsible for the effects of D1/5R activation on LTP, LTD, and depotentiation, and may contribute to the cognitive-enhancing properties of D1/5R drugs.

Conclusion:

Brief D1/5R activation produces delayed, sustained potentiation of synaptic field responses in SC-CA1 of the hippocampus. Like LTP potentiation by D1/5R activation, D1/5R potentiation of synaptic responses occurs on the order of 30-40 minutes. Furthermore, D1/5R potentiation occluded D1/5R enhancement of LTP

and LTP occluded D1/5R potentiation, suggesting that D1/5R potentiation of LTP and D1/5R potentiation of synaptic field responses are results of the same phenomenon.

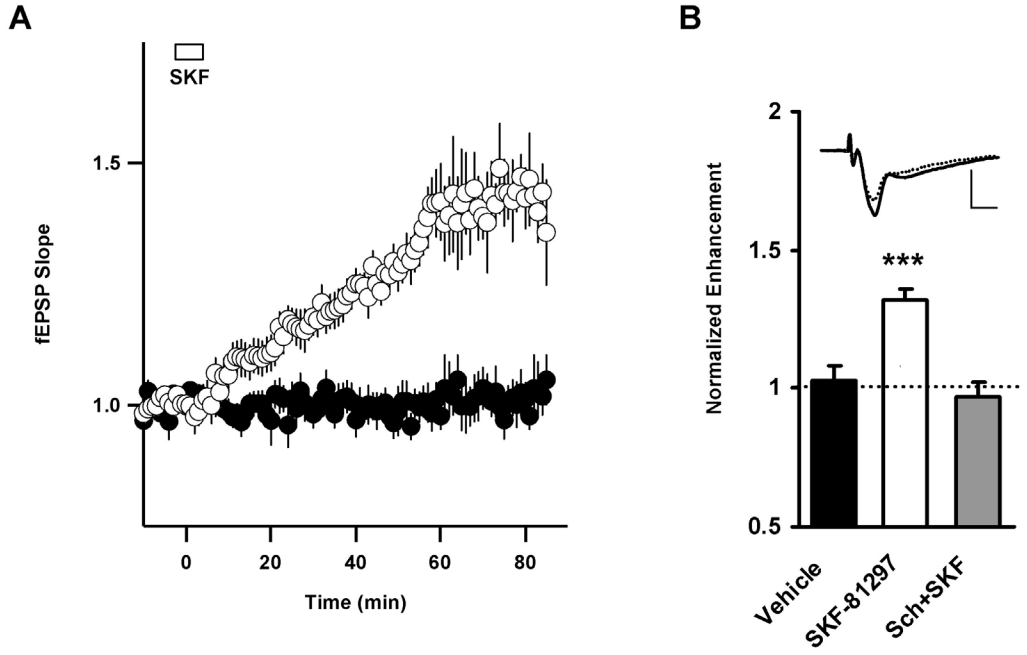

Figure 3.1: D1/5R activation induces TBS-independent potentiation. A) SKF-81297 potentiates synaptic field responses by direct D1/5R activation. Filled circles, vehicle; open circles, SKF-81297. Bar, SKF-81297. The D1/5R antagonist SCH-23390 prevents potentiation by SKF-81297. B) Bar graph representing SKF-81297 potentiation of synaptic field responses. Inset, reprentative field response before and after D1/5R potentiation. Scale: y-axis 1 mV, x-axis 5 ms.

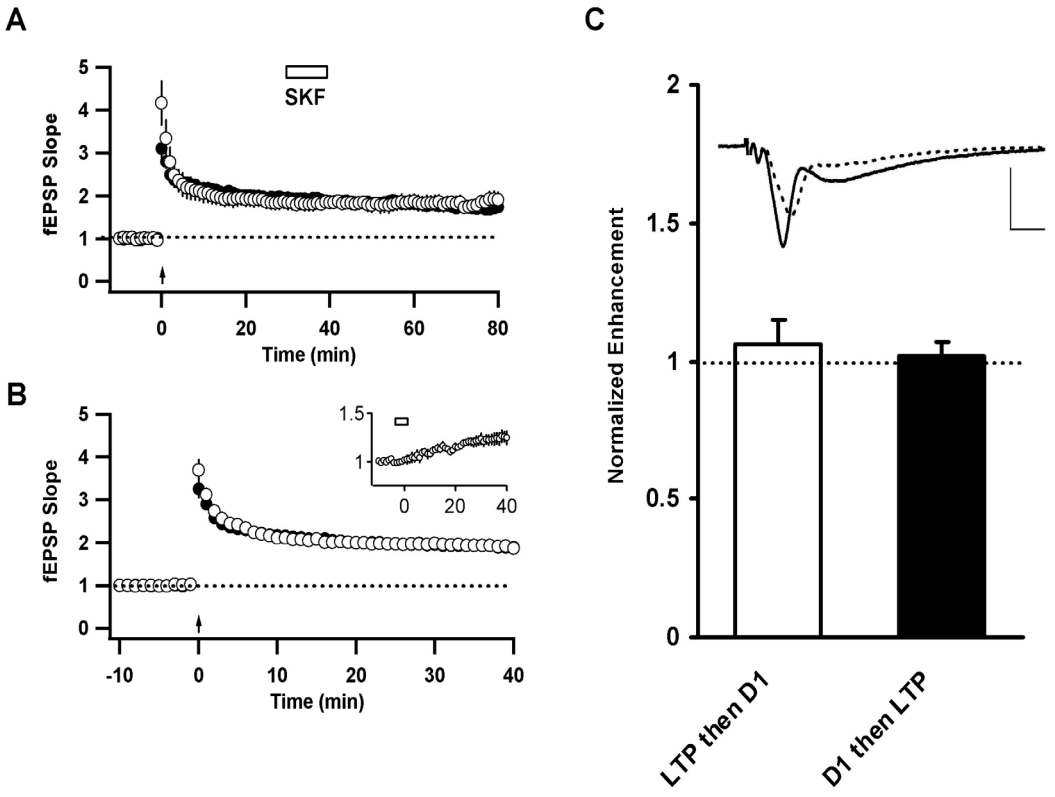

Figure 3.2: LTP occludes D1/5R potentiation and potentiation by D1/5R activation occludes D1/5R enhancement of LTP. A) SKF-81297 during LTP maintenance does not change field responses. For al panels: filled circles, SKF-81297; open circles, control; open bar, SKF-81297; arrow, 30 TBS. B) LTP induction during maintenance of D1/5R potentiation does not change the magnitude of LTP C) Bar graph representing outcome of occlusion experiments. Inset, representative response before and after LTP. Scale, y-axis 1 mV, x-axis 5 ms.

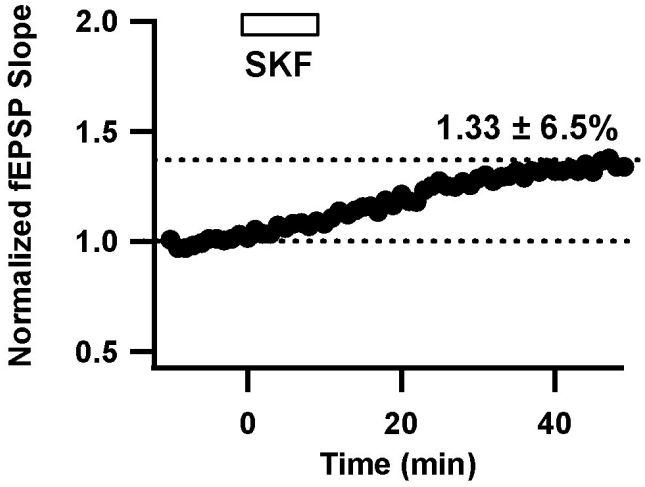

Supplemental Figure 3.1: D1/5R activation by SKF-81297 potentiates synaptic field responses with inhibitory signaling intact.

CHAPTER FOUR

MECHANISM OF DOPAMINE D1/5 RECEPTOR POTENTIATION OF SYNAPTIC FIELD RESPONSES

Summary:

Using field recordings in acute hippocampal slices, we demonstrate induction of D1/5R potentiation requires the activity of NR2B NMDARs. Expression and maintenance of D1/5R potentiation, however, do not require NMDAR activity. Further, we show that D1/5R activation in the absence of NMDAR activity has the continued ability to potentiate synaptic responses after direct D1/5R activation has ceased, indicating D1/5R activation triggers a persistent signal that can induce NMDAR-dependent plasticity as NMDARs become available. Although direct D1/5R activation and NMDAR activity are not simultaneously required for induction of D1/5R potentiation, synapse non-specific coincident post-synaptic activity is required. Finally, D1/5R potentiation requires the activity of PKA, PKC, and PKMζ. We conclude that D1/5R activation prolongs the temporal window for induction of NMDAR-dependent synaptic plasticity and resembles the maintenance phase of L-LTP. However unlike traditional LTP, D1/5R

potentiation is not synapse-specific, and may serve to increase the synaptic "gain" during salient experiences.

Introduction:

Traditional forms of synaptic plasticity are specific to a subset of synapses that receive patterns of coincident glutamate release and post-synaptic depolarization. Furthermore, they rely on a vast array of intracellular signals for induction, expression, and maintenance. When activated, $G_{\alpha s}$-coupled D1/5Rs enhance adelylate cyclase, increase cAMP, and activate PKA. Consistent with this, previous work has indicated essential roles for both PKA and PKC in mediating the various effects of D1/5R activation on neuronal function and synaptic plasticity (Klann et al 1991, 1993, Roberson and Sweatt 1996). Additionally, previous studies have shown atypical persistently activated PKC isoform PKMζ is necessary and sufficient for maintenance of late-phase LTP (Ling et al 2002, Sacktor et al 1993). Furthermore, inhibition of PKMζ has no effect on LTP induction or E-LTP expression (Serrano et al 2005). Using field recordings in acute hippocampal slices, we show that D1/5R activation prolongs the temporal window for induction of NMDAR-dependent synaptic plasticity and occurs independently of evoked activity. Additionally, D1/5R potentiation requires activity of PKA, PKC, and PKMζ. We conclude that D1/5R potentiation is a

novel, synapse non-specific form of E-LTP that resembles the maintenance phase of L-LTP. These findings help clarify the role of DA in mediating hippocampal memory and in diseases of aberrant DA signaling in the hippocampus.

Experimental Procedures:

Drugs and Solutions:

Artificial cerebrospinal fluid (ACSF) for slice experiments consisted of (in mM); NaCl 125, KCl 2.5, NaH_2PO_4 1.25, $MgCl_2$*6(H_2O) 1, $CaCl_2$*2(H_2O) 2, $NaHCO_3$ 25, and Dextrose 25. All drugs were aliquoted and stored at -20°C. Fresh drug aliquots were used for each experiment. To activate D1/5R receptors SKF-81297 (Tocris) in DMSO was used at 10 μM. To block NR2B NMDARS, Ifenprodil (Tocris) in ethanol was used at 3 μM. To block NMDA receptors, APV (Tocris) dissolved in 1 equivalent NaOH and water was used at 50 μM. To block $GABA_A$ signaling, picrotoxin (Sigma-Aldrich) in ethanol was used at 50 μM. To block L-type VGCCs, nimodipine (Tocris) was used at 10 μM. To inhibit PKA signaling, H89 (Tocris) in DMSO was used at 10 μM, or KT5720 (Tocris) in DMSO was used at 1 μM. To inhibit src-family tyrosine kinases, PP2 (Tocris) in DMSO was used at 10 μM. To inhibit PKC signaling, GFX109203X (Tocris) in DMSO was used at 10 μM. To inhibit PKMζ signaling, ZIP (Tocris) and scrambled ZIP (Tocris) in water was used at 5 μM.

Acute Slice Preparation:

Adult 6-12 wk. C57/BL6 mice (Jackson Labs) were anesthetized with isoflurane, rapidly decapitated, and brains were immediately placed in ice-cold cutting solution (in mM): sucrose 254, dextrose 10, NaH_2PO_4 1.25, $NaHCO_3$ 24, $CaCl_2$*2(H_2O) 2, $MgSO_4$*7(H_2O) 2, KCl 3) saturated with carbogen gas (95% O_2, 5% CO_2). 400 μm para-transverse hippocampal slices were made using a vibrating tissue slicer (Vibratome, St. Louis, MO) and transferred to a holding chamber containing room temperature ACSF. Slices were allowed to recover at least one hour before use.

Field Potential Recording:

Acute hippocampal slices were placed in a RC-26 submersion recording chamber (Warner, Hamden, CT) at room temperature. A stimulating electrode (CED255, FHC, Bowdoin, ME) was placed in the Schaffer Collaterals near CA2 and a glass recording electrode (1-2 MΩ) filled with ACSF was placed in the Schaffer Collaterals in CA1. Field responses were elicited with a biphasic stimulus delivered via a stimulus isolator (BSI-950, Dagan, Minneapolis, MN) and stimulation intensity was adjusted until field responses were within 30-60% of the linear response range. Field responses were recorded with an Axoclamp 2B amplifier (Axon instruments, Foster City, CA) and digitized using an ITC-18

digital/analog converter (Instrutech, Port Washington, NY). Responses were stored on a Dell PC. Data acquisition and analysis was conducted using custom software in Igor Pro (Wavemetrics). Group comparisons were made using paired or unpaired t-tests where appropriate.

Results:

Induction of D1/5R potentiation requires NR2B NMDA receptors

Because considerable time passes between activation of D1/5R receptors and expression of D1/5R potentiation, it is possible that NMDA activity is important not only during acute D1/5R activation, but after D1/5R washout as well. We next sought to determine the role of NMDAR activity in three phases of D1/5R potentiation: Induction, expression, and maintenance. Because involvement of $GABA_A$ signaling and L-type VGCCs had previously been excluded, drug-free ACSF was used unless otherwise stated.

Based on our previous finding that D1/5R enhancement of LTP required NR2B NMDARs, we hypothesized that if D1/5R potentiation is responsible for D1/5R enhancement of LTP, it too should require NMDAR activity and NR2B NMDARs. To investigate this, we applied SKF-81297 in the presence of the NMDA antagonist APV (50 μM) or the NR2B antagonist ifenprodil (3 μM) throughout the duration of recording and found no change in field response

following SKF-81297 application (Figure 4.1A, open circles APV, -3.5 ± 4.1%, n = 5, $p > 0.05$; grey circles ifenprodil, 3.7 ± 6%, n = 5, $p > 0.05$). This indicates that like D1/5R enhancement of LTP, D1/5R potentiation requires NMDAR activity with a specific requirement for NR2B subunits.

We next sought to investigate the role for NMDAR activity in the expression of D1/5R potentiation. We induced D1/5R potentiation with SKF-81297 (10 μM) applied for 10 minutes and added APV (50 μM) for the remainder of the experiment immediately upon SKF-81297 wash-out. We found that APV applied after induction of D1/5R potentiation did not prevent enhancement of the field response (Figure 4.1B, 29.6 ± 8.3%, n = 9, $p < 0.01$), suggesting that NMDAR activity is not required for expression of D1/5R potentiation.

Classical LTP induction requires coincident postsynaptic glutamate receptor activation and NMDAR activity. To determine if induction of D1/5R potentiation requires coincident D1/5R activation and NMDAR activity, we applied APV for 5 minutes preceding and throughout the SKF-81297 application. During washout of APV and SKF-81297, the D1/5R antagonist SCH-23390 (10 μM) was added for the remainder of the experiment to prevent residual direct D1/5R receptor activation. We found that under conditions of non-coincident D1/5R activation and NMDAR activation, D1/5R potentiation remained intact (Figure 4.1C, 26.6 ± 8.3, n = 5, $p < 0.05$). This suggests that brief D1/5R activation triggers a persistently activated signaling cascade that is maintained

after direct receptor activation has ceased, and activity of this signaling cascade is sufficient to induce potentiation via NMDARs without coincident direct D1/5R activation.

Finally, we sought to determine if maintenance of D1/5R potentiation requires NMDAR activity. D1/5R potentiation was induced using SKF-81297 (Figure 4.1D inset) and allowed to stabilize. Once expression of D1/5R potentiation stabilized, APV was applied for 10 min. and no reduction of D1/5R-potentiated responses was observed (Figure 4.1D, -4.5 ± 4.1%, $n = 5$, $p > 0.05$). This suggests that field responses under our conditions are entirely AMPAR and not NMDAR-mediated, and that maintenance of D1/5R potentiation results not from increased NMDA currents, but rather through an NMDAR-mediated change in signaling that influences AMPAR function.

We conclude that induction of D1/5R potentiation requires NMDAR activity (specifically NR2B), while expression and maintenance of D1/5R potentiation are independent of NMDAR activation. Furthermore, we conclude that D1/5R activation triggers persistent intracellular signaling that is permissive for the induction of potentiation. Through this mechanism, previous D1/5R activity gates induction of NMDAR-dependent synaptic plasticity as NMDARs becomes available. Through this mechanism, D1/5R activation increases the temporal window for induction of NMDAR-dependent synaptic plasticity.

Coincident post-synaptic activity and D1/5R activation are required for D1/5R potentiation

Hebbian forms of synaptic plasticity require coincident glutamate receptor activation and post-synaptic depolarization to activate NMDARs. Because our findings indicate that coincident D1/5R activation and NMDAR activity are not required for induction of D1/5R potentiation, we next sought to determine if D1/5R potentiation is Hebbian in that post-synaptic activity is required simultaneously with D1/5R activation

One possibility is that the repeated synaptic stimulation used to monitor field responses activates NMDARs and allows for induction of D1/5R potentiation. To address this, we turned off the stimulator after baseline recording, applied SKF-81297, and following 30 minutes of SKF-81297 washout, resumed stimulation. In the absence of synaptic stimulation, SKF-81297 potentiated synaptic responses (Figure 4.2A, 32.3 ± 8.8%, $n = 7$, $p < 0.05$) with no significant potentiation observed in interleaved control experiments (Figure 4.2A, 3 ± 4.0%, $n = 4$, $p > 0.05$). This implies that evoked activity is not required for D1/5R potentiation, and raises the possibility spontaneous synaptic activity may be sufficient to induce D1/5R potentiation.

To further investigate if coincident post-synaptic activity and D1/5R activation are required for induction of D1/5R potentiation, we blocked post-synaptic activity with kynurenic acid (KA, 2 mM). More specific AMPAR

antagonists could not be used because they do not readily wash out. Although KA blocks both AMPARs and NMDARs, necessity of coincident NMDAR and D1/5R activation for induction of D1/5R potentiation had previously been excluded, allowing effects of KA on D1/5R potentiation to be attributed to modulation of AMPAR activity. When SKF-81297 was applied in the presence of KA, we found no potentiation between SKF-81297 over the control condition (Figure 4.2B, -2.1 ± 7.6%, n = 4 control, n = 5 SKF, $p > 0.05$), indicating coincident post-synaptic AMPAR activity is required with direct D1/5R activation for D1/5R potentiation induction. One caveat of the previous experiment is that KA itself induced plasticity under control conditions. To rule out occlusion of D1/5R potentiation by KA-induced plasticity, we applied KA for 30 minutes following SKF-81297 application and found D1/5R potentiation to be intact (Figure 4.2C, 217.1 ± 28.5%, n = 4 control, n = 4 SKF, $p < 0.01$). Although D1/5R potentiation is Hebbian in that it requires coincident receptor binding and post-synaptic activity for induction, the magnitude of post-synaptic activity required appears to be much less than for traditional LTP and potentiation is not specific to synapses receiving evoked activity. This suggests that spontaneous activity alone may be sufficient to induce D1/5R potentiation.

D1/5R potentiation requires the activity of PKA, PKC, and PKM zeta

We next sought to investigate the intracellular signaling mechanisms that mediate D1/5R potentiation. D1/5R activation enhances adenlylate cyclase, increases cAMP, and activates PKA. To determine if PKA activity was required for D1/5R potentiation, we used the PKA inhibitor H89 (10 μM) and the more selective PKA inhibitor KT5720 (10 μM) to inhibit PKA, and found no effect of SKF-81297 on synaptic field responses in the presence of either H89 (Figure 4.3, lightest grey circles, 8.8 ± 11.7%, n = 5, $p > 0.05$) or KT5720 (Figure 4.3, next lightest grey circles, 0 ± 1.2%, n = 5, $p > 0.05$).

Furthermore, previous work has indicated a role for PKC in mediating the various effects of D1/5R activation on neuronal function and synaptic plasticity. To determine if PKC was involved in mediating D1/5R potentiation, we applied SKF-81297 in the presence of the selective PKC inhibitor GFX109203X (10 μM), and found no effect of SKF-81297 (Figure 7, medium grey circles, 4.4 ± 7.9%, n = 8, $p > 0.05$).

Finally, the persistently activated atypical PKC isoform PKMζ is necessary and sufficient for maintenance of late-phase LTP, while having no effect on LTP induction or E-LTP expression (Ling et el 2002, Serrano et al 2005). We hypothesized that if D1/5R potentiation resembled the maintenance phase of LTP that inhibition of PKMζ would prevent potentiation, while if D1/5R potentiation resembled the early phase of LTP, inhibition of PKMζ would produce no effect. In the presence of PKMζ inhibitory peptide ZIP (5 μM), we

found no potentiation by SKF-81297 (Figure 4.3, dark grey circles, -3.1 ± 12.1%, n = 5, $p > 0.05$), while potentiation remained intact in the presence of scrambled ZIP (Figure 4.3B, 26.6 ± 6.7%, n = 4, $p < 0.05$). This suggests that D1/5 potentiation may be similar to the maintenance phase of traditional LTP in that it requires PKMζ activity.

Discussion:

We showed that induction of D1/5R potentiation requires NR2B-NMDARs, while expression and maintenance of D1/5R potentiation is independent of NMDAR activity. Furthermore, induction of D1/5R potentiation does not require coincident NMDAR activity. This implies brief D1/5R activation triggers persistent changes in intracellular signaling that can induce potentiation as NMDARs become available. Unlike TBS-induced NMDAR-dependent synaptic plasticity, which has a temporal window for induction on the order of milliseconds, the window for induction of D1/5R NMDAR-dependent plasticity is on the order of minutes. Thus, D1/5R activation prolongs the temporal window for induction of NMDAR-dependent synaptic plasticity.

Unlike induction of LTP by TBS which requires NMDAR activity with the induction signal (TBS), D1/5R potentiation does not require NMDAR activity with the induction signal (direct D1/5R activation) and thus has a much wider

temporal window for induction. Unlike previous experiments that block NMDAR activity during LTP induction and prevent potentiation (Sarvey et al 1989), we found that blocking NMDARs during direct D1/5R activation did not prevent potentiation of synaptic responses. Additionally, we found blocking NMDARs during D1/5R expression did not prevent potentiation, nor did blocking NMDARs during D1/5R potentiation maintnance. These results indicate that the temporal window for NMDAR activity is much wider for induction of D1/5R potentiation than for induction of LTP, and that expression and maintenance of D1/5R potentiation are independent of NMDARs. During LTP induction by electrical stimulation, NMDAR activity is only possible during TBS because of channel block by magnesium and membrane depolarization via AMPARs is the mechanism gating induction of NMDAR-dependent synaptic plasticity. Because only synapses receiving evoked activity are potentiated, LTP only occurs at the specific subset of synapses receiving stimulation coincident with glutamate receptor activation. Like traditional LTP, induction of D1/5R potentiation requires coincident post-synaptic activity; however it is independent of evoked activity and is thus synapse non-specific.

In summary, D1/5R potentiation appears to work through an LTP-like NMDAR-dependent induction process, however unlike traditional LTP, D1/5 potentiation is synapse non-specific and does not require the induction signal to be coincident with NMDAR activation. The unique ability of D1/5R activation to

induce potentiation in a broad temporal manner without synaptic specificity may serve to increase the "gain" of synaptic responses during salient environmental experiences and may underlie the ability of D1/5R drugs to improve cognition during hippocampal behaviors.

Conclusion:

We conclude that brief D1/5R activation triggers persistent intracellular signaling which prolongs the temporal window for induction of NMDAR-dependent synaptic plasticity, however unlike traditional LTP, it does not require the induction signal be coincident NMDAR activity nor is it restricted to a subset of activated synapses. Furthermore, D1/5R potentiation produces E-LTP that resembles the maintenance phase of L-LTP. We suggest D1/5R potentiation is a novel form of plasticity that increases the "gain" of synaptic responses during salient environmental experiences and may underlie the ability of D1/5R drugs to improve cognition during hippocampal tasks.

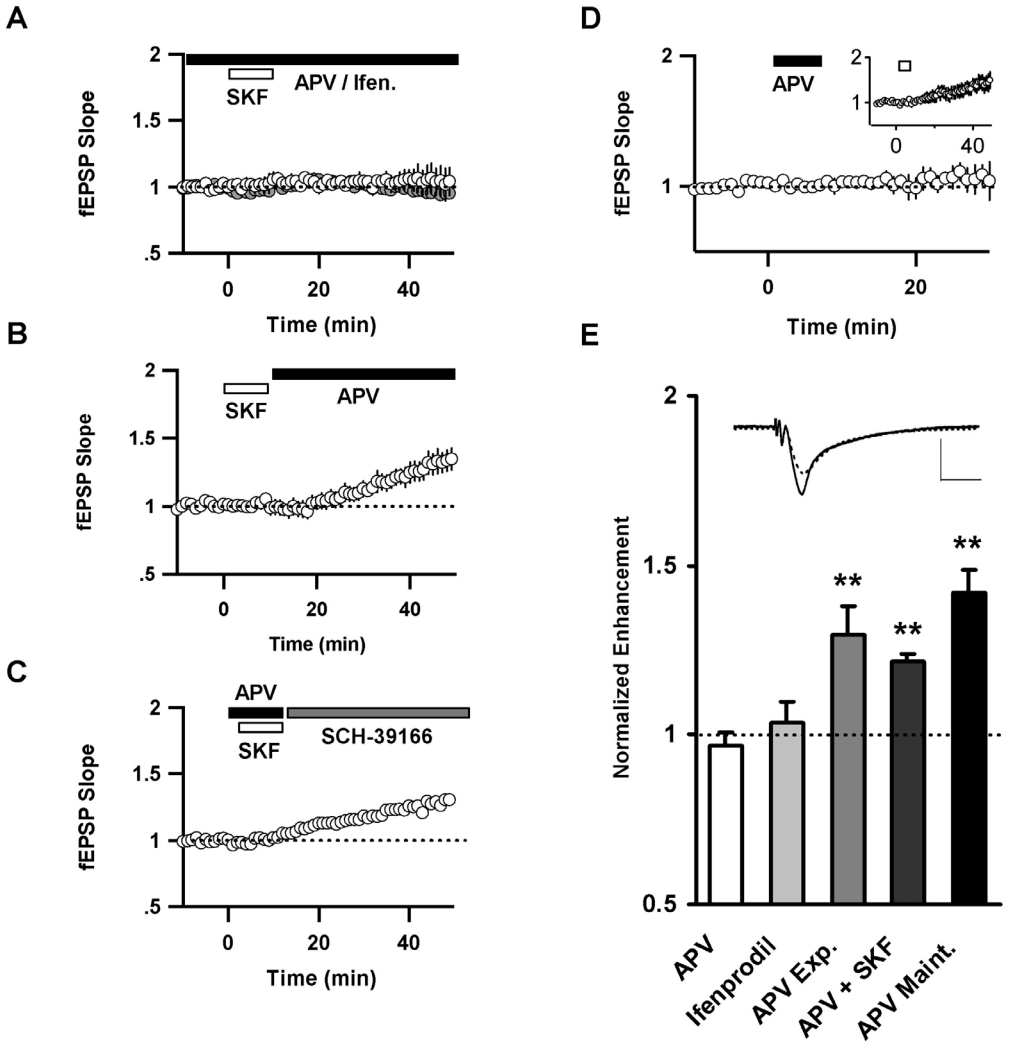

Figure 4.1: Induction of D1/5R potentiation requires NMDA receptors. A) NR2B NMDARs are required for D1/5R potentiation. For all panels: open bar SKF-81297; filled bar APV or ifenprodil; open circles, APV; closed circles, ifenprodil. B) NMDAR activity is not required for expression of D1/5R potentiation. C) D1/5R activation with induces potentiation without coincident NMDAR activity, grey bar D1/5R antagonist SCH-23390. D) NMDAR activity is not required for maintenance of D1/5R potentiation. E) Bar graph representing role of NMDAR activity in D1/5R potentiation. Inset, representative field response before and after D1/5R potentiation. Scale bar; 1 mV y-axis, 5 ms x-axis.

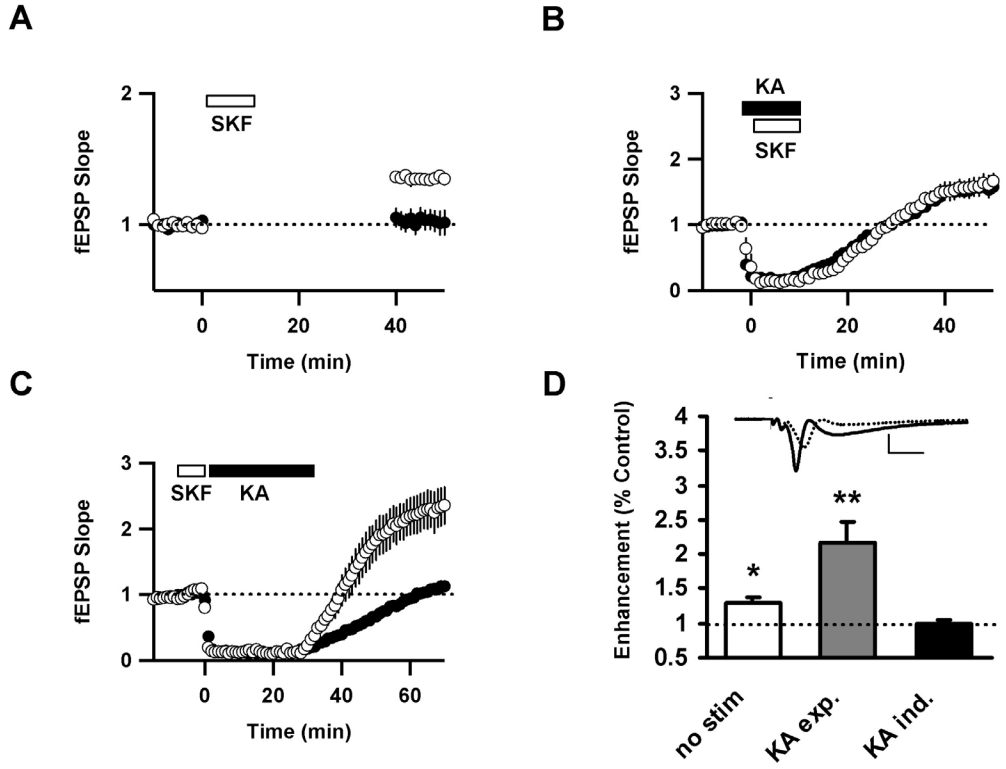

Figure 4.2: D1/5R potentiation requires coincident post-synaptic activity and D1/5R activation. A) SKF-81297 potentiates synaptic field responses in the absence of synaptic stimulation. For all panels, Ooen circles SKF-81297; filled circles control; open bar, SKF-81297; closed bar, KA. B) Post-synaptic activity coincident with D1/5R activation is required for D1/5R potentiation. C) Post-synaptic activity after D1/5R activation is not required for D1/5R potentiation. D) Bar graph representing activity-dependence of D1/5R potentiation. Inset; representative field response before and after D1/5R potentiation. Scale bar; 1 mV y-axis, 5 ms x-axis.

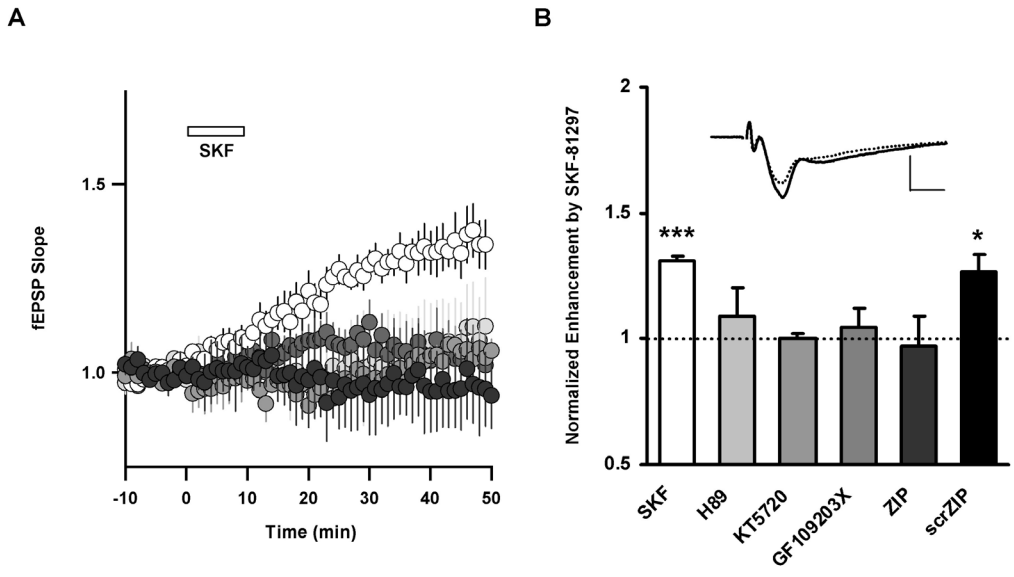

Figure 4.3: D1/5R potentiation requires the activity of PKA, PKC, and PKM zeta. A) Average D1/5R potentiation experiments. Open circles; SKF-81297 only. Light grey circles; SKF-81297 with PKA inhibitors H89 and KT5720. Medium grey circles; SKF-81297 with selective PKC inhibitor GF109203X. Dark grey circles; SKF-81297 with PKM zeta inhibitory peptide ZIP. B) Bar graph representing potentiation by SKF-81297. Inset; representative field response before and after D1/5R potentiation. Scale bar; 1 mV y-axis, 5 ms x-axis.

CHAPTER FIVE

MODULATION OF AMPA AND NMDA CURRENTS BY D1/5 ACTIVATION

Summary:

Using whole-cell voltage clamp recordings from CA1 pyramidal neurons in adult hippocampal slices, we found brief D1/5R activation potentiates both AMPA-mediated inward currents and NMDA-mediated outward currents without altering the AMPA-NMDAR ratio. Additionally, we found that consistent with an increase in NR2B contribution, the decay time constant of outward NMDA currents increased following D1/5R activation. We conclude that D1/5R modulation of glutamatergic receptor currents is consistent with the ability of ionotropic D1/5R agonists to potentiate glutamatergic neurotransmission and neuroplasticity.

Studies examining the effect of D1/5R activation on hippocampal synaptic plasticity, a cellular correlate of learning, suggest that D1/5R activation promotes the maintenance of potentiated synaptic strength (Otmakhova and Lisman 1996, Matthies et al 1997, Otmakhova and Lisman 1998, Williams et al 2006, Lemon

and Manahan-Vaughn 2006, Mockett et al 2007, Navakkode et al 2007, Granado et al 2008). One characteristic of synapses that have undergone potentiation such as LTP is the expression of a greater ratio of AMPA current to NMDA current, a property called the AMPA-NMDA ratio (Kauer et al 1988). It is thought that changes in AMPA-NMDA ratio seen following LTP induction results from an increased number of GluR1-containing AMPARs that have been translocated to the cell surface (Liu et al 2001). To determine if, as for LTP, D1/5R potentiation changes the AMPA-NMDA ratio, we used whole-cell voltage clamp recordings in acute hippocampal slices. Previously, it has been shown that D1/5R activation in CA1 potentiates EPSCs through both AMPA and NMDA glutamate receptors (Hatt et al 1995, Umemiya and Raymond 1997, Price and Raymond 1999, Zheng et al 1999, Yang 2000, Chen et al 2002, Tseng and O'Donnell 2004, Wirkner 2004, Whitman et al 2005), and we sought to determine if potentiation of AMPA and NMDARs following D1/5R activation modulated the AMPA-NMDA ratio in a manner similar to traditional LTP.

Experimental Procedures:

Drugs and Solutions:

Artificial cerebrospinal fluid (ACSF) for slice experiments consisted of (in mM); NaCl 125, KCl 2.5, NaH_2PO_4 1.25, $MgCl_2$*6(H_2O) 1, $CaCl_2$*2(H_2O) 2,

$NaHCO_3$ 25, and Dextrose 25. All drugs were aliquoted and stored at -20°C. Fresh drug aliquots were used for each experiment. To activate D1/5R receptors SKF-81297 (Tocris) in DMSO was added to ACSF to a final concentration of 10 μM. To block NMDA receptors, APV (Tocris) dissolved in 1 equivalent NaOH and water was used at 50 μM. To block $GABA_A$ signaling, picrotoxin (Sigma-Aldrich) in ethanol was used at 50 μM. To block L-type VGCCs, nimodipine (Tocris) was used at 10 μM. Cs-based internal solution for voltage-clamp recording contained (in mM) D-gluconic acid 110, CsOH 110, TEA-Cl 20, NaPhCr 10, NaGTP 0.3, MgATP 2, HEPES 20, EGTA 0.5, QX-314 5, Biocytin 0.1%).

Acute Slice Preparation:

Adult 6-12 wk. C57/BL6 mice (Jackson Labs) were anesthetized with isoflurane, rapidly decapitated, and brains were immediately placed in ice-cold cutting solution (in mM): sucrose 254, dextrose 10, NaH_2PO_4 1.25, $NaHCO_3$ 24, $CaCl_2$*2(H_2O) 2, $MgSO_4$*7(H_2O) 2, KCl 3) saturated with carbogen gas (95% O_2, 5% CO_2). 400 μm para-transverse hippocampal slices were made using a vibrating tissue slicer (Vibratome, St. Louis, MO) and transferred to a holding chamber containing room temperature ACSF. Slices were allowed to recover at least one hour before use.

Voltage Clamp Recording:

Whole-cell voltage clamp recordings made using a BVC-700 amplifier (Dagan, Minneapolis, MN). Patch-clamp electrodes were made from borosilicate glass with resistances of 3-5 MΩ in ACSF. Synaptic stimulation of CA1 pyramidal neurons was performed using a bipolar stimulating electrode (CED255, FHC, Bowdoin, ME) connected to stimulus isolator (BSI-950, Dagan, Minneapolis, MN). Stimulation intensity was adjusted to elicit responses that were 40-60% maximal within the linear response range. CA1 pyramidal neurons were visualized with an Olympus BX51-WI microscope equipped with IR-DIC optics. Data were stored on a computer (Dell) via an ITC-18 analog-to-digital converter (Instrutech, Port Washington, NY). Data acquision and analysis was performed using Igor Pro (Wavemetcics). Group comparisons were made using paired t-tests.

Results:

D1/5R activation potentiates AMPA and NMDA

To confirm previous reports of D1/5R potentiation of isolated AMPA and NMDA EPSCs under our experimental conditions and determine an AMPA-

NMDA ratio, we used whole-cell voltage clamp recording in acute hippocampal slices. After recording a stable baseline, the AMPA-NMDA ratio

was measured before and after 10 minute application of SKF-81297 (10 μM). Because we wanted to measure before and after drug treatment in the same cell, we could not use pharmacological tools to isolate AMPA and NMDA responses as done by others (Hatt et al 1995, Umemiya and Raymond 1997, Price and Raymond 1999, Zheng et al 1999, Yang 2000, Chen et al 2002, Tseng and O'Donnell 2004, Wirkner 2004, Whitman et al 2005). Instead, we recorded inward AMPA currents at -80 mV to reduce contribution of NMDA and VGCCs and measured outward NMDA currents at +60 mV, performing analysis on the outward EPSC only after the AMPA component had decayed completely (Figure 5.1).

In agreement with previous reports showing enhancement of both AMPA and NMDA currents in the hippocampus following D1/5R activation (Yang 2000), we found a significant increase in the total charge transfer (integral) of both AMPA EPSCs (Figure 5.2, control 3179.9 ± 739.3 pA, SKF-81297 4331.3 ± 736.1 pA, 142.5 ± 8.9%, $n = 6$, $p < 0.01$) and NMDA EPSCs (Figure 5.2, control 6240.6 ± 399.2 pA, SKF-81297 8558.07 ± 574.5 pA, 140.2 ± 13.8%, $n = 6$, $p < 0.05$). Additionally, the decay time constant of the NMDA component showed a significant increase (Figure 5.2, control 43.3 ± 4.0, SKF-81297 57.9 ± 4.5, 135.6 ± 8.8%, $n = 6$, $p < 0.05$) and the AMPA component showed a significant increase in peak (Figure 5.2, control 162.7 ± 37.7 pA, SKF-81297 205.9 ± 50.4 pA, 124.0 ± 3.8%, $n = 6$, $p < 0.05$). Because NR2B-EPSCs have a much slower decay

constant than NR2A-EPSCs, the increase in decay constant is consistent with an increase in NR2B surface expression (Vicini et al 1998). No significant change in the AMPA decay constant (Figure 5.2, control 13.2 ± 1.8, SKF-81297 14.4 ± 0.8, 115.8 ± 12.1%, n = 6, $p > 0.05$), NMDA peak (Figure 5.2, control 124.5 ± 25.3 pA, SKF-81297 152.8 ± 34.8 pA, 118.2 ± 8.3%, n = 6, $p > 0.05$), or AMPA-NMDA ratio was found (Figure 5.2, control 0.53 ± 0.14, SKF-81297 0.45 ± 0.06 107.1 ± 12.0%, n = 6, $p > 0.05$). One discrepancy to note is that D1/5R activation begins to modulate whole cell currents after only 10 minutes, while little if any effect is seen on the field response at this time point. It is possible that this discrepancy results from the increased sensitivity of whole-cell recording, which may allow for detection of subtle events that are not yet apparent at the level of a neuronal population.

Discussion:

While an increase in the AMPA/NMDA is characteristic of LTP (Kauer 1988), we do not see a change in the AMPA/NMDA ratio following D1/5R activation. This is likely due to the increases seen in both AMPA and NMDA receptor surface localization and synaptic currents. However, AMPA/NMDA was measured only 10 min. after SKF-81297 application, and its possible that a change might be detectable at a further time point. It has also been reported in the

cortex that increases in AMPA contribution initially following LTP induction via synaptic stimulation are accompanied by delayed increases in NMDA current that serves to maintain glutamate receptor contribution to synaptic transmission (Watt et al 2004). This suggests that stimulation-dependent LTP, like D1/5R potentiation, may eventually include potentiation of NMDA components in addition to AMPA components. In summary, in agreement with previous reports showing D1/5R activation potentiates pharmacologically isolated AMPA and NMDA currents, D1/5R activation potentiates both inward currents largely mediated by AMPARs and outward currents predominantly mediated by NMDARs under our experimental conditions. Unlike the characteristic increase in AMPA-NMDA ratio seen at synapses that have undergone LTP, we observed no change in the ratio of AMPA-NMDA following 10 minutes of D1/5R activation.

Conclusion:

We conclude that D1/5R activation potentiates AMPA-mediated inward currents and NMDA-mediated outward currents without altering the ratio of AMPA-NMDA. Consistent with upregulation of NR2B-NMDARs, the decay constant of the outward NMDA-mediated current is increased following 10 minutes of D1/5R activation while the decay constant of the AMPA-mediated inward component is unchanged. This modulation of glutamatergic currents likely underlies the ability

of D1/5R activation to potentiate glutamatergic neurotransmission and enhance synaptic plasticity.

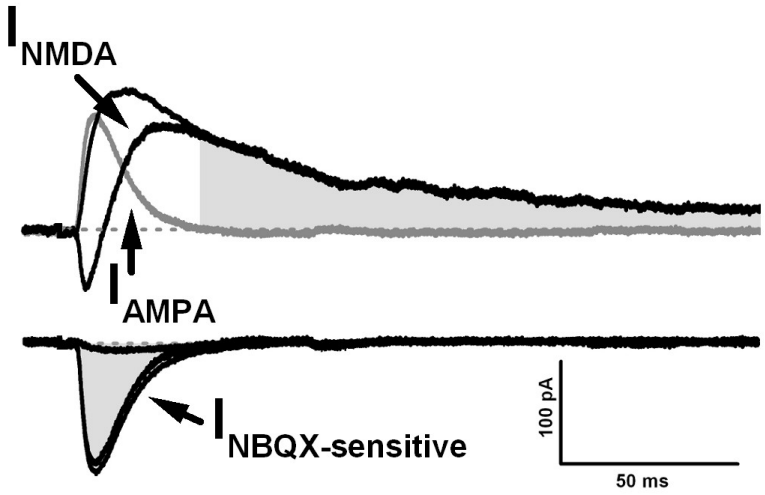

Figure 5.1: Analysis of outward and inward currents. Inward current, representative AMPA EPSCs taken at -80 mV. Outward current, representative NMDA EPSCs taken at +60 mV Scale bar; x-axis, 50 ms, y-axis, 100 pA. Gray trace represents kinetics of AMPA component to outward current. Gray shaded area illustrates part of inward and outward currents used for AMPA and NMDA analysis, respectively.

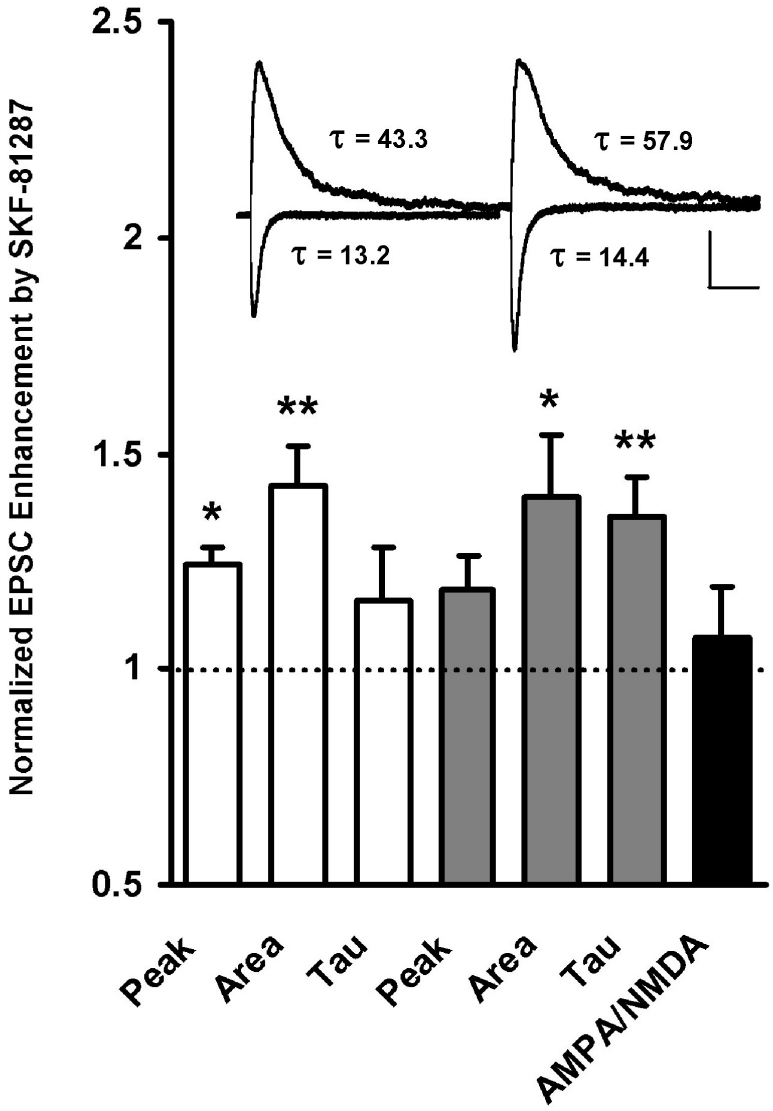

Figure 5.2: Modulation of AMPA and NMDA EPSCs by SKF-81297. Open bars, AMPAR modulation. Grey bars, NMDAR modulation. Inset; representative currents before and after D1/5R activation. Scale bar; 100 pA y-axis, 200 ms x-axis.

CHAPTER SIX

BIOCHEMICAL EFFECTS OF D1/5R ACTIVATION ON AMPA AND NMDA RECEPTORS

Summary:

Using pharmacology experiments in acute hippocampal slices, we found brief D1/5R activation induces lasting changes in cellular locations and biochemical state of AMPAR and NMDAR subunits. Following brief D1/5R activation, we found an increase in surface expression of GluR1 and NR2B subunits, and this increase required the activity of NR2B-NMDARs. Furthermore, PKA phosphorylation of GluR1 subunits increased, CamKII phosphorylation of GluR1 was decreased, and no changes were detected in fyn kinase phosphorylation of NR2B subunits. We conclude that brief D1/5R activation induces persistent NR2B-dependent increases in NR2B and GluR1 surface expression; however the phosphorylation results that accompany this increase are inconsistent with previous literature and further investigation is needed.

Introduction:

While the effect of D1/5R activation on NMDAR phosphorylation state and cellular localization has been well characterized in a variety of cultures, we sought to determine if similar changes in phosphorylation and cellular localization were consistent with the data obtained from field potential recordings in acute hippocampal slices. Previous studies show that following D1/5R activation, surface expression of NR1 and NR2B subunits is increased in striatal slices and cultures, in prefrontal cortical cultures, and in VTA slices (Dunah and Standeart 2001, Dunah et al 2004, Hallett et al 2006, Schilstrom et al 2006, Gao and Wolf 2008). One study indicated an increase in NR2A subunits as well (Dunah et al 2004). Furthermore, some studies found D1/5R induced increases in surface expression were accompanied by an increase in p-T1472 (phosphorylated by fyn tyrosine kinase) (Dunah et al 2004, Hallett et al 2006, Gao and Wolf 2008), while another found an increase in NR2B surface expression following D1/5R activation without any change in p-T1472 NR2B (Schilstrom et al 2006). Additionally, previous studies show D1/5R activation increases surface expression and synaptic incorporation of GluR1 subunits in cultured hippocampal, VTA, NAc, and PFC neurons (Wolf et al 2004, Gao et al 2006, Gao et al 2007), which are accompanied by increases in PKA phosphorylation at S-845 GluR1 and not CamKII/PKC phosphorylation at S-831 (Wolf et al 2004). In hippocampal and PFC-VTA co-cultures, increases in GluR1 surface expression are NMDAR-

dependent (Gao et al 2006, Gao and Wolf 2007), and in the PFC, increases in GluR1 synaptic incorporation require CamKII and PKA. (Gao et al 2006). Taken together, this data indicates that D1/5R activation modulates both AMPAR and NMDAR phosphorylation and cellular localization, giving D1/5Rs the potential to influence multiple and distinct stages of synaptic plasticity. Using slice pharmacology and biotin labeling of surface proteins in acute hippocampal slices, we found brief D1/5R activation induced lasting increases in surface AMPA and NMDARs, and we conclude that these changes are consistent with our data showing D1/5R potentiation of AMPA and NMDA EPSCs and synaptic field potentials.

Experimental Procedures:

Drugs and Solutions:

Artificial cerebrospinal fluid (ACSF) for slice experiments consisted of (in mM); NaCl 125, KCl 2.5, NaH2PO4 1.25, MgCl2*6(H2O) 1, CaCl2*2(H2O) 2, NaHCO3 25, and Dextrose 25. All drugs were aliquoted and stored at -20°C. Fresh drug aliquots were used for each experiment. To activate D1/5R receptors SKF-81297 (Tocris) in DMSO was added to ACSF to a final concentration of 10 μM. To block NR2B NMDARS, Ifenprodil (Tocris) in ethanol was used at 3 μM.

Acute Slice Preparation:

Adult 6-12 wk. C57/BL6 mice (Jackson Labs) were anesthetized with isoflurane, rapidly decapitated, and brains were immediately placed in ice-cold cutting solution (in mM): sucrose 254, dextrose 10, NaH2PO4 1.25, NaHCO3 24, CaCl2*2(H2O) 2, MgSO4*7(H2O) 2, KCl 3) saturated with carbogen gas (95% O2, 5% CO2). 400 μm para-transverse hippocampal slices were made using a vibrating tissue slicer (Vibratome, St. Louis, MO) and transferred to a holding chamber containing room temperature ACSF. Slices were allowed to recover at least one hour before use.

Slice Pharmacology:

Hippocampal slices were placed in small-volume (50 mL) holding chambers contaning carbogen-bubbled ACSF and allowed to equilibrate. 10 uM SKF-81297 and in some experiments, 3 uM ifenprodil was added to the holding chamber. Following drug treatment, slices were transferred to new chambers for drug wash-out. Slices were then transferred to a Petri dish containing ice-cold ACSF and hippocampi were further dissected from the surrounding tissue. Drug-treated hippocampi were immediately frozen on dry ice and stored at -80°C. Group comparisons were made using unpaired t-tests.

Biotin Surface Labeling:

Following drug treatment, slices were transferred to a Petri dish and allowed to incubate in a solution containing EZ-Link Sulfo-NHS-LC-LC-Biotin (1 mg/ mL, Pierce, Rockford IL) in ice-cold ACSF for 10 minutes. Slices were then washed with ice-cold TBS 3x 5 minutes to quench the biotin reaction. Hippocampi were dissected from surrounding tissue in ice-cold TBS and immediately frozen on dry ice and stored at -80°C.

Lysis buffer (NaCl 150 mM, Tris-HCL 50 mM, 0.5% Trition X-100, pH 7.5) containing protease inhibitor cocktail (Sigma Aldrich, St. Louis MO) was added to labeled tissue samples and samples were homogenized using sonication. Tissue lysate was incubated for 2 hrs with high capacity neutravidin agarose resin (Thermo Scientific, Rockfort IL) to bind labeled proteins. Avadin beads were washed with lysis butter 3 times to remove unbound proteins, and bound proteins were eluted with sample buffer containing DDT and heated to 100°C for 15 minutes. Immunoblotting was carried out using standard procedures. All antibodies were purchased from Upstate and used at 1:1,000 dilutions. Group comparisons were made using unpaired t-tests.

Results:

D1/5R activation induces an NR2B-dependent increase in surface-labeled GluR1 and NR2B protein.

It has previously been reported that D1/5R activation leads to increased surface expression of GluR1 and NR2B subunits in culture (Dunah and Standaert 2001, Dunah et al 2004, Hallett et al 2006, Gao and Wolf 2008). To determine if this could be a mechanism by which D1/5R activation leads to potentiated synaptic responses in an NMDA-dependent manner in acute hippocampal slices, we prepared slices as for field recording and used them in slice pharmacology experiments to examine AMPA and NMDA subunits for biochemical changes. As for field experiments, slices were allowed to equilibrate in standard ACSF, followed by bath application of SKF-81297 (10 μM) for 10 minutes. Slices were transferred back to standard ACSF for a 30 minute wash-out period and treated to biotinylate surface proteins. Tissue was immunobloted for total and surface-labeled proteins with GluR1 and NR2B antibodies (Upstate, 1: 1K). Consistent with previous reports, we found a significant increase in both surface GluR1 (Figure 6.1A, B, 23.3 ± 6.0%, n = 12 control, n = 11 SKF-81297, $p < 0.01$) and surface NR2B (Figure 6.1A, B, 26.9 ± 5.7%, n = 12 control, n = 11 SKF-81297, $p < 0.001$) with no change in total GluR1 (Figure 6.1A, D 2.3 ± 11.8%, n = 9 control, n = 10 SKF-81297, $p > 0.05$) or total NR2B (Figure 6.1A, D, 7.5 ± 13.2%, n = 5 control, n = 10 SKF-81297, $p > 0.05$).

To determine if, as for D1/5R potentiation, increases in surface expression were NR2B-dependent, we repeated the experiment in the presence of ifenprodil (3 μM). Under these conditions, we found no change in surface-labeled GluR1

(Figure 6.1A, C, -0.9 ± 16.1%, n = 8 control, n = 7 SKF-81297, $p > 0.05$) or NR2B (Figure 6.1A, C, -3.0 ± 12.8%, n = 8 control, n = 7 SKF-81297, $p > 0.05$). From this we conclude that D1/5R-mediated increases in GluR1 and NR2B surface expression are NR2B-dependent.

D1/5R activation increases PKA phosphorylation of GluR1 subunits

We next sought to examine if D1/5R activation induced phosphorylation changes on GluR1 and NR2B subunitsthat accompanied the increase in surface expression. D1/5Rs are G_s-coupled GPCRs, and upon DA binding activate activate adenylyl cyclase, increase cAMP, and activate PKA. Consequently, we expected to see an increase in PKA phosphorylation of GluR1 following D1/5R activation. Acute hippocampal slices were incubated in SKF-81297 (10 μM) for 10 min., then transferred to drug-free ACSF for a 30 minute washout period so that the treatment would be analogous to those used during field recordings. Hippocampi were dissected from surrounding tissue and immediately frozen either immediately after 10 min. SKF-81297 application or after the 30 min. washout period for comparison to field recordings at times when no potentiation was expressed and during maintenance of D1/5R potentiation. Tissue was then processed using standard western blot procedures and blots were probed with anti-phospho-S845 GluR1 antibody. As expected, phosphorylation at the PKA site S845 on GluR1 subunits significantly increased at both immediately after

SKF-81297 application (Figure 6.2A, 50.9 ± 15.6%, n = 14 control, n = 13 SKF-81297, $p < 0.05$) and 30 min. after SKF-81297 washout (Figure 6.2A, 157.6 ± 37.0%, n = 14 control, n = 15 SKF-81297, $p < 0.001$). No difference was seen in total GluR1 protein (Figure 6.2C, n = 5, $p > 0.05$).

Because D1/5R potentiation of synaptic field responses requires NMDAR activity, we hypothesized that if the increase in PKA phosphorylation of GluR1 subunits mediated D1/5R potentiation, it should also require NMDAR activity. To test this hypothesis, we repeated the D1/5R slice pharmacology experiment in the presence of APV (50 μM) and found no reduction in the ability of D1/5R activation to increase PKA phosphorylation of GluR1 immediately after 10 min. SKF-81297 application (Figure 6.3A, 67.3 ± 9.2%, n = 8 control, n = 7 SKF-81297, $p < 0.001$) or 30 min. after SKF-81297 washout (Figure 6.3B, 86.4 ± 13.6%, n = 8 control, n = 6 SKF-81297, $p < 0.001$). We conclude that because PKA phosphorylation is not prevented by blocking NMDAR activity, this mechanism is not likely responsible for the expression of D1/5R potentiation.

D1/5R activation causes an NMDAR-dependent decrease in PKC/CamKII phosphorylation of GluR1 subunits

Calcium influx through NMDARs during LTP induction has been shown to activate both CamKII and PKC, causing an increase in phosphorylation of GluR1 subunits at S-831, with a variety of CamKII and PKC isoforms required for both

LTP induction and maintenance. (Lovenger et al 1987, Colley et al 1990, Wang and Feng 1992, Sacktor et al 1993, Powell et al 1994, Barria et al 1997). Because D1/5R potentiation appears to share similarities with LTP, we hypothesized that like LTP, D1/5R activation increases phosphorylation at the CamKII/PKC site on GluR1, S-831. Incubating acute hippocampal slices in a 10 min. application of SKF-81297 (10 μM) followed by 30 min. washout as described previously, we found that contrary to our hypothesis, D1/5R activation decreased S-831 GluR1 phosphorylation both immediately after 10 min. SKF-81297 application (Figure 6.2B, -42.4 ± 5.1%, n = 28 control, n = 23 SKF-81297, $p < 0.001$) and after 30 min. washout (Figure 6.2B, 49.9 ± 6.4%, n = 28 control, n = 23 SKF-81297, $p < 0.001$).

To determine if D1/5R-induced decreases in CamKII/PKC phosphorylation of GluR1 could be responsible for D1/5R potentiation of synaptic responses, we repeated the experiment in the presence of APV (50 μM). We found that blocking NMDAR activity prevented the ability of D1/5R activation to modulate phosphorylation at the CamKII/PKC site on GluR1 both immediately after 10 min. SKF-81297 application (Figure 6.3B, -3.8 ± 3.3%, n = 8 control, n = 7 SKF-81297, $p > 0.05$) and after 30 min. washout (Fig. 6.3B, -1.2 ± 6.4%, n = 8 control, n = 6 SKF-81297, $p > 0.05$). We conclude that although the direction of modulation is opposite to that in the LTP literature, this NMDAR-dependent decrease in CamKII/PKC phosphorylation may be involved in the modulation of

AMPAR activity required for expression of D1/5R potentiation in synaptic field responses.

D1/5R activation does not change fyn tyrosine kinase phosphorylation on NR2B subunits

Previously it has been shown that D1/5R activation increases NR2B surface expression via fyn tyrosine kinase. To determine if fyn phosphorylation accompanied the increase in NR2B surface expression we found in acute hippocampal slices, we repeated D1/5R slice pharmacology experiments as previously described and probed for phosphorylation changes in the primary fyn site, T-1472 NR2B, and a secondary fyn site, T-1338 NR2B. Because no significant difference was seen between 10 min and 30 min timepoints, data were pooled. We found that following D1/5R activation, no change in phosphorylation at either T-1472 (Figure 6.4 A,B, 12.7 ± 8.7%, n = 5 control, n = 10 SKF-81297, $p > 0.5$) or T-1336 (Figure 6.4A,B, -9.9 ± 3.1%, n = 5 control, n = 10 SKF-81297, $p > 0.5$). No change was seen in total NR2B protein (Figure 6.4A,B, 7.5 ± 13.2%, n = 5 control, n = 10 SKF-81297, $p > 0.5$). While this data is inconsistent with previous studies showing an increase in p-T1472 following D1/5R activation, these studies were largely done in culture and in regions outside the hippocampus. Additionally, we found no loss of D1/5R LTP modulation in fyn KO mice, and this further supports our suggestion that a different src-family kinase may be

responsible for mediating the effects of D1/5R activation on NR2B function in the hippocampus.

Discussion:

We found that D1/5R activation, like LTP, induces a lasting increase in surface expression of GluR1 subunits that is sustained long after induction. We further found that D1/5R activation-induced increases in GluR1 surface expression were NMDAR-dependent, as were increases in GluR1 surface expression previously seen following LTP induction (Pickard et al 2001). In addition to increasing surface expression of AMPARs, LTP induction leads to a rapid increase in surface expression of NMDARs that is dependent on src-family kinases and PKC in the hippocampus (Grosshans et al 2002). This is similar to the mechanism we presented for D1/5R-mediated potentiation. We found that like LTP induction, D1/5R activation leads to increased NMDAR surface expression. In summary, potentiation by D1/5R activation, like LTP, results in NMDAR-dependent increases in both NMDAR (NR2B) and AMPAR (GluR1) surface expression. In agreement with our electrophysiological data, surface labeling experiments implicate a specific requirement for NR2B-NMDARs in mediating the effects of D1/5R activation.

Our results show that brief D1/5R activation induces sustained phosphorylation changes in GluR1 AMPAR subunits. Following D1/5R activation, phosphorylation by PKA at S845-GluR1 increasess, while phosphorylation by CamKII/PKC at S831-GluR1 decreases. Previous studies show that LTP induction in naïve synapses increases CamKII/PKC phosphorylation of GluR1, while LTP induction in depressed synapses increases GluR1 phosphorylation by PKA (Lee et al 2000). The same study also showed that LTD induction in potentiated synapses decreases CamKII/PKC GluR1 phosphorylation, while LTD induction in naïve synapses decreases PKA phosphorylation of GluR1 (Lee et al). In light of these findings, D1/5R activation induces GluR1 phosphorylation changes that are similar to those seen following potentiation of depressed synapses and depression of potentiated synapses. However, this is inconsistent with our functional data showing an LTP-like effect of D1/5R activation on synaptic responses. Furthermore, the D1/5R-induced increase in GluR1 PKA phosphorylation is independent of NMDAR activity, while the D1/5R-induced decrease in GluR1 CamKII/PKC phosphorylation is NMDAR-dependent. Because our electrophysiology data indicates that expression of D1/5R potentiation requires induction through NMDARs, the decrease in CamKII/PKC phosphorylation, because of its requirement for NMDAR activity, is of greater relevance than the increase in PKA phosphorylation to our physiology data. It remains unclear how a decrease in CamKII/PKC phosphorylation could be

functionally expressed as increased GluR1 surface expression and AMPA-mediated synaptic responses following D1/5R activation. Because the changes detected in CamKII/PKC phosphorylation following D1/5R activation are both novel and inconsistent with previously published literature, more investigation is required to interpret these findings.

Finally, we showed that contrary to previous studies done in non-hippocampal brain regions in slice and culture, we do not detect modulation of fyn phosphorylation of T1472 or T1336 on NR2B NMDAR subunits following D1/5R activation. Our functional data showing intact D1/5R potentiation in fyn KO mice is consistent with a lack of role for fyn tyrosine kinase in mediating the effects of D1/5R activation. While this is in contrast to previous reports implicating fyn tyrosine in D1/5R modulation of NMDARs, it is consistent with our physiology data. It is possible that a different src-family kinase mediates the effects of D1/5R activation in the hippocampus.

Conclusion:

In conclusion, we find that like LTP, D1/5R activation induces lasting, NMDAR-dependent increases in GluR1 and NMDAR (NR2B) surface expression. However, unlike LTP induction, D1/5R activation increases PKA phosphorylation and produces an NMDAR-dependent decrease in CamKII/PKC

phosphorylation of GluR1. We also find that in contrast to previous reports, D1/5R activation does not modulate fyn tyrosine kinase sites on NR2B subunits in acute hippocampal slices. The biochemical mechanisms underling D1/5R potentiation are complex, and further research is needed to interpret the novel changes in GluR1 phosphorylation that accompany D1/5R potentiation of synaptic responses. However, the increases in seen following D1/5R activation in NMDAR and AMPAR surface expression are consistent with changes seen in synapses potentiated by LTP, and lend mechanistic support to our functional data showing D1/5R potentiation of both glutamatergic currents and synaptic field responses.

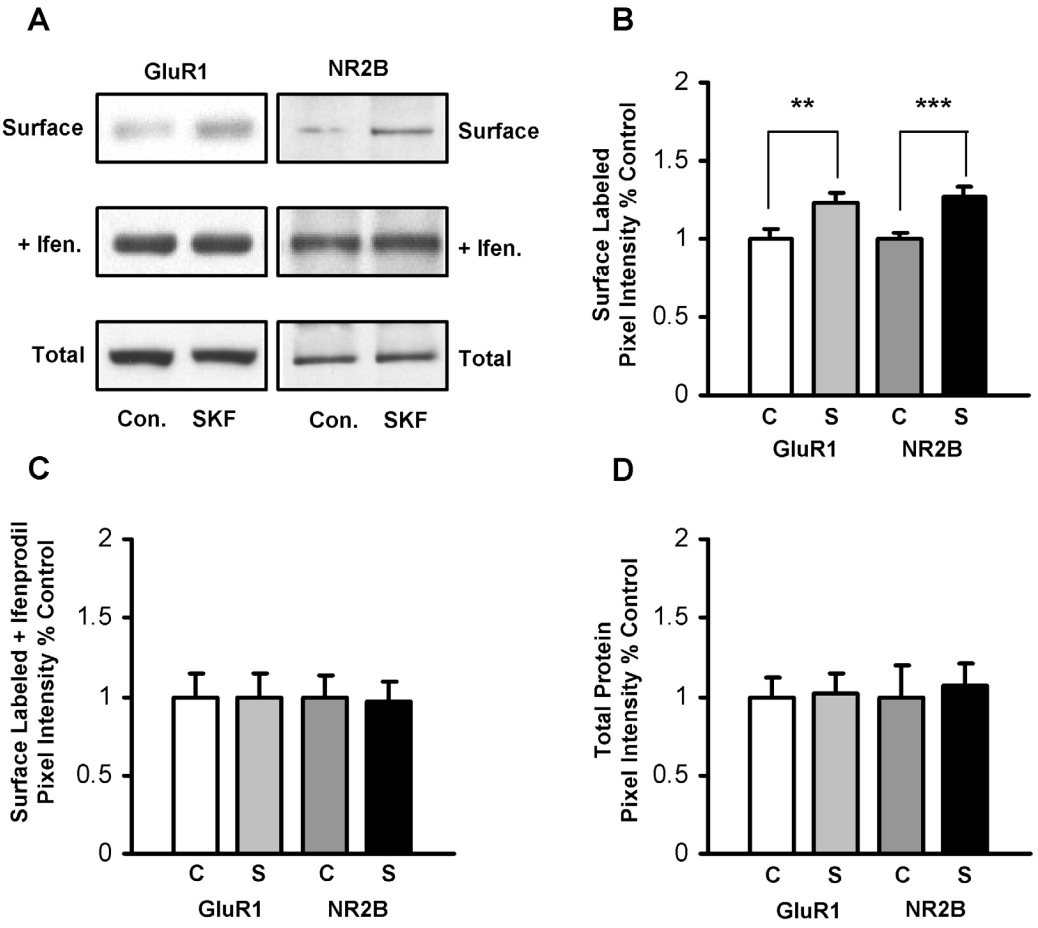

Figure 6.1: D1/5R activation induces an NR2B-dependent increase in surface-labeled GluR1 and NR2B protein. For all panels, C = control, S = SKF-81297. A) Representative blots from slice pharmacology experiments showing surface-labeled and total GluR1 and NR2B protein from control and SKF-81297-treated slices. B) Incubation in SKF-81297 followed by 30 min. drug washout induces an increase in surface labeled GluR1 and NR2B protein. C) Ifenprodil prevents the SKF-81297-induced increase in GluR1 and NR2B surface expression. D) Incubation in SKF-81297 followed by 30 min. drug washout does not change total protein levels of GluR1 or NR2B.

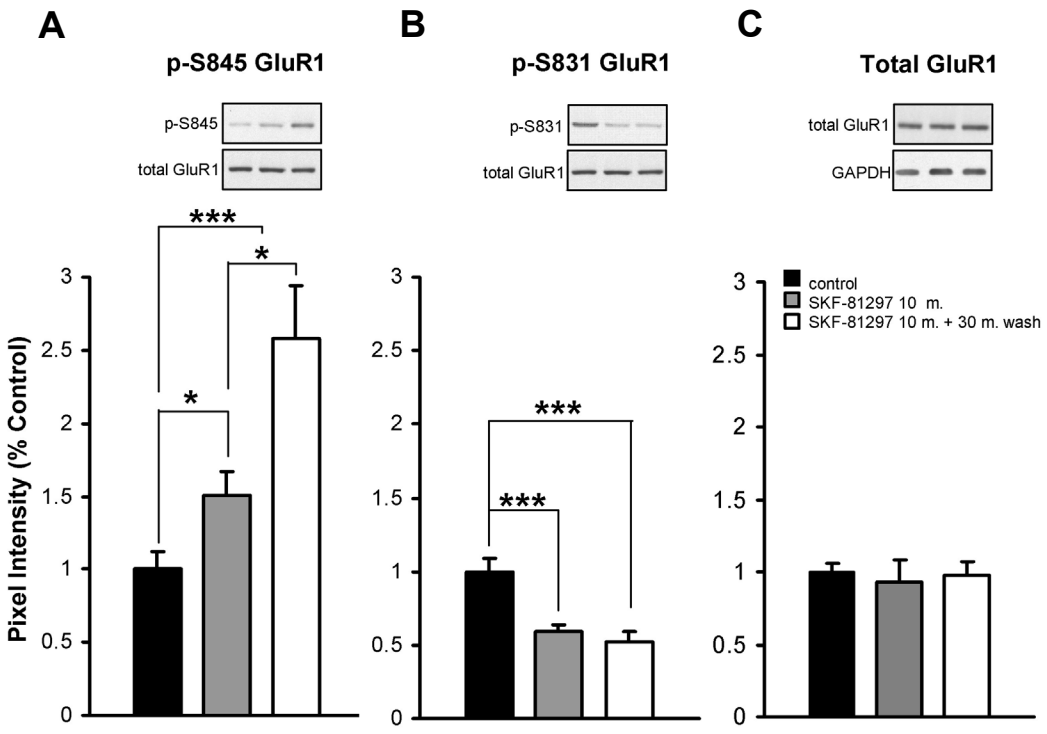

Figure 6.2: D1/5R activation increases GluR1 phosphorylation at S845 and decreases GluR1 phosphorylation at S831. A) Significant increase in p-S845 after 10 min. SKF-81297 application and after 30 min. washout. Inset, representative blot. B) Significant decrease in p-S831 after 10 min. SKF-81297 application and after 30 min. washout. Inset, representative blot. C) No change in total GluR1 protein levels following SKF-81297 application. Inset, representative blot.

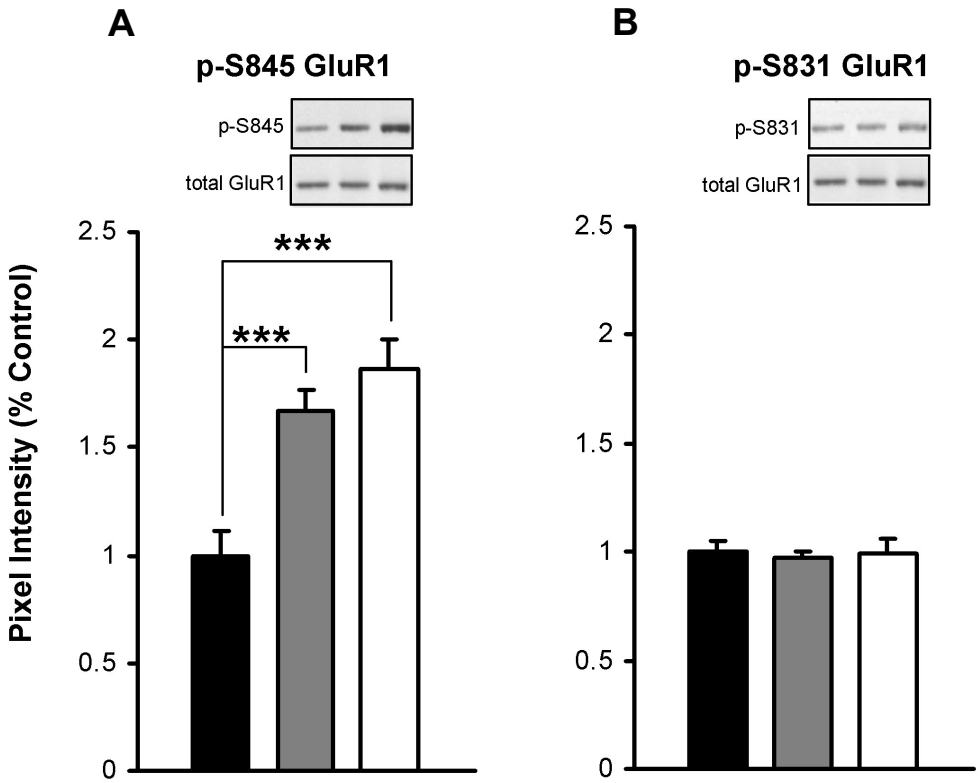

Figure 6.3: NMDAR activity is required for the D1/5R-induced decrease in GluR1 phosphorylation at S831 but not the D1/5R-induced increase in GluR1 phosphorylation at S845. A) Significant increase in p-S845 after 10 min. SKF-81297 application and after 30 min. washout in the presence of APV. Inset, representative blot. B) No change in p-S831 after 10 min. SKF-81297 application and after 30 min. washout in the presence of APV. Inset, representative blot.

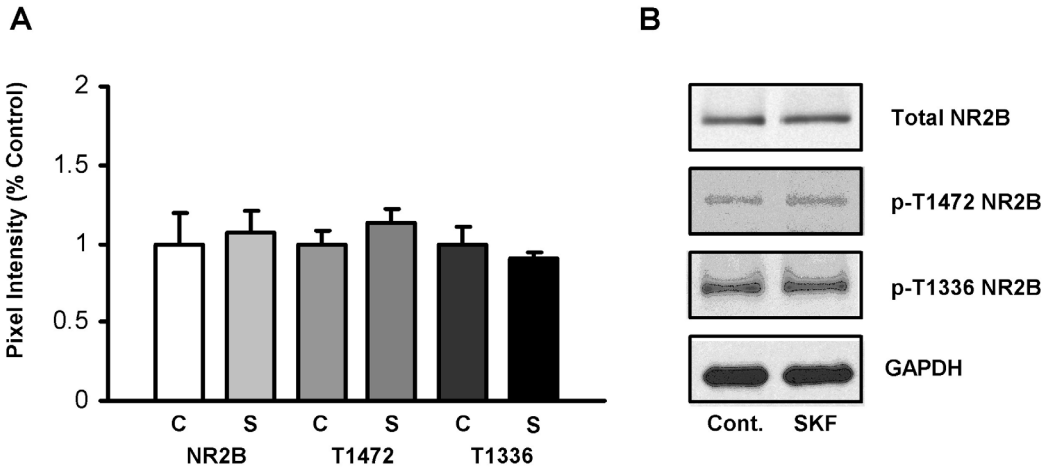

Figure 6.4: D1/5 activation does not change phosphorylation at Fyn tyrosine kinase sites T1472 or T1336 of the NR2B subunit in the hippocampus. A) After 10 minute SKF-81297 treatment followed by 30 minute washout, no change was seen in total NR2B protein normalized to GAPDH, in phospho-T1472 NR2B, or in phospho-T1336. B) Representatve blots showing effect of SKF on total, p-T1472, and p-T1336 NR2B, and GAPDH.

CHAPTER SEVEN

FACILITATION OF HIPPOCAMPAL LEARNING BY D1/5 ACTIVATION DURING MEMORY CONSOLIDATION

Summary:

Using extinction to contextual conditioned fear to measure hippocampal learning, we found that systemic D1/5R activation during memory consolidation facilitated extinction learning. Furthermore, systemic D1/5R activation after fear training enhanced memory retention measured one week later. We suggest that potentiation of glutamatergic neurotransmission following brief D1/5R activation acts as a consolidation promoter that may underlie the cognitive enhancing properties of D1/5R drugs.

Introduction:

D1/5 receptors (D1/5R) are important modulators of hippocampal learning and memory. Studies using local pharmacologic manipulation of D1/5R in area CA1 find that activation of D1/5R signaling improves learning and memory,

while the opposite effect is produced by inhibition of D1/5R activation (Packard and White 1991, Gasbarri et al 1996, Bevilaqua et al 1997, Bach et al 1999). Despite the fact that D1/5R enhancement of learning and memory has been well studied, the mechanism of D1/5R cognitive enhancement remains unknown. We suggest that D1/5R potentiation of glutamatergic neurotransmission may underlie the cognitive enhancing properties of D1/5R drugs.

One aspect of hippocampal memory on which the effects of D1/5R activation have yet to be well characterized is memory consolidation. While it has been shown that D1/5R activation in the hippocampus enhances retention of step-down inhibitory avoidance when given after training (Bevilaqua et al 1997), the effects of D1/5R activation on learning that occurs following memory reactivation and consolidation has yet to be determined.

Long-term memory formation within the hippocampus occurs through consolidation, a process where short-term memory traces stored via modifications in synaptic strength are solidified. A role for LTP in the consolidation of memory is supported by a number of studies that suggest not all relevant LTP-like phenomena are triggered immediately by environmental stimuli (Kim et al 1992, Guzowski and McGaugh 1997, Atkins et al 1998, Steele and Morris 1999, Guzowski et al 2000, Shimizu et al 2000, Day and Morris 2001, Brun et al 2001). Instead, there is a window between 0-4 hours whereby NMDAR activation is required to consolidate memories. (Santini et al 2001). To further support our

argument that D1/5R potentiation is an LTP-like phenomenon, we examined the effect of D1/5R activation during memory consolidation using the hippocampal task of extinction of contextual conditioned fear. We found that D1/5R activation given during the consolidation phase following contextual re-exposure facilitated extinction learning, and we suggest that D1/5R potentiation of glutamatergic neurotransmission may underlie the broad cognitive enhancing properties of D1/5R drugs evidenced during hippocampal tasks.

Experimental Procedures:

Drugs:

SKF-81297 was dissolved in 0.9% saline and made fresh daily. Injections were given with 1 ml insulin syringes and 28-gauge needles. Solutions were prepared at a volume of 5 ml/kg body weight.

Locomotor Activity:

Mice were placed in a fresh home cage with minimal bedding for 2 hr. Horizontal activity was monitored using photobeams linked to computer data acquisition software (San Diego Instruments). Two-way ANOVA was used to analyze the data.

Fear Conditioning:

Fear conditioning was conducted similar to described previously (Cai et al 2006) Briefly, adult (12 week old) C57/BL6 mice were placed in the shock context for 2 min., then a foot shock (0.5 mA, 2 seconds) was delivered three times with a one min. interstimulus interval. Mice remained were immediately returned to their home cage. Freezing behavior was monitored at 10-s intervals by an observer blind to the experimental manipulation. To test for contextual memory 24 h after training, mice were placed into the same training context for 5 min and scored for freezing behavior every 10 s. Extinction training involved daily 5 min exposures to the training context. Reminder shock (0.2 mA, 2 seconds) was delivered three times with a one min. interstimulus interval. A two-tailed t-test was used for two-group comparisons while a two-way ANOVA was used in experiments with multiple groups.

Results:

D1/5R activation increases locomotor activity

In order to examine the effects of D1/5R activation on hippocampal memory consolidation during extinction to contextual conditioned fear, we first determined the effect of SKF-81297 on locomotor activity. Because a freezing response is measured during fear conditioning, drugs that cause locomotor activation that are given during freezing measurements could confound the assessment of freezing

behavior. Adult 10-12 wk C57/BL6 mice were tested for locomotor response every daily. Day one mice were given saline, followed by 0.1, 0.5, and 1 mg/kg SKF-81297 on subsequent days. Each locomotor session consisted of one hour of habituation, followed by drug injection and one hour of locomotor measurement using X-Y beam breaks. Significant locomotor activation was seen at doses of 0.5 and 1 mg/kg SKF-81297 (Figure 7.1, $n = 12$, $p < 0.01$, paired t-test vs. SKF vs. saline). Because the 0.5 mg/kg SKF-81297 dose was minimal yet effective as assayed by locomotor activation, 0.5 mg/kg SKF-81297 was chosen for future experiments.

D1/5R activation facilitates extinction to conditioned fear

We next sought to determine if transient D1/5R activation could produce lasting LTP-like effects at the level of behavioral output. One classical function of the hippocampus is in memory consolidation. Many studies support a role for LTP in hippocampal memory consolidation and a requirement for NMDAR activity (Kim et al 1992, Guzowski and McGaugh 1997, Atkins et al 1998, Steele and Morris 1999, Guzowski et al 2000, Shimizu et al 2000, Day and Morris 2001, Brun et al 2001). D1/5R agonists are well-established to have broad cognitive-enhancing properties (Packard and White 1991, Bevilaqua et al 1997, Bach et al 1999, Gasbarri et al 1996), and we sought to determine if D1/5R activation could act as to promote consolidation and facilitates the conversion of short-term to

long-term memories in the hippocampus. Additionally, the resemblance between D1/5R potentiation and the maintenance phase of LTP makes D1/5R activation an ideal consolidation promoter.

To provide further functional relevance for D1/5R potentiation of glutamatergic neurotransmission, we tested the effect of D1/5R activation on extinction to contextual fear conditioning, a task that involves primarily the hippocampus (Sweatt JD, 2003). We chose to examine the effect of D1/5R activation on memory consolidation rather than memory formation due to the acute locomotor activating properties of D1/5R agonists as previously discussed. Animals were placed in the shock context and allowed to habituate. After shock training with only the context as a cue, mice were re-exposed to the shock context 24 hours later, assayed for freezing behavior, and given an I.P. injection of SKF-81297 (0.5 mg / kg) or saline upon removal from the context. Re-exposure to the context and assessment of freezing followed by SKF-81297 or saline injection was repeated every 24 hours until extinction occurred in both groups (6 days). Animals that received SKF-81297 exhibited extinguished freezing behavior significantly faster than animals receiving saline (Figure 7.2A, $n = 20$ each group, $p < 0.0001$ drug effect, $p < 0.0001$ day effect, ANOVA for repeated measures). To confirm that D1/5R activation facilitates extinction learning and was not causing mice to “forget” the salience of the context, animals were given a sub-threshold reminder shock 28 days after training. Animals that had forgotten the

pairing of aversive shock stimuli to context would be expected to differentially reinstate freezing behavior to these stimuli. The reminder shock however, reinstated freezing equally in both groups (Figure 7.2B, $n = 8$ each group, $p > 0.05$ drug effect, $p < 0.0001$ day effect). Finally, to determine the effect of SKF-81297 in the absence of memory reactivation, mice were given shock training and returned to their home cages. 6 hours later on the same day and for the next six days, mice received an I.P. injection of SKF-81297 (0.5 mg/kg) or saline in their home cage without re-exposure to the context. On day 7 mice were re-exposed to the context and assayed for freezing behavior. Mice that received SKF-81297 in their home cage froze significantly more on the test day than mice that received saline (Figure 7.2C, $n = 9$, $p < 0.05$). This demonstrates that repeated D1/5R activation, even in the absence of memory reactivation, can facilitate retention of freezing behavior measured a week later. We conclude that systemic D1/5R activation facilitates extinction learning in a hippocampal task and may have broad cognitive enhancing properties.

Discussion:

To demonstrate that D1/5R activation has functional relevance at the behavioral level as a consolidation promoter and to further support our argument that D1/5R potentiation is an LTP-like phenomenon, we tested the ability of global D1/5R

activation to facilitate memory consolidation to contextual conditioned fear. We found that similar to other LTP-like phenomena, D1/5R activation facilitates consolidation of memory during extinction learning to contextual conditioned fear. Mice that were given systemic D1/5R agonist after removal from a context paired with an aversive foot shock learned more quickly that the context was no longer paired with the aversive stimulus. During extinction learning, it is likely that LTP occurs not only in response to environmental cues during context-stimuli pairing, but also after contextual cues are no longer present during consolidation of the aversive memory (Santini et al 2001). It is in this latter period that we demonstrate the LTP-like ability of D1/5R activation to serve as a consolidation promoter. Additionally, we showed that in the absence of contextual re-exposure, repeated D1/5R activation facilitates retention of fear memory a week later. DA is released in response to both rewarding and aversive events, and even in the absence of exogenous D1/5R activation, it is possible that the activity of D1/5R receptors is serving not only as a salience signal by enhancing glutamatergic neurotransmission during environmental stimuli, but promotes memory consolidation and retention of the conditions surrounding salient environmental events.

Conclusion:

We conclude D1/5R activation serves as consolidation promoter at the level of cognitive behavioral output. Using extinction to contextual conditioned fear, we found that systemic D1/5R activation facilitated extinction learning by enhancing memory consolidation. We also found that in the absence of memory reactivation, D1/5R activation enhanced memory retention. We conclude that the cognitive-enhancing properties of D1/5R drugs facilitate hippocampal learning and memory consolidation.

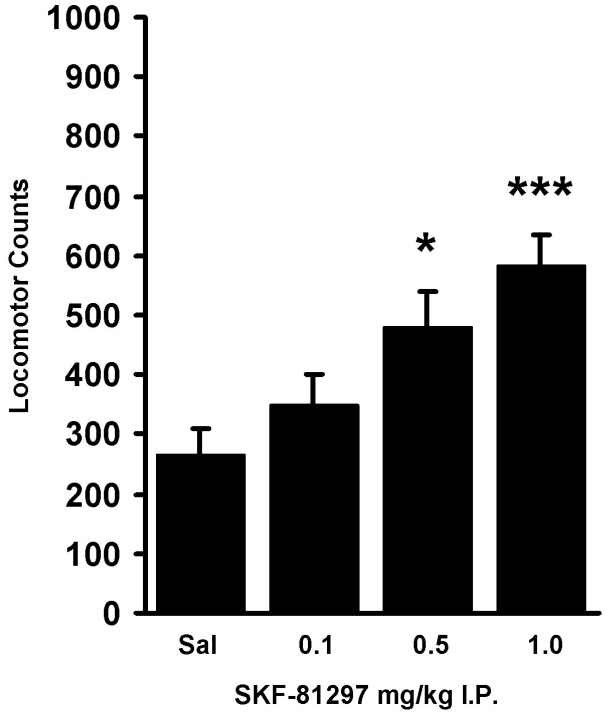

Figure 7.1: Systemic D1/5R increases locomotor activity. Systemic SKF-81297 causes locomotor activation ($n = 12$, $p > 0.05$ for 0.1 mg/kg; $p < 0.01$ for 0.5 and 1 mg/kg).

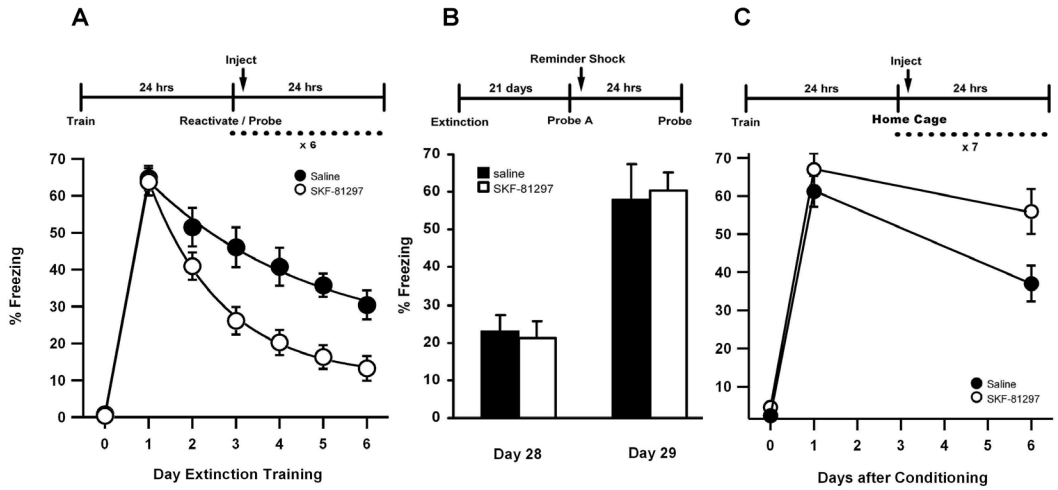

Figure 7.2: Systemic D1/5R activation during memory consolidation facilitates extinction learning to conditioned fear. A) SKF-81297 (0.5 mg/kg I.P.) given after memory reactivation by exposure to the context facilitates extinction learning. Filled circles, saline; open circles, SKF-81297. B) A reminder shock reinstates freezing in SKF-81297 and control groups. Filled bar, saline; open bar, SKF-81297. C) SKF-81297 given daily starting 6 hrs. after fear training facilitates memory retention without re-exposure to the context.

CHAPTER EIGHT

CONCLUSION

Summary:

Dopamine D1/5R activation has well-characterized effects on glutamate receptor function, synaptic plasticity, and behavioral output, however a mechanism linking the molecular changes to functional and behavioral output has yet to be determined. We used pharmacological and genetic manipulation of components downstream of the D1/5R to examine the mechanism underlying D1/5R potentiation of glutamatergic neurotransmission. Using field recordings and surface-labeling of glutamate receptor subunits in acute hippocampal slices, we found that enhancement of synaptic responses by D1/5R activation occurs through a pathway involving NR2B-NMDARs, PKA, PKC, PKMζ, and tyrosine kinase, and that at the cellular level, D1/5R activation induces increases in surface NR2B and GluR1 subunits in an NR2B-NMDAR-dependent manner. Additionally, we showed that D1/5R activation acts as a consolidation signal facilitating extinction learning. We suggest that this mechanism may underlie the broad cognitive-enhancing properties of D1/5R pathway activation, and that

perturbances in this DA/glutamate signaling cascade in the hippocampus may be involved in neuropathologies such as schizophrenia and addiction.

Effect of D1/5R activation on LTP induction.

D1/5R activation during TBS enhances the magnitude of LTP in hippocampal SC-CA1 synapses (Otmakova and Lisman 1996), yet the precise mechanism for this remains unknown. Illuminating the effects of D1/5R activation on LTP is relevant to understanding the broad cognitive-enhancing properties of D1/5R activation on behaviors mediated by the hippocampus and other brain regions, which rely on modulation of synaptic plasticity (Packard and White 1991, Bevilaqua et al 1997, Bach et al 1999, Gasbarri et al 1996). Based on evidence for positive modulatory interactions between D1/5R activation and NR2B-NMDARs (Dunah and Standaert 2001, Dunah et al 2004, Hallett et al 2006, Gao and Wolf 2008) and evidence supporting a role for NR2B in LTP (reviewed in Yashiro and Philpot 2008) we hypothesized that NR2B-NMDARs mediated the enhancing effect of D1/5R activation on LTP. Since NMDARs are necessary for LTP induction, we sought to determine which NMDA subunit was responsible for the effect of D1/5R activation on LTP. We found that NR2B-NMDARs were required for D1/5R enhancement of LTP. Additionally, brief D1/5R activation produced a delayed, sustained enhancement of synaptic responses in the absence of LTP induction. This implies that although direct

D1/5R activation was only present during the induction phase of LTP (during TBS) D1/5R activation was not modulating LTP during induction. We presented evidence that D1/5R synaptic potentiation occurs in an NMDA-dependent, evoked activity-independent, synapse-non-specific manner. However, post-synaptic activity coincident with D1/5R activation was required, and the source of post-synaptic activity may be spontaneous glutamate release. We further showed that D1/5R modulation of LTP and D1/5R modulation of synaptic responses share similar mechanisms requiring NR2B NMDARs, share similar time courses, and share similar magnitudes of potentiation. Although a late-phase (>120 min), synapse-specific, protein synthesis-dependent form of D1/5R potentiation has previously been reported (Huang and Kandel 1995, Navakkode et al 2007), our description is the first to report an early-phase D1/5R potentiation that resembles the maintenance phase of LTP and the first to provide a mechanism linking early-phase D1/5R potentiation to D1/5R potentiation of synaptic plasticity. Our results suggest that D1/5R activation may work through NR2Bs and LTP-like machinery to cause evoked activity-independent potentiation of synaptic responses.

D1/5R potentiation of synaptic responses and LTP share overlapping mechanisms

D1/5R potentiation, like LTP, requires NMDAR activity. If D1/5R potentiation and TBS share similar mechanisms, LTP induction with TBS should occlude D1/5R potentiation by saturating the machinery. When we tested this by

inducing LTP and following it with application of D1/5R agonist during the expression phase, we found no additional effect of D1/5R activation. LTP occluded the effects of D1/5R activation, indicating that D1/5R potentiation and LTP may share some mechanistic similarities. We attempted the reverse by inducing potentiation with D1/5R activation and then inducing LTP with TBS. We found that D1/5R potentiation occluded D1/5R enhancement of LTP, however D1/5R potentiation did not occlude the induction of LTP. This is possibly because D1/5R activation did not saturate the mechanism of potentiation as did TBS. This supports our claim that D1/5R potentiation of LTP and D1/5R potentiation of synaptic responses are results of the same phenomenon. It is possible that this mechanism is also responsible for the reversing effect of D1/5R activation LTD and the inhibitory effect of D1/5R activation on depotentiation that others have reported (Otmakhova and Lisman 1998, Mockett et al 2007).

The similarity between potentiation induced by D1/5R activation and synaptic stimulation during LTP induction is further supported by our finding that D1/5R activation, like LTP, induces a lasting increase in surface expression of GluR1 subunits that is sustained long after induction. The increase in GluR1 surface expression resulting from D1/5R stimulation is NMDAR-dependent, like the increase in GluR1 surface expression seen with LTP induction (Pickard et al 2001). Additionally, it has been reported that LTP induction by synaptic stimulation leads to a rapid increase in surface NMDARs that is dependent on src-

family kinases and PKC in the hippocampus (Grosshans et al 2002). We present a similar mechanism for D1/5R-mediated potentiation that shows necessity of src-family kinases and PKC and results in an increase in surface NR2B-NMDARs. In summary, potentiation by D1/5R activation, like LTP, is delayed in onset, sustained in magnitude long after induction, dependent on NMDAR activity, and involves increases in NMDAR and AMPAR currents and surface expression.

Differences between D1/5R potentiation and LTP

Unlike stimulation-dependent induction of LTP which has a brief temporal requirement for NMDA activation, the window for NMDA activity during D1/5R potentiation is relatively broad. We found that blocking NMDA receptors during acute D1/5R activation did not block potentiation of synaptic responses, unlike experiments done by others where blocking NMDA receptors specifically during LTP induction prevents potentiation (Sarvey et al 1989). We also found that blocking NMDA receptors after washout of D1/5R activation did not block potentiation. These results indicate that the critical period for NMDA activity is much wider for induction of D1/5R potentiation than for induction of LTP. During LTP induction by electrical stimulation, NMDAR activity is only possible during TBS because of channel block by magnesium, while membrane depolarization is the mechanism that gates induction via NMDARs. Because only active synapses are potentiated, LTP only occurs at a specific subset of synapses.

During LTP induction by D1/5R activation, however, it is possible that the signaling cascade remains active long after direct D1/5R activation has ceased. This signaling cascade may both persistently up-regulate NMDARs and act on these NMDARs to induce potentiation, resulting in a much wider temporal window for induction.

While an increase in the AMPA/NMDA is characteristic of LTP, we do not see a change in the AMPA/NMDA ratio following D1/5R activation. This is likely due to the increases seen in both AMPA and NMDA receptor surface localization and synaptic currents. However, AMPA/NMDA was measured only 10 minutes after SKF-81297 application, and its possible that a change might be detectable at a further time point. It has also been reported in the cortex that increases in AMPA contribution initially following LTP induction via synaptic stimulation are accompanied by delayed increases in NMDA current that serves to maintain glutamate receptor contribution to synaptic transmission (Watt et al 2004). Finally, while LTP of naïve synapses is accompanied by an increase in CamKII/PKC phosphorylation, but not PKA phosphorylation, of GluR1 subunits. However, we found that D1/5R activation induces an NMDAR-dependent decrease in CamKII/PKC phosphorylation and an NMDAR-independent increase in PKA phosphorylation of GluR1. These phosphorylation changes resemble those seen during depression of potentiated synapses and during potentiation of depressed synapses, respectively. This data illustrates that although D1/5R

potentiation and LTP share some functional similarity, they are characterized by mechanistically distinct changes in the biochemical states of glutamate receptors. In summary, D1/5R delayed potentiation appears to work through a protracted LTP-like NMDAR-dependent induction process.

Relevance to memory consolidation

Long-term memory formation within the hippocampus occurs when short-term memory traces stored via modifications in synaptic strength in the hippocampus are solidified through the process of consolidation. A role for LTP in the consolidation of memory is supported by a number of studies that suggest not all relevant LTP-like phenomena are triggered immediately by environmental stimuli (Kim et al 1992, Guzowski and McGaugh 1997, Atkins et al 1998, Steele and Morris 1999, Guzowski et al 2000, Shimizu et al 2000, Day and Morris 2001, Brun et al 2001). To demonstrate that D1/5R activation has functional relevance at the behavioral level to enhance consolidation, we show that D1/5R activation facilitates consolidation of memory during extinction learning to contextual conditioned fear. When mice were given systemic D1/5R agonist during the consolidation period, they more rapidly learned that the context was no longer paired with an aversive stimulus. During extinction learning, it is likely that LTP occurs not only in response to environmental cues during within session context-stimuli pairing, but also between sessions when contextual cues are no longer

present during consolidation of the extinction learning. It is in this latter period that we demonstrate the LTP-like ability of D1/5R activation to serve as a consolidation signal. Additionally, we showed that in the absence of contextual re-exposure, repeated D1/5R activation facilitates retention of fear memory a week later. Our finding that D1/5R potentiation resembles the maintenance phase of LTP is consistent with our behavioral data supporting the role of D1/5R activation as a consolidation signal. DA is released in response to both rewarding and aversive events (Iverson and Iverson 2007), and even in the absence of exogenous D1/5R activation, it is likely that the activity of D1/5R receptors is serving not only as a salience signal that potentiates glutamatergic neurotransmission during environmental stimuli, but also enhances consolidation and memory retention of the conditions surrounding salient events.

CHAPTER NINE

OPTIMISATION OF EXPERIMENTAL CONDITIONS

Summary:

In order to determine the mechanism of D1/5R enhancement of LTP, we first characterized the effect of pharmacological antagonists on synaptic field responses and LTP. Inhibitory signaling through $GABA_A$ receptors reduced SC-CA1 synaptic field responses by nearly half. Additionally, both L-type and T-type VGCCs made measurable contributions to synaptic field responses. In isolated NMDA fEPSPs, NR2B-NMDARs contributed to over half the synaptic response. Next, we sought to optimize a protocol for inducing LTP. We characterized a number of LTP induction protocols, and LTP induction by 30 TBS was chosen for future experiments, as LTP induction was reliable in the absence of L-type VGCCs and NR2B-NMDARs. As reported by others, we found D1/5R enhancement of LTP under our experimental conditions. Furthermore, we excluded the involvement of $GABA_A$ or L-type VGCC signaling in mediating the effects of D1/5R activation on LTP.

Introduction:

Previous studies show D1/5R activation decreases inhibitory $GABA_A$ signaling and increases currents through L-type voltage-gated calcium channels (VGCCs; Byrnes et al 1997, Galarraga et al 1997, Hernandez-Lopez et al 1997, Liu et al 2004, Hernández-Echeagaray et al 2006). Decreases in inhibition following D1/5R activation potentially enhance synaptic field responses in the absence of LTP induction, while increases in L-type VGCC current potentially facilitate LTP induction via an NMDAR-independent mechanism. We hypothesized that D1/5R activation works through NMDARs to enhance LTP induction, and it became necessary to prevent potential confounds using specific pharmacological inhibitors of $GABA_A$s and L-type VGCCs. Our first goal was to characterize the effects of pharmacological inhibitors on synaptic field responses and LTP to determine optimal drug concentrations for future experiments.

Previous LTP studies use a variety of LTP induction protocols. We further sought to determine a "physiologically relevant" induction protocol to use in our experiments. An optimal protocol would be weak enough not to saturate LTP machinery and allow detection of LTP modulation, yet strong enough to induce LTP in the absence of L-type VGCC and NR2B-NMDAR signaling. Finally, we sought to replicate previous work and confirm brief D1/5R activation prior to LTP induction could enhance LTP under our experimental conditions.

Experimental Procedures:

Acute Hippocampal Slice Preparation

Adult 6-12 wk. C57/BL6 mice (Jackson Labs) were anesthetized with isoflurane, rapidly decapitated, and brains were immediately placed in ice-cold cutting solution (in mM): sucrose 254, dextrose 10, NaH_2PO_4 1.25, $NaHCO_3$ 24, $CaCl_2$*2(H_2O) 2, $MgSO_4$*7(H_2O) 2, KCl 3) saturated with carbogen gas (95% O_2, 5% CO_2). 400 µm para-transverse hippocampal slices were made using a vibrating tissue slicer (Vibratome, St. Louis, MO) and transferred to a holding chamber containing room temperature ACSF. Slices were allowed to recover at least one hour before use.

Synaptic Field Recording

Acute hippocampal slices were placed in a RC-26 submersion recording chamber (Warner, Hamden, CT) at room temperature. A stimulating electrode (CED255, FHC, Bowdoin, ME) was placed in the Schaffer Collaterals near CA2 and a glass recording electrode (1-2 MΩ) filled with ACSF was placed in the Schaffer Collaterals in CA1. Field responses were elicited with a biphasic stimulus delivered via a stimulus isolator (BSI-950, Dagan, Minneapolis, MN) and stimulation intensity was adjusted until field responses were within 30-60%

of the linear response range. Field responses were recorded with an Axoclamp 2B amplifier (Axon instruments, Foster City, CA) and digitized using an ITC-18 digital/analog converter (Instrutech, Port Washington, NY). Responses were stored on a Dell PC. Data acquisition and analysis was conducted using custom software in Igor Pro (Wavemetrics).

Drugs and Solutions

Artificial cerebrospinal fluid (ACSF) for slice experiments consisted of (in mM); NaCl 125, KCl 2.5, NaH_2PO_4 1.25, $MgCl_2$*6(H_2O) 1, $CaCl_2$*2(H_2O) 2, $NaHCO_3$ 25, and Dextrose 25. All drugs were aliquoted and stored at -20°C. Fresh drug aliquots were used for each experiment. To activate D1/5R receptors SKF-81297 (Tocris) in DMSO was added to ACSF to a final concentration of 10 μM. To block NR2B NMDARS, Ifenprodil (Tocris) in ethanol was used at 3 μM. To block NMDA receptors, APV (Tocris) dissolved in 1 equivalent NaOH and water was used at 50 μM. To block $GABA_A$ signaling, picrotoxin (Sigma-Aldrich) in ethanol was used at 50 μM. To block L-type VGCCs, nimodipine (Tocris) was used at 10 μM. To block AMPARs, NBQX (Tocris) was used at 50 μM.

Statistics and analysis:

Experimental conditions were interleaved and group comparisons were made using either paired or unpaired two-tailed student's t-tests. Results were considered statistically significant if P value was less than 0.05.

Results:

Determination of LTP induction protocol

We first sought to optimize a protocol for LTP induction. An ideal protocol would induce robust LTP, yet not be so strong that modulation of LTP would be undetectable due to saturation. Previously, high-frequency stimulation (HFS) has been used to study D1/5R modulation of LTP (Otmakhova and Lisman 1996). High frequency stimulation is a strong induction protocol, and we thought theta-burst stimulation (TBS), which mimics the neural activity of a behaving animal, would be more physiologically relevant. Furthermore, by varying the number of theta bursts during induction, different magnitudes of LTP can be induced. It is possible a greater effect of D1/5R activation on LTP might be measurable with TBS compared to HFS.

Hippocampal field responses were evoked using a stimulating electrode placed in the SC and measured with a recording electrode placed in the striatum radiatum (SR) of CA1 (Figure 9.1 A). To ensure modulation of field responses could be detected, responses within the linear range of stimulation were used

(Figure 9.1 B). Three different LTP induction protocols were tested: 2 TBS, 50 Hz stimulation for 1 min., and 10 TBS (Figure 9.1 C). We found significant LTP in response to each stimulation protocol measured by the average increase in field response 30-40 min. following LTP induction. 2 TBS produced moderate LTP (Figure 9.2 A, 19.8 ± 6.1%, $n = 5$, $p < 0.05$), as did 50 Hz stimulation for 1 minute (Figure 9.2 B, 20.0 ± 6.4% $n = 8$ $p < 0.01$). A larger magnitude of LTP was produced using 10 TBS (Figure 9.2 C, 41.6 ± 10.1% $n = 6$, $p < 0.05$). These results are summarized in Figure 9.2 D. We conclude 10 TBS produces robust LTP and choose it for subsequent experiments.

Characterization of drug effects on SC-CA1 field response

In order to isolate D1/5R effects to modulation of NMDARs, it was necessary to use drugs to block $GABA_A$ receptors and L-type voltage VGCCs, both of which can modulate LTP and are modulated by D1/5R activation (Byrnes et al 1997, Galarraga et al 1997, Hernandez-Lopez et al 1997, Liu et al 2004, Hernández-Echeagaray et al 2006). We found that removing $GABA_A$ inhibition produced a near doubling of synaptic response (Figure 9.3, 93.6 ± 29.4% $n = 5$, $p < 0.05$). Following stable baseline recording, the $GABA_A$ antagonist picrotoxin (50 μM) was bath-applied for 10 min. and the response was monitored another 10 min. The increase in synaptic field response was determined by comparing average

response 10 min. following picrotoxin application to average response during 10 min. baseline.

VGCCs also contributed to SC-CA1 synaptic responses. Blocking L- and T-type VGCCs with nimodipine (10 μM) and nickel chloride (100 μM) reduced the synaptic response (Figure 9.4, 52.7 ± 7.1%, n = 3, p = 0.05). Following baseline recording, nimodipine and nickel chloride were bath-applied for 10 min. and the average response for 10 min. following VGCC antagonist application was measured and compared to the average response during 10 min. baseline. After the response in nimodipine and nickel chloride stabilized, the specific NR2B-NMDAR antagonist ifenprodil (3 μM, Williams et al 1993) was added on top of the VGCC antagonists. This resulted in a significant reduction in synaptic response (Figure 9.4, 65.0 ± 4.7%, n = 3, $p < 0.01$).

Although synaptic field responses are mostly due to current through AMPARs, we sought to determine what contribution NR2B-NMDARs made to isolated NMDA field responses to confirm the action of ifenprodil. Using NBQX (10 μM) and a very high stimulation intensity, we evoked NMDAR field responses. Following stable baseline, we bath-applied ifenprodil (3 μM) for 10 minutes. This produced a significant decrease in NMDA-fEPSP area (Figure 9.5, 19.8 ± 5.6%, n = 4, $p < 0.0001$). From these experiments examining the effect of pharmacological antagonists on synaptic field responses, we conclude that $GABA_A$,VGCCs, and NR2B-NMDARs all make significant contributions to

synaptic responses in SC-CA1, and manipulations that modulate these receptors and channels have the potential to effect synaptic field responses.

Characterization of drug effects on LTP

Prior to investigating D1/5R modulation of LTP, is was necessary to characterize the effects of antagonists that would be used on LTP induction to ensure that LTP could reliably be induced using our experimental conditions. We also sought to replicate the finding reported by Otmakhova and Lisman of D1/5R-mediated enhancement of LTP under our experimental conditions. As previously mentioned, the L-type VGCC antagonist nimodipine is required to rule out D1/5R modulation of L-type VGCCs in D1/5R potentiation of LTP, as D1/5R activation could modulate LTP induction through this mechanism in addition to NMDARs. We found that blocking L-type VGCCs with nimodipine (10 μM) did not prevent the induction of LTP with 10 TBS (Figure 9.6, 53.9 ± 25.4, $n = 4$, $p < 0.05$).

To replicate previous reports of D1/5R-mediated enhancement of LTP under conditions to isolate D1/5R effects to NMDARs during LTP induction, we bath-applied the D1/5R agonist SKF-81297 (10 μM) for 10 min. prior to LTP induction with 10 TBS. Picrotoxin (50 μM) and nimodipine (10 μM) were included throughout the experiment, and control and SKF-81297 experiments were interleaved to avoid systematic bias. We found that as previously reported in drug free ACSF using HFS, 10 min. D1/5R activation also potentiates LTP

induced by 10 TBS in the presence of picrotoxin and nimodipine (Figure 9.7, control LTP: 41.6 ± 10.2; n = 6. SKF-%81297 LTP: 102.0 ± 26.4%; n = 7. $p < 0.01$ 2-tailed unpaired t-test). Because we reproduced this initial finding under our experimental conditions, we concluded that we could now begin to pharmacologically explore the mechanism responsible for D1/5R enhancement of LTP.

We hypothesized that D1/5R enhancement of LTP required NR2B-NMDARs, and to test this hypothesis we sought to repeat the D1/5 LTP

However, LTP failed to be induced by 10 TBS in the presence of ifenprodil (Figure 9.8, n = 5, $p > 0.05$). This was not surprising given ifenprodil blocked a considerable amount of NMDAR response as shown in Figure 9.4 and Figure 9.5. To overcome this, we used a stronger stimulation of 30 TBS and found that in the presence of ifenprodil, LTP could be reliably induced (Figure 9.8, 51.3 ±13.3%, n = 4, $p < 0.01$). Given this, we concluded that for future experiments to determine the mechanism of D1/5R enhancement of LTP, an induction protocol of 30 TBS should be used.

Discussion:

Prior to dissecting a mechanism for a phenomenon with pharmacological tools, it is important to first systematically examine effects of those pharmacological

agents on both specific and non-specific targets. Optimization of experimental conditions and tools is essential to creating a strong foundation for future experiments. In order to test specific hypothesis regarding the mechanism for D1/5R enhancement of LTP, we sought to isolate effectors of D1/5R activation that potentially influence LTP. Because previous studies show that D1/5R activation decreases inhibition, increases current through L-type VGCCs (Byrnes et al 1997, Galarraga et al 1997, Hernandez-Lopez et al 1997, Liu et al 2004, Hernández-Echeagaray et al 2006), and could influence induction of LTP, it we removed the contribution of these mechanisms. When inhibition, L-type VGCCs, and a subset of NMDARs were blocked, the LTP induction protocol had to be optimized to produce a reliable amount of LTP without saturation. Finally, to confirm that our system was capable of reproducing published results, we replicated D1/5 enhancement of LTP under our experimental conditions.

Conclusion:

We conclude that using an optimized LTP induction protocol of 30 TBS, we can induce LTP with a subset of NMDARs active (in the presence of ifenprodil) and that D1/5R enhancement of LTP occurs without changes in L-type VGCC or inhibitory contribution.

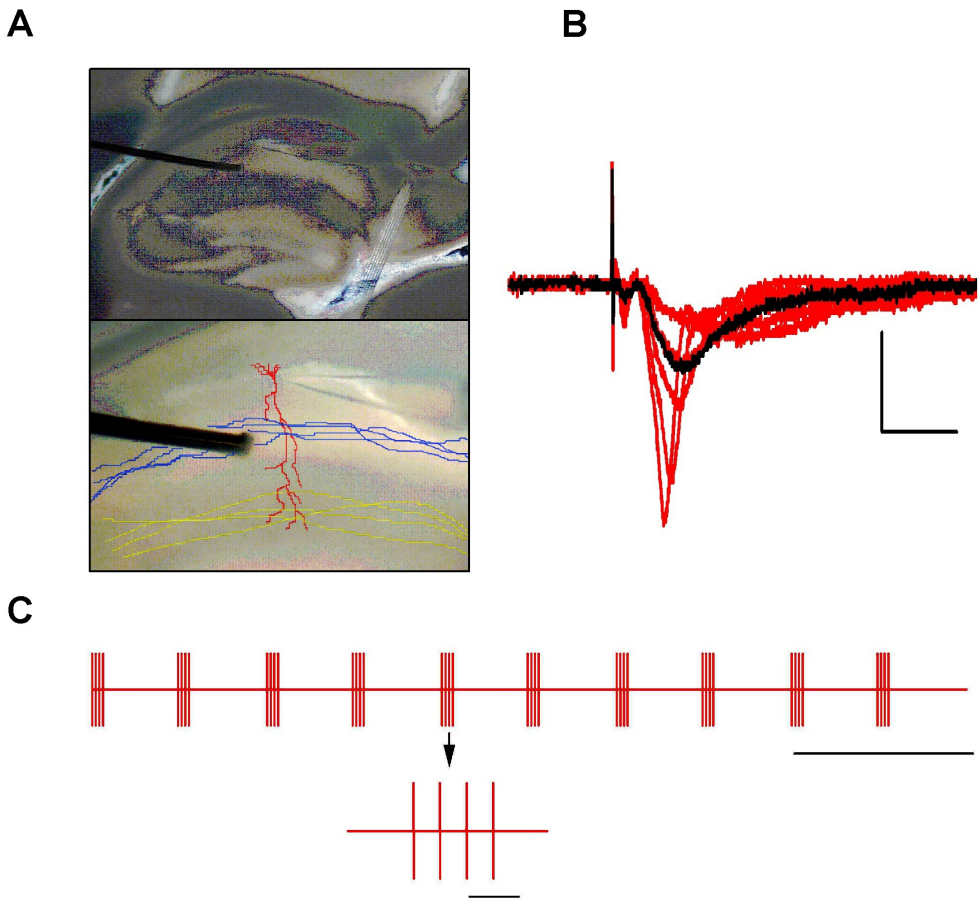

Figure 9.1: Experimental Recording Configuration.
A) Image of hippocampal slice and position of stimulating (metal) and recording (glass) electrodes in SC-CA1 (blue). Orientation of CA1 pyramidal neurons is shown in red. Yellow indicates the temporo-ammonic pathway. B) Representative field response elicited by optimal stimulation intensity shown in black. Red indicates response to entire range of stimulation intensities. Scale bar: 1 mV y-axis; 10 ms x-axis. C) Theta-burst stimulation. One theta burst consists of four 0.1 ms bi-phasic pulses separated delivered at 100 Hz. Each burst is delivered every 200 ms. Top scale bar, 500ms. Bottom scale bar, 20 ms.

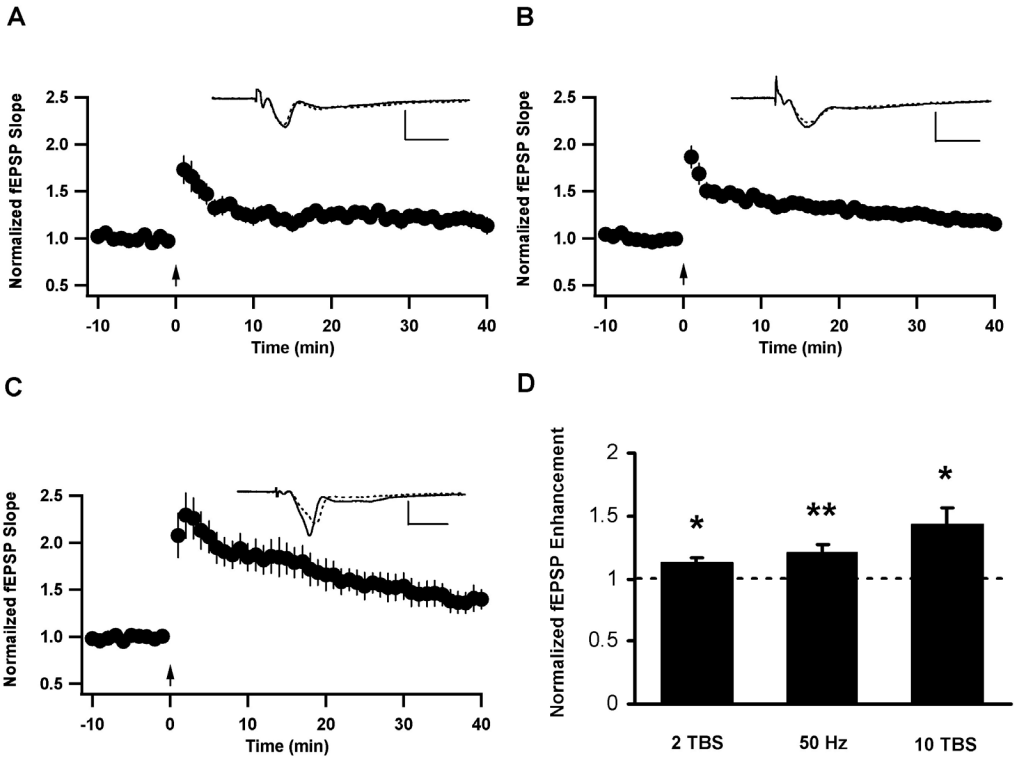

Figure 9.2: Characterization of LTP Induction Protocols. A) LTP induced by 2 TBS. B) LTP induced by 50 Hz stimulation for 60 sec. C) LTP induced by 10 TBS. For all panels: inset: dotted trace, average baseline; solid trace, average 30-40 minutes after LTP induction. Scale Bar: 1 mV y-axis, 10 ms x-axis. D) Bar graph comparing amount LTP resulting from each induction protocol.

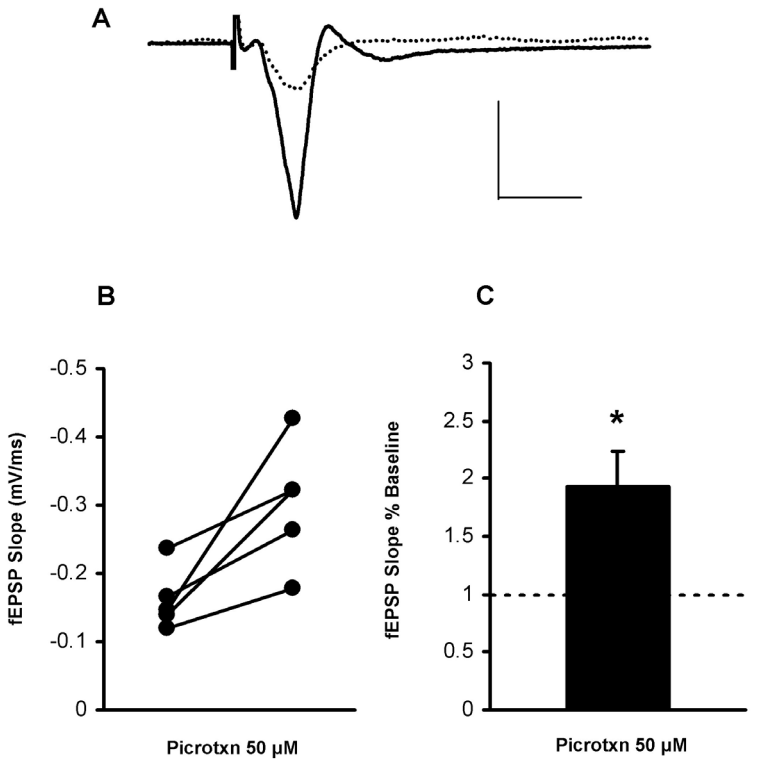

Figure 9.3: Effect of $GABA_A$ inhibition on synaptic field response
A) Representative trace before (dotted) and after (solid) 50 µM picrotoxin application. B) Connected dots represent outcomes of individual experiments. C) Removing $GABA_A$ inhibition increases the synaptic field response.

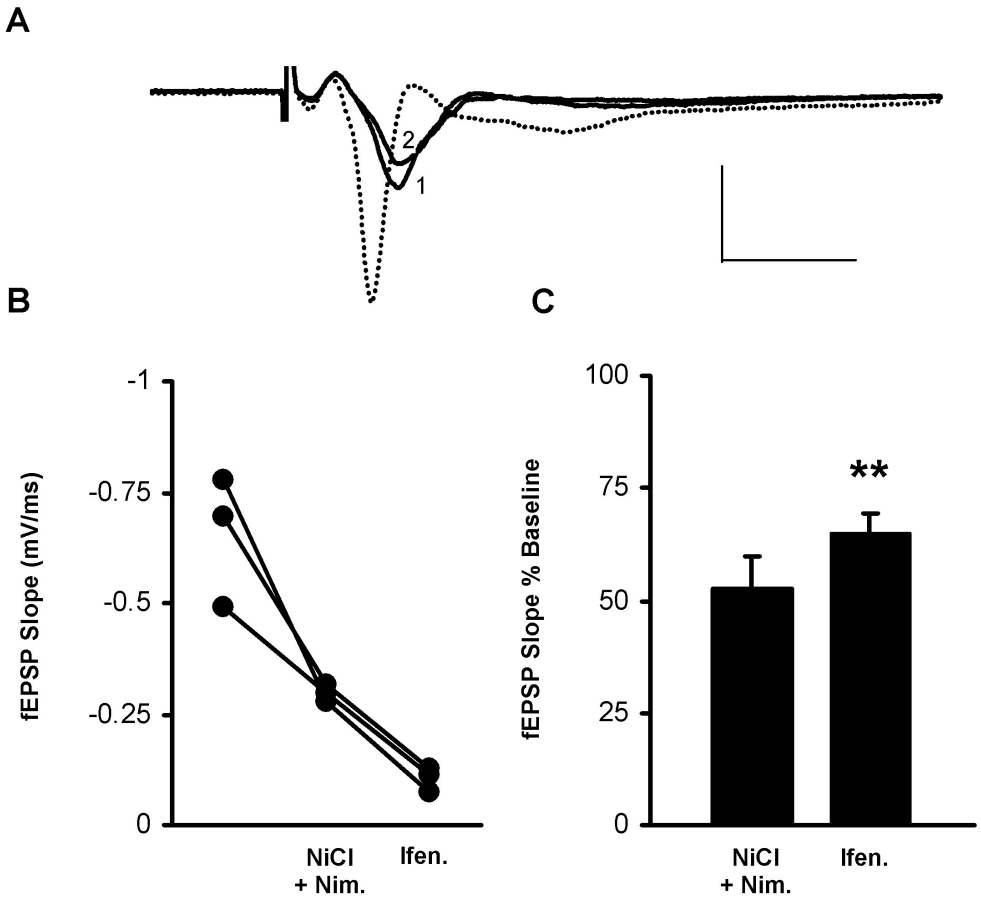

Figure 9.4: Effect of L-type and T-type VGCCs and NR2B-NMDARs on synaptic field response. A) Representative trace before (dotted) and after NiCl (1) and ifenprodil (2) application. Scale bar: 1 mV y-axis; 10 ms x-axis. B) Connected dots represent outcomes of individual experiments. C) Blocking VGCCs and NR2B NMDARs reduces the synaptic field response.

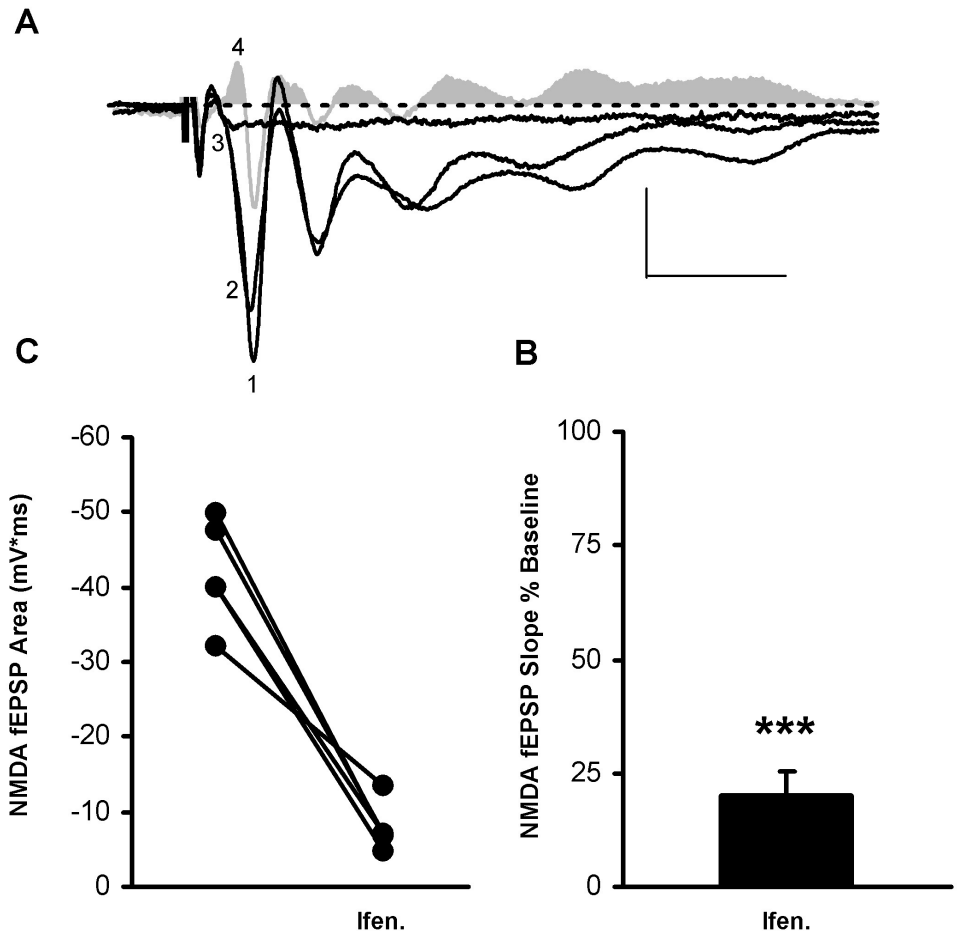

Figure 9.5: Effect of NR2B-NMDARs on isolated NMDA fEPSPs.
A) Representative trace before (1) and after (2) and ifenprodil application and after APV application (3). Gray trace (4) represents ifenprodil-sensitive component of NMDA fEPSP. bar: 0.5 mV y-axis; 20 ms x-axis B) Connected dots represent outcomes of individual experiments. C) Blocking NR2B NMDARs reduces isolated NMDAR field response.

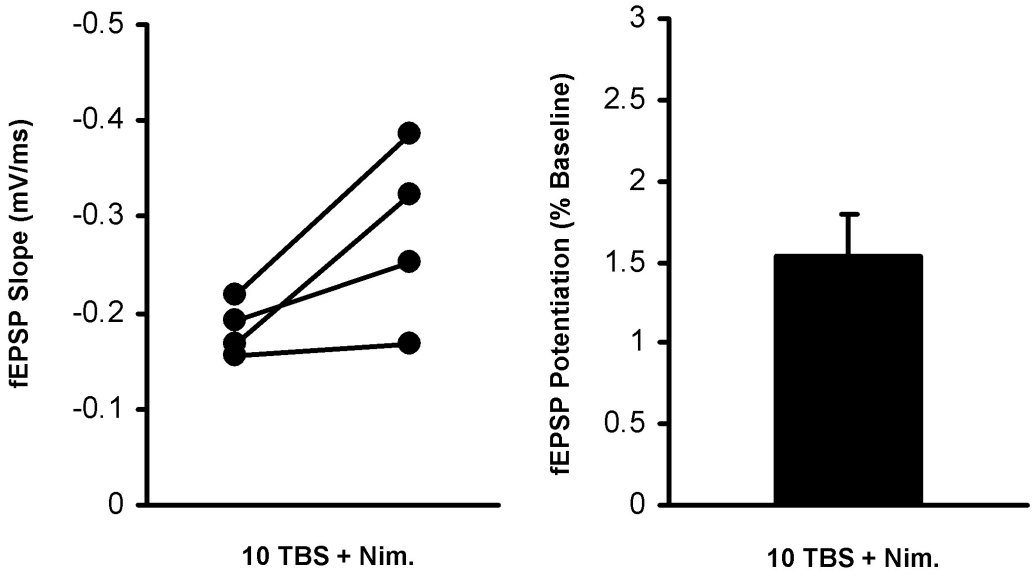

Figure 9.6: LTP induction at SC-CA1 synapses does not require L-type VGCCs

A) Connected dots represent outcome of individual experiments. B) Bar graph representing amount of LTP induced from 10 TBS in the presence of nimodipine.

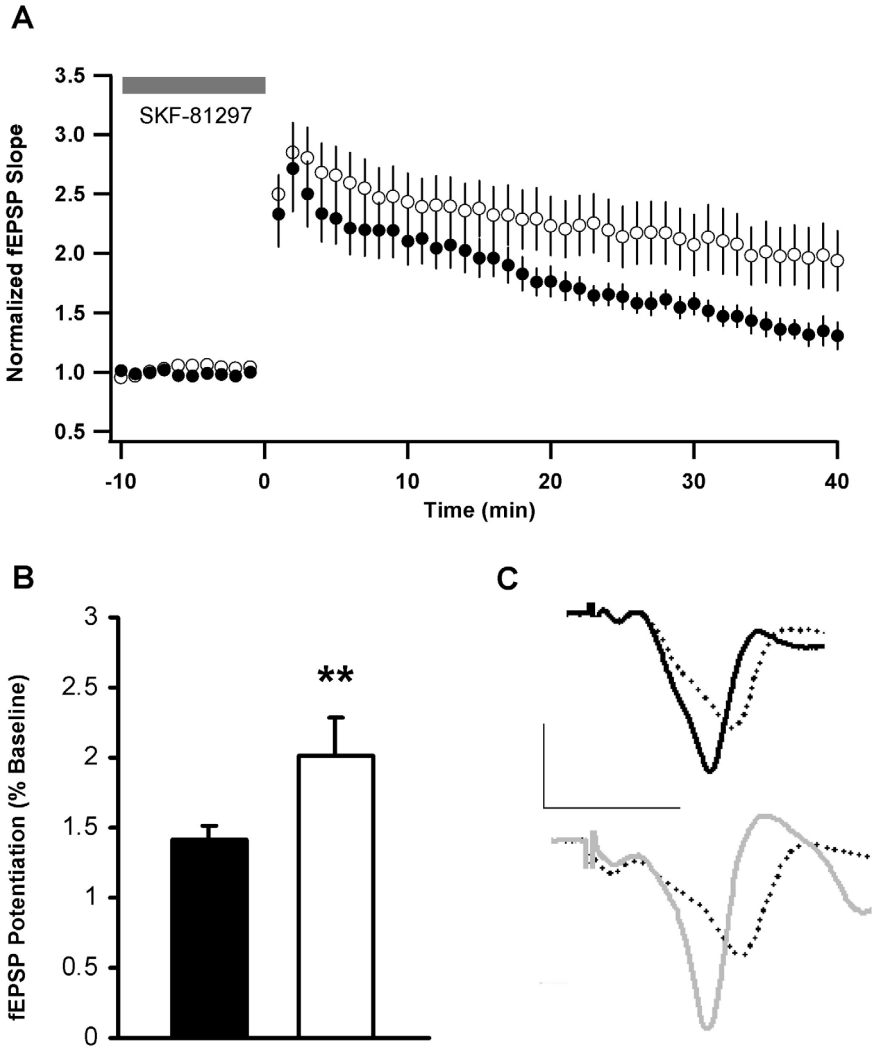

Figure 9.7: Effect D1/5R activation enhances LTP

A) SKF-81297 enhances LTP in the presence of nimodipine and picrotoxin. B) Bar graph representing LTP enhancement by D1/5R activation. C) Representative LTP traces (baseline, dashed; black, control; grey, SKF-81297).

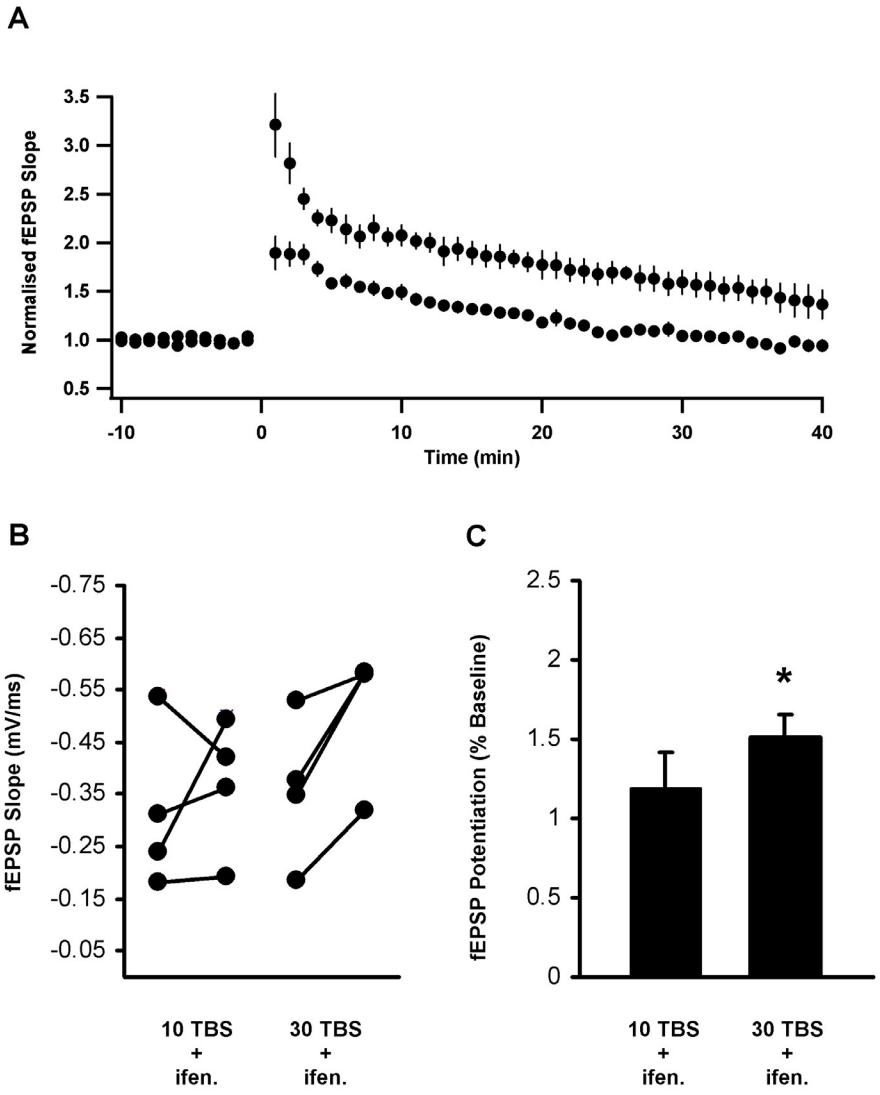

Figure 9.8: Effect of Ifenprodil on LTP induction

A) LTP induced by 10 TBS was blocked by ifenprodil, however 30 TBS could induce LTP in the presence of ifenprodil. B) Connected dots represent outcomes of individual experiments. C) Bar graph representing amount of LTP in each condition.

APPENDIX

DATA ACQUISITION AND ANALYSIS MACROS FOR IGOR PRO

Written by Leah Leverich and Don Cooper Ph.D

Field EPSP Data Acquisition Macro:

Used for online monitoring of field EPSP slope and peak measurements and to maintain digital record of experimental manipulations. Variations of this macro were used to acquire inward and outward whole-cell EPCS data. Data acquisition macro is first illustrated with screen shots.

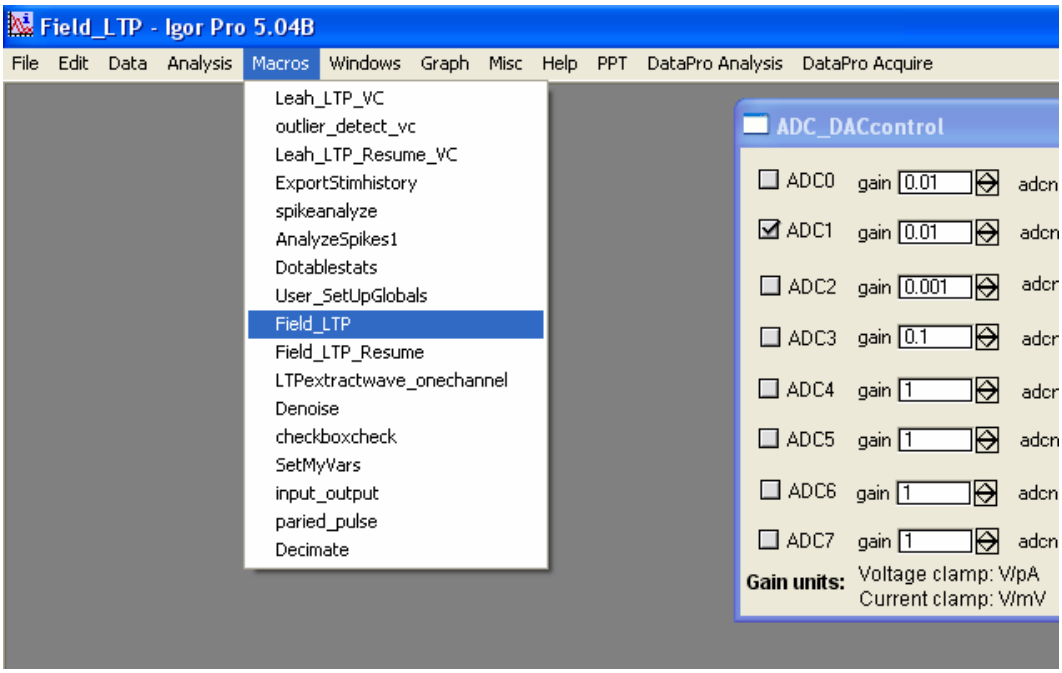

Appendix 1.1: Field Data Acquisition Program in Datapro5.
Select Field_LTP from the macros menu.

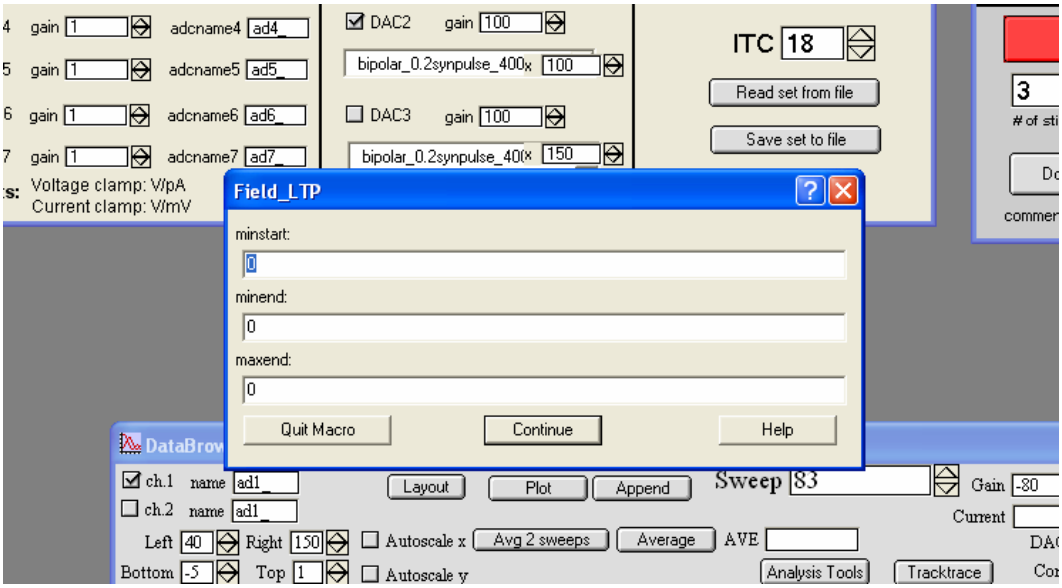

Appendix 1.2: Enter in user programmable variables. These are the x-values the program uses to determine the maximum and minimum y values of the fEPSP in order to calculate the slope and peak.

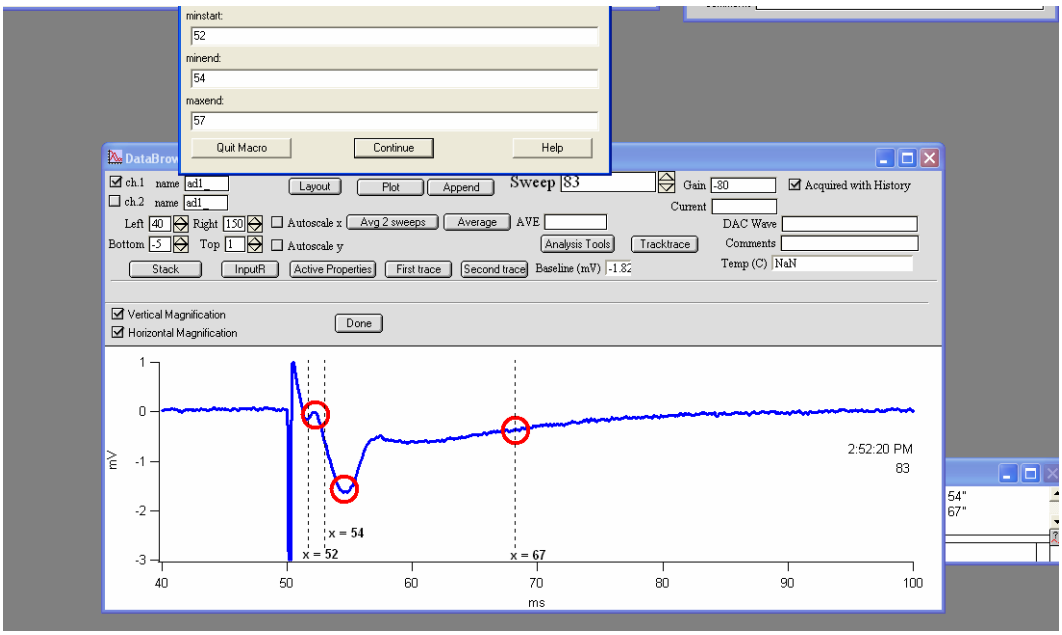

Appendix 1.3: Explanation of user programmable variables. Representative fEPSP with minimum, maximum, and end-range values circled in red. Dashed lines represent the x-values entered by the user that allow the programs to determine these values. Note: mark-up does not appear in actual program.

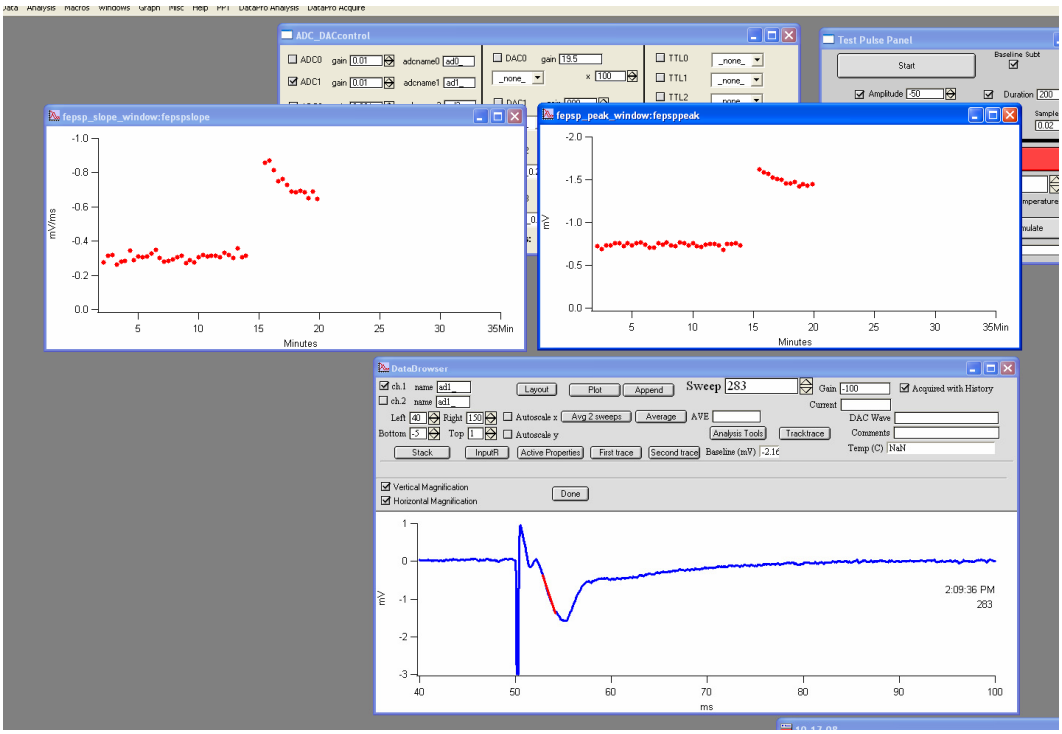

Appendix 1.4: Online monitoring of fEPSP peak and slope. Left graph shows slope vs time, and right graph shows peak vs. time, of representative response in data browser window below. The fit for line plotted in fEPSP slope is appended to response in databrowser window for online monitoring of fit function.

Igor code for Field_LTP data acquisition macro; comments are in bold.

```
#pragma rtGlobals=1
// Use modern global access method.

Macro Field_LTP(minstart,minend,maxend)
// user defined variables. The range (minstart, minend) sets where to find minimum point of fepsp after fiber volly. Range (minend, maxend) sets where to find peak of fepsp
variable howlong,stimint, starttime, endtime, baseline, peak, slpstart, slpend, fepsphalfmax,  peakloc, leftpt, rtpt
//variables that are only used in this macro
variable  minstart,minend,maxstart,maxend, initialslopeslope, finalslopeslope, slopechangeslope, initialpeakslope, finalpeakslope, slopechangepeak
variable slpstartloc, slpendloc, fibervollymax, fibervollymaxloc, fepspmin, fepspminloc, fepspmax, fepspmaxloc
variable/G universaltime,howlong2, time2, peak_avgbaseline, slope_avgbaseline, Gminstart, Gminend, Gmaxend
//global variables, can be accessed from other macros

    howlong=60
// sets duration of baseline recording
    stimint=20
// time between stimulations
    maxstart=minend
    Gminstart=minstart
// makes user-defined paramaters global variables so they can be used in LTP Resume program
    Gminend=minend
    Gmaxend=maxend
//dowindow/k fepsp_peak_baseline_window // kills window if it has aleady been called (prevents multiple windows from accumulating)
  dowindow/k fepsp_peak_window
  dowindow/k fepsp_slope_window
    howlong2=howlong
    universaltime=datetime
// sets starting time of experiment in number of seconds since 1904, will be used as x-value of points (in seconds) of fepsp peak and slope waves in windows
    time2=0
  make/o/n=10000 fepspslope
```

```
// created wave named "fepspslope" that will be used to store slope values
    fepspslope=nan
// makes points in the wave not appear on graph until they are defined
  make/o/n=10000 fepsppeak
    fepsppeak=nan
  make/o/n=10000 percentpeakbaseline
    percentpeakbaseline=nan
  make/o/n=10000 percentslopebaseline
    percentslopebaseline=nan

    DoDataAcq()
// runs macro that delivers stimulus and acquires data
    SaveStimHistory(0)
// runs macro that saves stimulus information to stim history

  smooth 10,$newwave1
  wavestats/q/r=(1, 48) $newwave1
    baseline=v_avg
// determines baseline by averaging first 48 ms of  wave before stimulus
artifact
  wavestats/q/r=(minstart,minend) $newwave1
    fepspmin=v_max
// determines minimum value of fepsp
  findlevel/q/r=(minstart,minend) $newwave1, fepspmin
    fepspminloc=v_levelx
// finds x coordinate that corresponds to "epspmin" y-value, value will be
used for slope-fitting
  wavestats/q/r=(maxstart,maxend) $newwave1
    fepspmax=v_min
// determines maximum fEPSP amplitude
  findlevel/q/r=(maxstart,maxend) $newwave1, fepspmax
    fepspmaxloc=v_levelx
// finds corresponding x coordinate to max epsp value, will be used for slope
fitting
    fepsppeak[time2]=fepspmax-baseline
// subtracts baseline from epsp max, giving an absolute amplitude. Sets this
as y-value for a point in wave "fepsppeak" (appears in fepsp peak window),
x-vaue is time in seconds
    fepsphalfmax=(((fepspmax-fepspmin)/2)+fepspmin)
    slpstart=fepsphalfmax-(0.3*(fepspmax-fepspmin))
// finds y-value on fepsp that is 20% between the max and min
```

```
    slpend=fepsphalfmax+(0.3*(fepspmax-fepspmin))
// finds y-value on fepsp that is 80% between the max and min
  findlevel/q/r=(fepspminloc, fepspmaxloc) $newwave1 slpstart
    slpstartloc=v_levelx
// finds x-value of 20% y-coordinate
  findlevel/q/r=(fepspminloc, fepspmaxloc) $newwave1 slpend
    slpendloc=v_levelx
// finds x-value of 80% y-coordinate
  duplicate/o/r=(fepspminloc, fepspmaxloc) $newwave1 newwaveslope
  appendtograph newwaveslope
// highlights (in red) the portion of the fepsp that will be used in slope fitting
(allows user-defined variables to be checked for accuracy)
  dowindow/f databrowser
  CurveFit/w=0/q line $newwave1(slpstartloc, slpendloc) /d
// fits epsp slope. Uses 20%-80% of the peak amplitude
    fepspslope[time2]=(W_coef[1])
// makes slope value the y-coordinate of point in wave "fepspslope" that
appears in window, x-value is time
//runs window macro
    fepsp_peak_window()
    fepsp_slope_window()
  dowindow/f databrowser

do

// beginning of "do loop," program will keep looping this next portion until
defined conditions are met (in this case, 20  seconds have passed)

  sleep/s stimint
//program pauses for inter-stimulus interval
  dowindow/k fepsp_peak_window
  dowindow/k fepsp_slope_window
  dowindow/f databrowser
  removefromgraph newwaveslope
// prevents waves from accumulating in databrowser
    time2=(datetime-universaltime)
// number of seconds since last time the number of seconds since 1904 were
counted, should be 20 seconds later (that's how long the program slept), this
will be the new  x-value for peak and slope points

    DoDataAcq()
```

```
    SaveStimHistory(0)

// the commands in rest of the "do loop" serve the same function as they did
above, unless otherwise noted
  smooth 10,$newwave1
  wavestats/q/r=(1, 48) $newwave1
    baseline=v_avg
  wavestats/q/r=(minstart,minend) $newwave1
    fepspmin=v_max
  findlevel/q/r=(minstart,minend) $newwave1, fepspmin
    fepspminloc=v_levelx
  wavestats/q/r=(maxstart,maxend) $newwave1
    fepspmax=v_min
  findlevel/q/r=(maxstart,maxend) $newwave1, fepspmax
    fepspmaxloc=v_levelx
    fepsppeak[time2]=fepspmax-baseline
    fepsphalfmax=(((fepspmax-fepspmin)/2)+fepspmin)
    slpstart=fepsphalfmax-(0.3*(fepspmax-fepspmin))
    slpend=fepsphalfmax+(0.3*(fepspmax-fepspmin))
  findlevel/q/r=(fepspminloc, fepspmaxloc) $newwave1 slpstart
    slpstartloc=v_levelx
  findlevel/q/r=(fepspminloc, fepspmaxloc) $newwave1 slpend
    slpendloc=v_levelx
  duplicate/o/r=(fepspminloc, fepspmaxloc) $newwave1 newwaveslope
  appendtograph newwaveslope
  dowindow/f databrowser
  CurveFit/w=0/q line $newwave1(slpstartloc, slpendloc) /d
    fepspslope[time2]=(W_coef[1])
    fepsp_peak_window()
    fepsp_slope_window()
  dowindow databrowser
  setscale/p x,0,0.016,"Min",fEPSPpeak,fEPSPslope, percentpeakbaseline,
percentslopebaseline
// sets scale of peak and slope waves

while (time2<=howlong2*60))

  dowindow/f fepsp_peak_window
  dowindow/f fepsp_slope_window
// makes sure these window are visible when the program ends
```

```
EndMacro

---------------------------------------------------------------------------  // window
macros

Window fepsp_peak_window() : Graph
  PauseUpdate; Silent 1
  Display /W=(487.5,44,935.25,270.5) fepsppeak
  ModifyGraph mode=3
  ModifyGraph marker=19
  ModifyGraph msize=2
  Label left "mV"
  Label bottom "Minutes"
  SetAxis left 0,-4
  SetAxis bottom 0,60
EndMacro
-------------------------------------------------------------------------------------------------
Window fepsp_slope_window() : Graph
  PauseUpdate; Silent 1
  Display /W=(15.75,44,477,270.5) fepspslope
  ModifyGraph mode=3
  ModifyGraph marker=19
  ModifyGraph msize=2
  Label left "mV/ms"
  Label bottom "Minutes"
  SetAxis left 0,-1.75
  SetAxis bottom 0,60
EndMacro

-------------------------------------------------------------------------------------------------

// the commands in the Field_LTP_Resume macro do the same thing as in the
Field_LTP macro unless otherwise stated

Macro Field_LTP_Resume ()
variable howlong,stimint,starttime,endtime,baseline, peak,slpstart, slpend,
epsphalfmax,  peakloc, leftpt, rtpt
variable slpstartloc, slpendloc, minstart,minend,maxstart,maxend
variable  fibervollymax, fibervollymaxloc, fepspmin, fepspminloc, fepspmax,
fepspmaxloc, fepsphalfmax, avgbaseline, fepspslopevalue
```

```
variable/g  time2=time2, howlong2, universaltime, peak_avgbaseline,
slope_avgbaseline, Gminstart, Gminend, Gmaxend
    howlong=60
    stimint=20
    minstart=Gminstart
    minend=Gminend
    maxend=Gmaxend
    maxstart=minend
    time2=datetime-universaltime
    howlong2=(howlong)+time2/60
  dowindow/k fepsp_peak_window
  dowindow/k fepsp_slope_window
  dowindow databrowser

    DoDataAcq()
    SaveStimHistory(0)

  smooth 10,$newwave1
  wavestats/q/r=(1, 48) $newwave1
    baseline=v_avg
  wavestats/q/r=(minstart,minend) $newwave1
    fepspmin=v_max
  findlevel/q/r=(minstart,minend) $newwave1, fepspmin
    fepspminloc=v_levelx
  wavestats/q/r=(maxstart,maxend) $newwave1
    fepspmax=v_min
  findlevel/q/r=(maxstart,maxend) $newwave1, fepspmax
    fepspmaxloc=v_levelx
    fepsppeak[time2]=fepspmax-baseline
    percentpeakbaseline[time2]=fepsppeak[time2]/peak_avgbaseline
    fepsphalfmax=(((fepspmax-fepspmin)/2)+fepspmin)
    slpstart=fepsphalfmax-(0.3*(fepspmax-fepspmin))
    slpend=fepsphalfmax+(0.3*(fepspmax-fepspmin))
  findlevel/q/r=(fepspminloc, fepspmaxloc) $newwave1 slpstart
    slpstartloc=v_levelx
  findlevel/q/r=(fepspminloc, fepspmaxloc) $newwave1 slpend
    slpendloc=v_levelx
  duplicate/o/r=(fepspminloc, fepspmaxloc) $newwave1 newwaveslope
  appendtograph newwaveslope
  dowindow/f databrowser
  CurveFit/w=0/q line $newwave1(slpstartloc, slpendloc) /d
```

```
    fepspslope[time2]=(W_coef[1])
    percentslopebaseline[time2]=fepspslope[time2]/slope_avgbaseline
    fepsp_slope_window()
    fepsp_peak_window()

do

  sleep/s stimint
  dowindow/k/f fepsp_peak_window
  dowindow/k/f fepsp_slope_window
  dowindow databrowser
  removefromgraph newwaveslope
    time2=(datetime-universaltime)
  NextSweep()
  execute "Updatesweep()"

    DoDataAcq()
    SaveStimHistory(0)

  smooth 10,$newwave1
  wavestats/q/r=(1, 48) $newwave1
    baseline=v_avg
  wavestats/q/r=(minstart,minend) $newwave1
    fepspmin=v_max
  findlevel/q/r=(minstart,minend) $newwave1, fepspmin
    fepspminloc=v_levelx
  wavestats/q/r=(maxstart,maxend) $newwave1
    fepspmax=v_min
  findlevel/q/r=(maxstart,maxend) $newwave1, fepspmax
    fepspmaxloc=v_levelx
    fepsppeak[time2]=fepspmax-baseline
    fepsphalfmax=(((fepspmax-fepspmin)/2)+fepspmin)
    slpstart=fepsphalfmax-(0.3*(fepspmax-fepspmin))
    slpend=fepsphalfmax+(0.3*(fepspmax-fepspmin))
  findlevel/q/r=(fepspminloc, fepspmaxloc) $newwave1 slpstart
    slpstartloc=v_levelx
  findlevel/q/r=(fepspminloc, fepspmaxloc) $newwave1 slpend
    slpendloc=v_levelx
  duplicate/o/r=(fepspminloc, fepspmaxloc) $newwave1 newwaveslope
  appendtograph newwaveslope
  dowindow/f databrowser
```

```
  CurveFit/w=0/q line $newwave1(slpstartloc, slpendloc) /d
    fepspslope[time2]=(W_coef[1])
  wavestats/q/r=(0, time2) fepspslope
    fepsp_peak_window()
    fepsp_slope_window()
  dowindow databrowser
  setscale/p x,0,0.016,"Min",fEPSPpeak,fEPSPslope, percentpeakbaseline,
percentslopebaseline

while (time2<=howlong2*60))

  dowindow/f fepsp_peak_window
  dowindow/f fepsp_slope_window

EndMacro
```

Data Extraction Macro:

Extracts numerical values for data stored in fEPSP Slope and fEPSP Peak waves in Field_LTP data acquisition macro.

```
#pragma rtGlobals=1

macro LTPextractwave_onechannel()
silent 1
variable i,p
make/o/n=500 fepsp_p
fepsp_p=nan
make/o/n=500 fepsp_s
fepsp_s=nan
make/o/n=500 fepsp_x
fepsp_x=nan
i=0
p=0
edit fepsp_x ,fepsp_p, fepsp_s

do

if(abs(fepsppeak[i])>=0))
 fepsp_p[p]=fepsppeak[i]
fepsp_s[p]=fepspslope[i]
fepsp_x[p]=i
p+=1
endif

i+=1

while(p<=500)

end
```

Analysis of Paired Pulse Facilitation:

This macro was used to compute paired pulse facilitation ratios from pulses delivered at a range of inter-stimulus intervals.

```
macro paried_pulse (wavenmbr)
string basenm
variable wavenmbr, baseline, fepsp1max, fepsp2max, PPR

sprintf basenm, "%s%d", "avg_", wavenmbr

wavestats/q/r=(1,48) $basenm
baseline=v_avg

wavestats/q/r=(54,67) $basenm
fepsp1max=v_min-baseline

wavestats/q/r=(104, 120) $basenm
fepsp2max=v_min-baseline

PPR=fepsp2max/fepsp1max

print fepsp1max, fepsp2max, ppr
end
```

Input/Output Analysis Macro:

This macro was used to analyze the ratio of fEPSP amplitude to fiber volley amplitude, a measure of synaptic connectivity.

```
---------------------------------------------------------------------------------------------
macro input_output(wavenmbr1, wavenmbr2, wavenmbr3, wavenmbr4,
wavenmbr5, wavenmbr6, wavenmbr7)
variable wavenmbr1, baseline, fibervollymax, fepspmax, wavenmbr2, wavenmbr3
variable wavenmbr4, wavenmbr5, wavenmbr6, wavenmbr7
string basenm, basenm2, basenm3, basenm4, basenm5, basenm6, basenm7
string x_label

make/o/n=10 fibervollyamp
make/o/n=10 fepspamp

sprintf basenm, "%s%d","avg_", wavenmbr1

wavestats/q/r=(10, 48) $basenm
baseline=v_avg
print v_avg
wavestats/q/r=(51,53) $basenm
fibervollymax=v_min
fibervollyamp[0]=fibervollymax-baseline
wavestats/q/r=(54,67) $basenm
fepspmax=v_min
fepspamp[0]=fepspmax-baseline

edit fibervollyamp
appendtotable fepspamp

sprintf basenm2, "%s%d","avg_", wavenmbr2

wavestats/q/r=(10, 48) $basenm2
baseline=v_avg
print v_avg
wavestats/q/r=(51,53) $basenm2
fibervollymax=v_min
fibervollyamp[1]=fibervollymax-baseline
wavestats/q/r=(54,67) $basenm2
fepspmax=v_min
fepspamp[1]=fepspmax-baseline
```

```
sprintf basenm3, "%s%d","avg_", wavenmbr3

wavestats/q/r=(10, 48) $basenm3
baseline=v_avg
print v_avg
wavestats/q/r=(51,53) $basenm3
fibervollymax=v_min
fibervollyamp[2]=fibervollymax-baseline
wavestats/q/r=(54,67) $basenm3
fepspmax=v_min
fepspamp[2]=fepspmax-baseline

sprintf basenm4, "%s%d","avg_", wavenmbr4

wavestats/q/r=(10, 48) $basenm4
baseline=v_avg
print v_avg
wavestats/q/r=(51,53) $basenm4
fibervollymax=v_min
fibervollyamp[3]=fibervollymax-baseline
wavestats/q/r=(54,67) $basenm4
fepspmax=v_min
fepspamp[3]=fepspmax-baseline

sprintf basenm5, "%s%d","avg_", wavenmbr5

wavestats/q/r=(10, 48) $basenm5
baseline=v_avg
print v_avg
wavestats/q/r=(51,53) $basenm5
fibervollymax=v_min
fibervollyamp[4]=fibervollymax-baseline
wavestats/q/r=(54,67) $basenm5
fepspmax=v_min
fepspamp[4]=fepspmax-baseline

sprintf basenm6, "%s%d","avg_", wavenmbr6

wavestats/q/r=(10, 48) $basenm6
baseline=v_avg
```

```
print v_avg
wavestats/q/r=(51,53) $basenm6
fibervollymax=v_min
fibervollyamp[5]=fibervollymax-baseline
wavestats/q/r=(54,67) $basenm6
fepspmax=v_min
fepspamp[5]=fepspmax-baseline

sprintf basenm7, "%s%d","avg_", wavenmbr7

wavestats/q/r=(10, 48) $basenm7
baseline=v_avg
print v_avg
wavestats/q/r=(51,53) $basenm7
fibervollymax=v_min
fibervollyamp[6]=fibervollymax-baseline
wavestats/q/r=(54,67) $basenm7
fepspmax=v_min
fepspamp[6]=fepspmax-baseline

end
```

AMPA / NMDA and EPSC analysis macro:

This macro calculates the peak, area, and decay constant of inward (AMPA) and outward (NMDA) currents and computes the AMPA / NMDA measured with whole-cell voltage clamp recording.

```
#pragma rtGlobals=1
//calculates area, tau, ampa nmda ratio for up to 3 conditions

macro AMPA_NMDA(wavenmbr_ampa1, wavenmbr_nmda1,wavenmbr_ampa2,
wavenmbr_nmda2,wavenmbr_ampa3, wavenmbr_nmda3)
variable wavenmbr_ampa1, wavenmbr_nmda1, wavenmbr_ampa2,
wavenmbr_nmda2
variable wavenmbr_ampa3, wavenmbr_nmda3
variable amplitude1a, adjfactor1a, baseline1a, amplitude1n, adjfactor1n,
baseline1n
variable amplitude2a, adjfactor2a, baseline2a, amplitude2n, adjfactor2n,
baseline2n
variable amplitude3a, adjfactor3a, baseline3a, amplitude3n, adjfactor3n,
baseline3n
string basenm1a, basenm1n, Normal1a, normal1n, basenm2a
basenm2n,Normal2a, normal2n
string basenm3a, basenm3n, Normal3a, normal3n
string x_label
variable peak1a, peak1aloc, peak1n, peak1nloc, peak2a, peak2aloc, peak2n,
peak2nloc
variable peak3a, peak3aloc, peak3n, peak3nloc
make/o/n=2 ratio_ampa_nmda
make/o/n=2 tau_ampa
make/o/n=2 tau_nmda
make/o/n=2 ampa_area
make/o/n=2 nmda_area

//calculates area of ampa response during condition1

sprintf basenm1a, "%s%d","avg_",wavenmbr_ampa1
wavestats/q/r=(203,800) $basenm1a
display $basenm1a
ModifyGraph lsize($basenm1a)=2,rgb($basenm1a)=(0,0,0)
setaxis bottom 190,700
setaxis/a left
```

```
wavestats/q/r=(90,190) $basenm1a
baseline1a=v_avg
$basenm1a-=baseline1a
wavestats/q/r=(203,800) $basenm1a
peak1a=v_min
findlevel/q/r=(203,800) $basenm1a, peak1a
peak1aloc=v_levelx
duplicate/o/r=(peak1aloc, 260) $basenm1a fit1a
curvefit/q exp_xoffset fit1a/d
appendtograph fit_fit1a
ModifyGraph lsize(fit_fit1a)=2,rgb(fit_fit1a)=(0,65280,0)
tau_ampa[0]=k2
duplicate/o/r=(203,260) $basenm1a area1a
ampa_area [0]=abs(area (area1a))
 appendtograph area1a
```

//calculates area of nmda response during condition1

```
sprintf basenm1n, "%s%d","avg_",wavenmbr_nmda1
wavestats/q/r=(90,190) $basenm1n
baseline1n=v_avg
$basenm1n-=baseline1n
appendtograph $basenm1n
ModifyGraph lsize($basenm1n)=2,rgb($basenm1n)=(0,0,0)
wavestats/q/r=(203,800) $basenm1n
peak1n=v_max
print peak1n
findlevel/q/r=(203,800) $basenm1n, peak1n
peak1nloc=v_levelx
print peak1nloc
duplicate/o/r=(peak1nloc, 400) $basenm1n fit1n
curvefit/q exp_xoffset fit1n/d
appendtograph fit_fit1n
ModifyGraph lsize(fit_fit1n)=2,rgb(fit_fit1n)=(0,65280,0)
tau_nmda[0]=k2
duplicate/o/r=(240,400) $basenm1n area1n
nmda_area [0]=area (area1n)
ratio_ampa_nmda[0]=abs(area(area1a))/area(area1n)

appendtograph area1n
```

//calculates area of ampa response during condition2

```
sprintf basenm2a, "%s%d","avg_",wavenmbr_ampa2
wavestats/q/r=(203,800) $basenm2a
appendtograph $basenm2a
ModifyGraph lsize($basenm2a)=2,rgb($basenm2a)=(0,0,0)
setaxis bottom 190,700
setaxis/a left

wavestats/q/r=(90,190) $basenm2a
baseline2a=v_avg
$basenm2a-=baseline2a
wavestats/q/r=(203,800) $basenm2a
peak2a=v_min
findlevel/q/r=(203,800) $basenm2a, peak2a
peak2aloc=v_levelx
duplicate/o/r=(peak2aloc, 260) $basenm2a fit2a
curvefit/q exp_xoffset fit2a/d
appendtograph fit_fit2a
ModifyGraph lsize(fit_fit2a)=2,rgb(fit_fit2a)=(0,65280,0)
tau_ampa[1]=k2
duplicate/o/r=(203,260) $basenm2a area2a
ampa_area [1]=abs(area (area2a))
appendtograph area2a
```

//calculates area of nmda response during condition2

```
sprintf basenm2n, "%s%d","avg_",wavenmbr_nmda2
wavestats/q/r=(90,190) $basenm2n
baseline2n=v_avg
$basenm2n-=baseline2n
appendtograph $basenm2n
ModifyGraph lsize($basenm2n)=2,rgb($basenm2n)=(0,0,0)
wavestats/q/r=(203,800) $basenm2n
peak2n=v_max
print peak2n
findlevel/q/r=(203,800) $basenm2n, peak2n
peak2nloc=v_levelx
print peak2nloc
duplicate/o/r=(peak2nloc, 400) $basenm2n fit2n
```

```
curvefit/q exp_xoffset fit2n/d
appendtograph fit_fit2n
ModifyGraph lsize(fit_fit2n)=2,rgb(fit_fit2n)=(0,65280,0)
tau_nmda[1]=k2
duplicate/o/r=(240,400) $basenm2n area2n
nmda_area [1]=area (area2n)
ratio_ampa_nmda[1]=abs(area(area2a))/area(area2n)
appendtograph area2n


edit ampa_area
appendtotable nmda_area
appendtotable ratio_ampa_nmda
appendtotable tau_ampa
appendtotable tau_nmda
end
```

//calculates area of ampa response during condition3

```
sprintf basenm3a, "%s%d","avg_",wavenmbr_ampa3
wavestats/q/r=(203,800) $basenm3a
appendtograph $basenm3a
ModifyGraph lsize($basenm3a)=2,rgb($basenm3a)=(0,0,0)
setaxis bottom 190,700
setaxis/a left

wavestats/q/r=(90,190) $basenm3a
baseline3a=v_avg
$basenm3a-=baseline3a
wavestats/q/r=(203,800) $basenm3a
peak3a=v_min
findlevel/q/r=(203,800) $basenm3a, peak3a
peak3aloc=v_levelx
duplicate/o/r=(peak3aloc, 800) $basenm3a fit3a
curvefit/q exp_xoffset fit3a/d
appendtograph fit_fit3a
ModifyGraph lsize(fit_fit3a)=2,rgb(fit_fit3a)=(0,65280,0)
tau_ampa[2]=k2
duplicate/o/r=(203,800) $basenm3a area3a
ampa_area [2]=abs(area (area3a))
```

//calculates area of nmda response during condition3

```
sprintf basenm3n, "%s%d","avg_",wavenmbr_nmda3
wavestats/q/r=(90,190) $basenm3n
baseline3n=v_avg
$basenm3n-=baseline3n
appendtograph $basenm3n
ModifyGraph lsize($basenm3n)=2,rgb($basenm3n)=(0,0,0)
wavestats/q/r=(203,800) $basenm3n
peak3n=v_max
print peak3n
findlevel/q/r=(203,800) $basenm3n, peak3n
peak3nloc=v_levelx
print peak3nloc
duplicate/o/r=(peak3nloc, 800) $basenm3n fit3n
curvefit/q exp_xoffset fit3n/d
appendtograph fit_fit3n
ModifyGraph lsize(fit_fit3n)=2,rgb(fit_fit3n)=(0,65280,0)
tau_nmda[2]=k2
duplicate/o/r=(203,800) $basenm3n area3n
nmda_area [2]=area (area3n)
ratio_ampa_nmda[2]=abs(area(area3a))/area(area3n)

EndMacro
```

BIBLIOGRAPHY

1. Atkins CM, Selcher JC, Petraitis JJ, Trzaskos JM, Sweatt JD. The MAPK cascade is required for mammalian associative learning. Nat Neurosci. 1998 Nov;1(7):602-9.

2. Baldessarini RJ, Tarazi FI. Brain dopamine receptors: a primer on their current status, basic and clinical. Harv Rev Psychiatry. 1996 Mar-Apr;3(6):301-25.

3. Banke TG, Bowie D, Lee H, Huganir RL, Schousboe A, Traynelis SF. Control of GluR1 AMPA receptor function by cAMP-dependent protein kinase. J. Neurosci. January 2000 20 (1): 89–102.

4. Bannon MJ, Roth RH. Pharmacology of mesocortical dopamine neurons. Pharmacol Rev 1983 35: 53-68

5. Barkley, R.A. Attention-deficit hyperactivity disorder. Sci. Am. 279 1998, pp. 66–71.

6. Berger A. and Posner M.I.. Pathologies of brain attentional networks. Neurosci. Biobehav. Rev. 24 2000, pp. 3–5.

7. Bernabeu R, Cammarota M, Izquierdo I, Medina JH. Involvement of hippocampal AMPA glutamate receptor changes and the cAMP/protein kinase A/CREB-P signalling pathway in memory consolidation of an avoidance task in rats. Braz J Med Biol Res. 1997 Aug;30(8):961-5.

8. Berridge KC, Robinson TE. Dopamine D1-like receptors and reward-related incentive learning. Neurosci Biobehav Rev 1998 22: 335-345

9. Boehm J, Kang MG, Johnson RC, Esteban J, Huganir RL, Malinow R. Synaptic incorporation of AMPA receptors during LTP is controlled by a PKC phosphorylation site on GluR1. Neuron. 2006 Jul 20;51(2):213-25.

10. Boehm J, Kang MG, Johnson RC, Esteban J, Huganir RL, Malinow R. Synaptic incorporation of AMPA receptors during LTP is controlled by a PKC phosphorylation site on GluR1. Neuron July 2006 51 (2): 213–25.

11. Brun VH, Ytterbo K, Morris RG, Moser MB, Moser EI. Retrograde amnesia for spatial memory induced by NMDA receptor-mediated long-term potentiation. J Neurosci. 2001 Jan 1;21(1):356-62.

12. Byrnes EM, Reilly A, Bruno JP. Effects of AMPA and D1 receptor activation on striatal and nigral GABA efflux. Synapse. 1997 Jul;26(3):254-68.

13. Cepeda C, Colwell CS, Itri JN, Chandler SH, Levine MS. Dopaminergic modulation of NMDA-induced whole cell currents in neostriatal neurons in slices: contribution of calcium conductances. J Neurophysiol. 1998 Jan;79(1):82-94.

14. Cepeda C, Levine MS. Where do you think you are going? The NMDA-D1 receptor trap. Sci STKE. 2006 May 2;2006(333):pe20.

15. Chao SZ, Ariano MA, Peterson DA, Wolf ME. D1 dopamine receptor stimulation increases GluR1 surface expression in nucleus accumbens neurons. J Neurochem. 2002 Nov;83(3):704-12.

16. Chen BS, Roche KW. Regulation of NMDA receptors by phosphorylation. Neuropharmacology. 2007 Sep;53(3):362-8. Epub 2007 Jun 2. Review.

17. Chen L, Yang CR. Interaction of dopamine D1 and NMDA receptors mediates acute clozapine potentiation of glutamate EPSPs in rat prefrontal cortex. J Neurophysiol. 2002 May;87(5):2324-36.

18. Crump FT, Dillman KS, Craig AM. cAMP-dependent protein kinase mediates activity-regulated synaptic targeting of NMDA receptors. The Journal of neuroscience. 2001;21:5079–5088.

19. Cull-Candy S, Brickley S, Farrant M. NMDA receptor subunits: diversity, development and disease. Current opinion in neurobiology. 2001;11:327–335.

20. Day M, Morris RG. Memory consolidation and NMDA receptors: discrepancy between genetic and pharmacological approaches. Science. 2001 Aug 3;293(5531):755.

21. Delgado JY, Coba M, Anderson CN, Thompson KR, Gray EE, Heusner CL, Martin KC, Grant SG, O'Dell TJ. NMDA receptor activation dephosphorylates AMPA receptor glutamate receptor 1 subunits at threonine 840. J Neurosci. 2007 Nov 28;27(48):13210-21.

22. Delgado JY, Coba M, Anderson CN. NMDA receptor activation dephosphorylates AMPA receptor glutamate receptor 1 subunits at threonine 840. J. Neurosci. November 2007 27 (48): 13210–21.

23. Derkach V, Barria A, Soderling TR . Ca2+/calmodulin-kinase II enhances channel conductance of alpha-amino-3-hydroxy-5-methyl-4-isoxazolepropionate type glutamate receptors. Proc. Natl. Acad. Sci. U.S.A. March 1999 96 (6): 3269–74.

24. Dunah AW, Sirianni AC, Fienberg AA, Bastia E, Schwarzschild MA, Standaert DG. Dopamine D1-dependent trafficking of striatal N-methyl-D-aspartate glutamate receptors requires Fyn protein tyrosine kinase but not DARPP-32. Mol Pharmacol. 2004 Jan;65(1):121-9.

25. Dunah AW, Standaert DG. Dopamine D1 receptor-dependent trafficking of striatal NMDA glutamate receptors to the postsynaptic membrane. J Neurosci. 2001 Aug 1;21(15):5546-58.

26. Dunah AW, Yasuda RP, Wolfe BB. Developmental regulation of tyrosine phosphorylation of the NR2D NMDA glutamate receptor subunit in rat central nervous system. Journal of neurochemistry. 1998;71:1926–1934.

27. Everett BJ, Parkinson JA, Olmstead MC, Arroyo M, Robledo P, Robbins TW. Associative processes in addiction and reward. The role of amygdala-ventral striatal subsystems. Ann N Y Acac Sci 1999 877: 412-438

28. Flores-Hernández J, Cepeda C, Hernández-Echeagaray E, Calvert CR, Jokel ES, Fienberg AA, Greengard P, Levine MS. Dopamine enhancement of NMDA currents in dissociated medium-sized striatal neurons: role of D1 receptors and DARPP-32.J Neurophysiol. 2002 Dec;88(6):3010-20.

29. Galarraga E, Hernández-López S, Reyes A, Barral J, Bargas J. Dopamine facilitates striatal EPSPs through an L-type Ca2+ conductance. Neuroreport. 1997 Jul 7;8(9-10):2183-6.

30. Girault JA, Greengard P. The neurobiology of dopamine signaling. Arch Neurol. 2004 May;61(5):641-4.

31. Gao C, Sun X, Wolf ME. Activation of D1 dopamine receptors increases surface expression of AMPA receptors and facilitates their synaptic incorporation in cultured hippocampal neurons.J Neurochem. 2006 Sep;98(5):1664-77. Epub 2006 Jun 27.

32. Gao C, Wolf ME. Dopamine alters AMPA receptor synaptic expression and subunit composition in dopamine neurons of the ventral tegmental area cultured with prefrontal cortex neurons. J Neurosci. 2007 Dec 26;27(52):14275-85.

33. Gao C, Wolf ME. Dopamine receptors regulate NMDA receptor surface expression in prefrontal cortex neurons. J Neurochem. 2008 Aug 13.

34. Gardner GJ, Ashby CR Jr. Heterogeneity of the mesotelencephalic dopamine fibers: physiology and pharmacology. Neurosci Biobehav Rev 2000 24: 115-118

35. Gasbarri A, Sulli A, Packard MG. The dopaminergic mesencephalic projections to the hippocampal formation in the rat. Prog Neuropsychopharmacol Biol Psychiatry. 1997 Jan;21(1):1-22.

36. Granado N, Ortiz O, Suárez LM, Martín ED, Ceña V, Solís JM, Moratalla R. D1 but not D5 dopamine receptors are critical for LTP, spatial learning, and LTP-Induced arc and zif268 expression in the hippocampus. Cereb Cortex. 2008 Jan;18(1):1-12. Epub 2007 Mar 29.

37. Gray, J. Feldon, J.N. Rawlins, D.R. Hensley and A.D. Smith , The neuropsychology of schizophrenia. Behav. Brain Sci. 14 1991, pp. 1–20.

38. Greger IH, Ziff EB, Penn AC. Molecular determinants of AMPA receptor subunit assembly. Trends Neurosci. August 2007 30 (8): 407–16.

39. Grosshans DR, Clayton DA, Coultrap SJ, Browning MD. LTP leads to rapid surface expression of NMDA but not AMPA receptors in adult rat CA1. Nat Neurosci. 2002 Jan;5(1):27-33.

40. Guzowski JF, Lyford GL, Stevenson GD, Houston FP, McGaugh JL, Worley PF, Barnes CA. Inhibition of activity-dependent arc protein expression in the rat hippocampus impairs the maintenance of long-term potentiation and the consolidation of long-term memory. J Neurosci. 2000 Jun 1;20(11):3993-4001.

41. Guzowski JF, McGaugh JL. Antisense oligodeoxynucleotide-mediated disruption of hippocampal cAMP response element binding protein levels impairs consolidation of memory for water maze training. Proc Natl Acad Sci U S A. 1997 Mar 18;94(6):2693-8.

42. Hallett PJ, Spoelgen R, Hyman BT, Standaert DG, Dunah AW. Dopamine D1 activation potentiates striatal NMDA receptors by tyrosine phosphorylation-dependent subunit trafficking. J Neurosci. 2006 Apr 26;26(17):4690-700.

43. Hatt H, Schmidt KF, Smith DO. Dopaminergic modulation of glutamate-activated channels in the central nervous system. J Neural Transm Suppl. 1995;46:77-86.

44. Hayashi Y, Shi SH, Esteban JA, Piccini A, Poncer JC, Malinow R. Driving AMPA receptors into synapses by LTP and CaMKII: requirement for GluR1 and PDZ domain interaction. Science (journal) March 2000 287 (5461): 2262–7.

45. Hernández-Echeagaray E, Cepeda C, Ariano MA, Lobo MK, Sibley DR, Levine MS. Dopamine reduction of GABA currents in striatal medium-sized spiny neurons is mediated principally by the D(1) receptor subtype. Neurochem Res. 2007 Feb;32(2):229-40. Epub 2006 Sep 22.

46. Hernandez-Lopez S, Bargas J, Surmeier D, Reyes A, Galgarraga E. D1 receptor activation enhances evoked discharge in neostriatal medium spiny neurons by modulating an L-type Ca2+ conductance. J Neurosci. 1997 May 1;17(9):3334-42.

47. Hsu KS. Characterization of dopamine receptors mediating inhibition of excitatory synaptic transmission in the rat hippocampal slice. J Neurophysiol. 1996 Sep;76(3):1887-95.

48. Huang YY, Kandel ER. D1/D5 receptor agonists induce a protein synthesis-dependent late potentiation in the CA1 region of the hippocampus. Proc Natl Acad Sci U S A. 1995 Mar 28;92(7):2446-50.

49. Ito HT, Schuman EM. Frequency-dependent gating of synaptic transmission and plasticity by dopamine. Front Neural Circuits. 2007;1:1. Epub

50. J O'Keefe and J Dostrovsky, The hippocampus as a spatial map. Preliminary evidence from unit activity in the freely-moving rat. Brain Res 34 (1971), pp. 171–175.

51. Jarrard LE. On the role of the hippocampus in learning and memory in the rat. Behav Neural Biol. 1993 Jul;60(1):9-26.

52. Jean-Antoine Girault, MD, PhD; Paul Greengard, PhD. The Neurobiology of Dopamine Signaling. Arch Neurol. 2004;61:641-644.

53. Jonas P, Sakmann B. Glutamate receptor channels in isolated patches from CA1 and CA3 pyramidal cells of rat hippocampal slices. J Physiol. 1992 Sep;455:143-71.

54. Jonas P. AMPA-type glutamate receptors--nonselective cation channels mediating fast excitatory transmission in the CNS. EXS. 1993;66:61-76

55. Kaphzan H, O'Riordan KJ, Mangan KP, Levenson JM, Rosenblum K. NMDA and dopamine converge on the NMDA-receptor to induce ERK activation and synaptic depression in mature hippocampus. PLoS ONE. 2006 Dec 27;1:e138.

56. Kauer JA, Malenka RC, Nicoll RA. A persistent postsynaptic modification mediates long-term potentiation in the hippocampus. Neuron. 1988 Dec;1(10):911-7.

57. Muller D, Joly M, Lynch G. Contributions of quisqualate and NMDA receptors to the induction and expression of LTP. Science. 1988 Dec 23;242(4886):1694-7.

58. Muller D, Lynch G. Long-term potentiation differentially affects two components of synaptic responses in hippocampus. Proc Natl Acad Sci U S A. 1988 Dec;85(23):9346-50.

59. Kauer JA, Malenka RC. Synaptic plasticity and addiction. Nat Rev Neurosci. 2007 Nov;8(11):844-58. Kim JJ, Fanselow MS, DeCola JP, Landeira-Fernandez J. Selective impairment of long-term but not short-term conditional fear by the N-methyl-D-aspartate antagonist APV. Behav Neurosci. 1992 Aug;106(4):591-6.

60. Klann E, Chen SJ, Sweatt JD. Mechanism of protein kinase C activation during the induction and maintenance of long-term potentiation probed using a selective peptide substrate. Proc Natl Acad Sci U S A. 1993 Sep 15;90(18):8337-41.

61. Klann E, Chen SJ, Sweatt JD. Persistent protein kinase activation in the maintenance phase of long-term potentiation. J Biol Chem. 1991 Dec 25;266(36):24253-6.

62. Kohr G, Seeburg PH. Subtype-specific regulation of recombinant NMDA receptor-channels by protein tyrosine kinases of the src family. The Journal of physiology. 1996;492(Pt 2):445–452.

63. Lan JY, Skeberdis VA, Jover T, Grooms SY, Lin Y, Araneda RC, Zheng X, Bennett MV, Zukin RS. Protein kinase C modulates NMDA receptor trafficking and gating. Nature neuroscience. 2001;4:382–390

64. Laruelle M, Kegeles LS, Abi-Dargham A. Glutamate, dopamine, and schizophrenia: from pathophysiology to treatment. Ann N Y Acad Sci. 2003 Nov;1003:138-58.

65. Lee HK, Barbarosie M, Kameyama K, Bear MF, Huganir RL. Regulation of distinct AMPA receptor phosphorylation sites during bidirectional synaptic plasticity. Nature. 2000 Jun 22;405(6789):955-9.

66. Legendre P and Westbrook GL. Ifenprodil blocks N-methyl-D-aspartate receptors by a two-component mechanism. Molecular Pharmacology 08/01/1991, Volume 40, Issue 2, pp. 289-298,

67. Lemon N, Manahan-Vaughan D. Dopamine D1/D5 receptors gate the acquisition of novel information through hippocampal long-term potentiation and long-term depression. J Neurosci. 2006 Jul 19;26(29):7723-9.

68. Liu JC, DeFazio RA, Espinosa-Jeffrey A, Cepeda C, de Vellis J, Levine MS. Calcium modulates dopamine potentiation of N-methyl-D-aspartate responses: electrophysiological and imaging evidence. J Neurosci Res. 2004 May 1;76(3):315-22.

69. Lu WY, Xiong ZG, Lei S, Orser BA, Dudek E, Browning MD, MacDonald JF. G-protein-coupled receptors act via protein kinase C and Src to regulate NMDA receptors. Nature neuroscience. 1999;2:331–338.

70. Lu W, Man H, Ju W, Trimble WS, MacDonald JF, Wang YT. Activation of synaptic NMDA receptors induces membrane insertion of new AMPA receptors and LTP in cultured hippocampal neurons. Neuron. 2001 Jan;29(1):243-54.

71. Mangiavacchi S, Wolf ME. D1 dopamine receptor stimulation increases the rate of AMPA receptor insertion onto the surface of cultured nucleus accumbens neurons through a pathway dependent on protein kinase A. J Neurochem. 2004 Mar;88(5):1261-71.

72. Markram H, Segal M. Activation of protein kinase C suppresses responses to NMDA in rat CA1 hippocampal neurones. The Journal of physiology. 1992;457:491–501.

73. Matthies H, Becker A, Schröeder H, Kraus J, Höllt V, Krug M. Dopamine D1-deficient mutant mice do not express the late phase of hippocampal long-term potentiation. Neuroreport. 1997 Nov 10;8(16):3533-5.

74. Mayer ML. Glutamate receptor ion channels. Curr Opin Neurobiol. 2005 Jun;15(3):282-8.

75. Missale C, Fiorentini C, Busi C, Collo G, Spano PF. The NMDA/D1 receptor complex as a new target in drug development. Curr Top Med Chem. 2006;6(8):801-8.

76. Moagenson GY, Jones DL, Cim CY. From motivation to action: functional interface between the limbic system and the motor system. Prog Neurobiol 1980 14: 69-97

77. Mockett BG, Guévremont D, Williams JM, Abraham WC. Dopamine D1/D5 receptor activation reverses NMDA receptor-dependent long-term depression in rat hippocampus. J Neurosci. 2007 Mar 14;27(11):2918-26.

78. Nakazawa T, Komai S, Tezuka T, Hisatsune C, Umemori H, Semba K, Mishina M, Manabe T, Yamamoto T. Characterization of Fyn-mediated tyrosine phosphorylation sites on GluR epsilon 2 (NR2B) subunit of the N-methyl-D-aspartate receptor. The Journal of biological chemistry. 2001;276:693–699.

79. Navakkode S, Sajikumar S, Frey JU. Synergistic requirements for the induction of dopaminergic D1/D5-receptor-mediated LTP in hippocampal slices of rat CA1 in vitro. Neuropharmacology. 2007 Jun;52(7):1547-54. Epub 2007 Mar 12.

80. Nestler EJ. The neurobiology of cocaine addiction. Sci Pract Perspect. 2005 Dec;3(1):4-10.

81. Otmakhova NA, Lisman JE. D1/D5 dopamine receptor activation increases the magnitude of early long-term potentiation at CA1 hippocampal synapses. J Neurosci. 1996 Dec 1;16(23):7478-86.

82. Otmakhova NA, Lisman JE. D1/D5 dopamine receptors inhibit depotentiation at CA1 synapses via cAMP-dependent mechanism. J Neurosci. 1998 Feb 15;18(4):1270-9.

83. Otmakhova NA, Lisman JE. Dopamine selectively inhibits the direct cortical pathway to the CA1 hippocampal region. J Neurosci. 1999 Feb 15;19(4):1437-45.

84. Packard MG, White NM. Dissociation of hippocampus and caudate nucleus memory systems by posttraining intracerebral injection of dopamine agonists. Behav Neurosci. 1991 Apr;105(2):295-306.

85. Philpson OT. Afferent projections to the ventral tegmental area of Tsai and interfasicular nucleus: a horseradish peroxidase study in the rat. J Comp Neurol 1979 187: 117-143

86. Pickard L, Noël J, Duckworth JK, Fitzjohn SM, Henley JM, Collingridge GL, Molnar E. Transient synaptic activation of NMDA receptors leads to the insertion of native AMPA receptors at hippocampal neuronal plasma membranes. Neuropharmacology. 2001 Nov;41(6):700-13.

87. Price CJ, Kim P, Raymond LA. D1 dopamine receptor-induced cyclic AMP-dependent protein kinase phosphorylation and potentiation of striatal glutamate receptors. J Neurochem. 1999 Dec;73(6):2441-6.

88. Raman IM, Tong G, Jahr CE. Beta-adrenergic regulation of synaptic NMDA receptors by cAMP-dependent protein kinase. Neuron. 1996;16:415–421.

89. Roberson ED, Sweatt JD. Transient activation of cyclic AMP-dependent protein kinase during hippocampal long-term potentiation. J Biol Chem. 1996 Nov 29;271(48):30436-41.

90. Rosenmund C, Stern-Bach Y, Stevens CF) The tetrameric structure of a glutamate receptor channel" Science (journal) June 1998 280 (5369): 1596–9.

91. Sacktor TC, Osten P, Valsamis H, Jiang X, Naik MU, Sublette E. Persistent activation of the zeta isoform of protein kinase C in the maintenance of long-term potentiation. Proc Natl Acad Sci U S A. 1993 Sep 15;90(18):8342-6.

92. Santini E, Muller RU, Quirk GJ. Consolidation of extinction learning involves transfer from NMDA-independent to NMDA-dependent memory. J Neurosci. 2001 Nov 15;21(22):9009-17.

93. Sarvey JM, Burgard EC, Decker G. Long-term potentiation: studies in the hippocampal slice. J Neurosci Methods. 1989 May;28(1-2):109-24.

94. Schilström B, Yaka R, Argilli E, Suvarna N, Schumann J, Chen BT, Carman M, Singh V, Mailliard WS, Ron D, Bonci A. Cocaine enhances NMDA receptor-mediated currents in ventral tegmental area cells via dopamine D5 receptor-dependent redistribution of NMDA receptors. J Neurosci. 2006 Aug 16;26(33):8549-58.

95. Shimizu E, Tang YP, Rampon C, Tsien JZ. NMDA receptor-dependent synaptic reinforcement as a crucial process for memory consolidation. Science. 2000 Nov 10;290(5494):1170-4

96. Skeberdis VA, Chevaleyre V, Lau CG, Goldberg JH, Pettit DL, Suadicani SO, Lin Y, Bennett MV, Yuste R, Castillo PE, Zukin RS. Protein kinase A regulates calcium permeability of NMDA receptors. Nature neuroscience. 2006;9:501–510.

97. Smith WB, Starck SR, Roberts RW, Schuman EM. Dopaminergic stimulation of local protein synthesis enhances surface expression of GluR1 and synaptic transmission in hippocampal neurons. Neuron. 2005 Mar 3;45(5):765-79.

98. Squire, L R; Cohen, N J; Nadel, L. Memory Consolidation. Weingartner H, Parker E. , editors. Hillsdale, NJ: Erlbaum; 1984. pp. 185–210.

99. Steele RJ, Morris RG. Delay-dependent impairment of a matching-to-place task with chronic and intrahippocampal infusion of the NMDA-antagonist D-AP5. Hippocampus. 1999;9(2):118-36.

100. Sun X, Milovanovic M, Zhao Y, Wolf ME. Acute and chronic dopamine receptor stimulation modulates AMPA receptor trafficking in nucleus accumbens neurons cocultured with prefrontal cortex neurons. J Neurosci. 2008 Apr 16;28(16):4216-30.

101. Sun X, Zhao Y, Wolf ME. Dopamine receptor stimulation modulates AMPA receptor synaptic insertion in prefrontal cortex neurons. J Neurosci. 2005 Aug 10;25(32):7342-51.

102. Sweat, JD. Mechanisms of memory. Elsevier academic press, San Diego. Copyright 2003.

103. Takasu MA, Dalva MB, Zigmond RE, Greenberg ME. Modulation of NMDA receptor-dependent calcium influx and gene expression through EphB receptors. Science. 2002;295:491–495.

104. Tarazi FI, Baldessarini RJ.J Regional localization of dopamine and ionotropic glutamate receptor subtypes in striatolimbic brain regions. Neurosci Res. 1999 Feb 15;55(4):401-10.

105. Tseng KY, O'Donnell P. Dopamine-glutamate interactions controlling prefrontal cortical pyramidal cell excitability involve multiple signaling mechanisms. J Neurosci. 2004 Jun 2;24(22):5131-9.

106. Umemiya M, Raymond LA. Dopaminergic modulation of excitatory postsynaptic currents in rat neostriatal neurons. J Neurophysiol. 1997 Sep;78(3):1248-55.

107. Varela JA, Hirsch SJ, Chapman D, Leverich LS, Greene RW. D1/5 modulation of synaptic NMDA receptor currents. J Neurosci, accepted Jan. 2009.

108. Vicini S, Wang JF, Li JH, Zhu WJ, Wang YH, Luo JH, Wolfe BB, Grayson DR. Functional and pharmacological differences between recombinant N-methyl-D-aspartate receptors. J Neurophysiol. 1998 Feb;79(2):555-66.

109. Watt AJ, Sjöström PJ, Häusser M, Nelson SB, Turrigiano GG. A proportional but slower NMDA potentiation follows AMPA potentiation in LTP. Nat Neurosci. 2004 May;7(5):518-24. Epub 2004 Mar 28.

110. Weinberger D.R. Implications of normal brain development for the pathogenesis of schizophrenia. Arch. Gen. Psychiatry 44 1987, pp. 660–669.

111. Williams K. Ifenprodil discriminates subtypes of the N-methyl-D-aspartate receptor: selectivity and mechanisms at recombinant heteromeric receptors. Mol Pharmacol. 1993 Oct;44(4):851-9.

112. Williams K., Ifenprodil, a Novel NMDA Receptor Antagonist : Site and Mechanism of Action. Current Drug Targets, Volume 2, Number 3, September 2001 , pp. 285-298(15)

113. Williams S, Mmbaga N, Chirwa S. Dopaminergic D1 receptor agonist SKF 38393 induces GAP-43 expression and long-term potentiation in hippocampus in vivo. Neurosci Lett. 2006 Jul 10;402(1-2):46-50. Epub 2006 May 3.

114. Wirkner K, Krause T, Köles L, Thümmler S, Al-Khrasani M, Illes P. D1 but not D2 dopamine receptors or adrenoceptors mediate dopamine-induced potentiation of N-methyl-d-aspartate currents in the rat prefrontal cortex. Neurosci Lett. 2004 Nov 30;372(1-2):89-93.

115. Wittmann M, Marino MJ, Henze DA, Seabrook GR, Conn PJ. Clozapine potentiation of N-methyl-D-aspartate receptor currents in the nucleus accumbens: role of NR2B and protein kinase A/Src kinases. J Pharmacol Exp Ther. 2005 May;313(2):594-603. Epub 2005 Jan 19.

116. Wolf ME, Sun X, Mangiavacchi S, Chao SZ. Psychomotor stimulants and neuronal plasticity. Neuropharmacology. 2004;47 Suppl 1:61-79.

117. www.brainmap.org

118. Yang CR, Chen L.Targeting prefrontal cortical dopamine D1 and N-methyl-D-aspartate receptor interactions in schizophrenia treatment. Neuroscientist. 2005 Oct;11(5):452-70.

119. Yang SN. Sustained enhancement of AMPA receptor- and NMDA receptor-mediated currents induced by dopamine D1/D5 receptor activation in the hippocampus: an essential role of postsynaptic Ca2+. Hippocampus. 2000;10(1):57-63.

120. Yashiro K, Philpot BD, Regulation of NMDA receptor subunit expression and its implications for LTD, LTP, and metaplasticity. Neuropharmacology, in press July 23 2008.

121. Zheng P, Zhang XX, Bunney BS, Shi WX. Opposite modulation of cortical N-methyl-D-aspartate receptor-mediated responses by low and high concentrations of dopamine. Neuroscience. 1999;91(2):527-35.

122. Zheng X, Zhang L, Wang AP, Bennett MV, Zukin RS. Protein kinase C potentiation of N-methyl-D-aspartate receptor activity is not mediated by phosphorylation of N-methyl-D-aspartate receptor subunits. Proceedings of the National Academy of Sciences of the United States of America. 1999;96:15262–15267.